ENGINEERING BACTERIAL CO_2 FIXATION TO ENHANCE BIOFUEL AND BIOCHEMICAL YIELDS

by

Alan Gregory Fast

A dissertation submitted to the Faculty of the University of Delaware in partial fulfillment of the requirements for the degree of Doctor of Philosophy in Chemical Engineering

Summer 2017

ENGINEERING BACTERIAL CO_2 FIXATION

TO ENHANCE BIOFUEL AND BIOCHEMICAL YIELDS

by

Alan Gregory Fast

Approved: _____

Eric M. Furst, Ph.D.
Chair of the Department of Chemical and Biomolecular Engineering

Approved: _____

Babatunde A. Ogunnaike, Ph.D.
Dean of the College of Engineering

Approved: _____

Ann L. Ardis, Ph.D.
Senior Vice Provost for Graduate and Professional Education

I certify that I have read this dissertation and that in my opinion it meets the academic and professional standard required by the University as a dissertation for the degree of Doctor of Philosophy.

Signed: _____

Eleftherios Terry Papoutsakis, Ph.D.
Professor in charge of dissertation

I certify that I have read this dissertation and that in my opinion it meets the academic and professional standard required by the University as a dissertation for the degree of Doctor of Philosophy.

Signed: _____

Maciek R. Antoniewicz, Ph.D.
Member of dissertation committee

I certify that I have read this dissertation and that in my opinion it meets the academic and professional standard required by the University as a dissertation for the degree of Doctor of Philosophy.

Signed: _____

Wilfred Chen, Ph.D.
Member of dissertation committee

I certify that I have read this dissertation and that in my opinion it meets the academic and professional standard required by the University as a dissertation for the degree of Doctor of Philosophy.

Signed: _____

Shawn W. Jones, Ph.D.
Member of dissertation committee

ACKNOWLEDGMENTS

I would like to begin my acknowledgements by thanking my advisor Terry Papoutsakis. His mentorship, characterized by intelligence, energy, drive and patience, has been essential for my success in this program. Terry's ability to interrogate biological systems with probing, detailed scientific questions all the while maintaining an eye on the bigger picture is a quality I will aspire to emulate throughout my career. I would also like to thank my committee, Maciek Antoniewicz, Wilfred Chen, and Shawn Jones, for their valuable input that challenged me and allowed me to view my research through fresh eyes.

It is impossible to express in words my gratitude to my parents, Chuck and Wendy Fast, who have taught me to treat others with dignity, kindness, and respect and instilled in me the value of lifelong learning. Both engineers themselves, my parents have also given me every opportunity to explore my passion for science, sending me to science camp, helping construct Science Olympiad rockets, and taking me to the emergency room when my own homemade experiments went awry. Their gifts to me can never be repaid in full, though I will try. Thanks also to my siblings, Shannon and Aaron, who inspire me with their openness, courage, and drive. I'm so excited to see what you will do in the future. To my grandparents, thanks for your love, encouragement, and wit. To "Substitute Grandma" DJ, thanks for being an aspirational figure in my life who embodies intelligence and mindfulness. And to Doris, thanks for being the "family we choose."

To my fellow lab members, you have been a second family to me, sharing countless backroom lunches, Oktoberfest cup towers, running club “runs,” rides in the Taco, and WaWa sandwiches by Ursula, not to mention technical assistance for all things science. Thanks to Stefan, Pani, Shawn, Dinesh, Keerthi, Mohab, Kyle Z., Kyle B., Jinlin, Chen-Yuan, Stephan, Stephanie, Elli, Julia, Kamil, Alex (aka Eric, aka #), Erica, Hannah, Mike, Yongbo, Dr. Bi, Lisa S., Lisa W., Brian, Bryan, and Vanessa. Special thanks to Nich, Sergios, and Dani for being excellent roommates, colleagues, and friends. It’s amazing to know so many intelligent and talented people all over the world, and I can’t wait to come crash on your couches.

Thanks to the rest of my Delaware crew – especially, Ben, Kathy, Bryan, Jill, Mr. Swift, and Devesh – who have always been there for a good laugh when it was needed the most through, both the challenges of first year classes and onwards. To Rick and Shawn, your friendship has been invaluable to me for the past few years, and I can’t imagine having made it without you.

TABLE OF CONTENTS

LIST OF TABLES

LIST OF FIGURES

ABSTRACT

The mass production of biofuels and chemicals through microbial fermentation is renewable solution to combat climate change through decreased greenhouse gas emissions. The primary factor affecting the economic viability of next generation biofuel fermentations is the cost of feedstock and feedstock pretreatment. One way to mitigate high feedstock costs is by maximizing feedstock conversion to the product of interest. The ability to achieve high mass yields from carbohydrate fermentations, however, is impeded by CO_2 loss during glycolysis through the decarboxylation of pyruvate when forming acetyl-CoA, whereby one third of hexose carbons cannot be recovered as useful products. One route to improving glycolytic yields is through the incorporation of CO_2 fixation pathways that can recapture CO_2 lost during fermentation.

Stoichiometric analysis of the six natural carbon fixation pathways shows that the best suited pathway for industrial fermentation is the Wood-Ljungdahl pathway (WLP), an anaerobic pathway that directly reduces CO_2 to form the biological building block, acetyl-CoA, using electrons derived from glycolysis or from a wide array of inorganic sources including molecular CO and H_2. Under mixotrophic fermentation, in which both gases and carbohydrates are consumed concurrently, 100% of carbohydrate carbons can be recovered in products, up from the 66% of carbohydrate carbon that can be recovered in traditional fermentation.

The viability of mixotrophic fermentation was tested in four bacteria that natively contain the WLP. All four acetogens demonstrated the capability to simultaneously consume sugars and gases by producing metabolites at yields higher than that which could be achieved through heterotrophic fermentation alone. Additionally, we showed through ^{13}C labeling that, in the case of *Clostridium ljungdahlii*, gas incorporation occurs concurrently with sugar consumption and that the relative rates of gas and sugar production allow for more than 40% of acetate to be derived from the carbon fixation rather than glycolysis thereby validating the concept of acetogenic fermentation.

Engineering the WLP in the established industrial organism *C. acetobutylicum* would allow for the conversion of carbohydrates into butanol, acetone, and ethanol at higher yields than would otherwise be possible. In an attempt to achieve this goal, we focused on expressing 11 core genes coding for enzymes and accessory proteins, which required the development of a novel clostridial genetic system using two co-existing plasmids combined with a method to integrate a subset of the WLP genes into the *C. acetobutylicum* chromosome. While the engineered Wood-Ljungdahl pathway in *C. acetobutylicum* showed functionality of the Eastern branch of the pathway due to

the formation of labeled 5,10-methylenetetrahydrofolate from labeled formate and a functional Western branch of the Wood-Ljungdahl pathway in the formation of CO from CO_2, the connection of these two branches was not observed in any labeling of acetyl-CoA observed in the acetate and butyrate pools. Further efforts were undertaken to characterize the expression and activity of the vital CODH/ACS enzyme that catalyzes the reduction of CO_2 to CO and the condensation of CO with a methyl-group to form acetyl-CoA, and both activities were demonstrated through *in vivo* assays. Further engineering will be required to bring a functional heterologous WLP to fruition.

Chapter 1

INTRODUCTION

1.1 Developing platform organisms for biofuel production

The microbial production of biofuels and commodity chemicals from renewable feedstocks is vital to reducing global dependence on fossil fuels and decreasing greenhouse gas emissions. One of the primary factors affecting the economic viability of next generation biofuel processes is the cost of feedstock and feedstock pretreatment, which can exceed 50% of total operating expenditure (Gnansounou and Dauriat 2010, Klein-Marcuschamer, Oleskowicz-Popiel et al. 2012). The 2016 Department of Energy 2016 Billion-Ton Report identified that the US feedstock capacity could be most easily increased using alternative feedstocks, such as agricultural wastes and cellulosic biomass. However, the majority of domestic biofuel production comes from the fermentation of corn mash (Fairley 2011), and recent rises in global food and energy prices highlight the need for feedstocks that do not directly compete with the food supply, such as cellulosic biomass. Currently, however, cellulosic-biofuel production in the US lags behind projections. The previous 2013 cellulosic biofuel mandate was six million gallons, but production only reached 800,000 gallons in 2015 (Service 2014, Klein-Marcuschamer and Blanch 2015, Papoutsakis 2015). Many factors impact the costs associated with substrates and their utilization: substrate sourcing and availability, variability in substrate composition and purity, extent of necessary pretreatment, cellular flexibility in efficient and simultaneous utilization of various substrates, and complete substrate utilization. One major associated factor determining process viability is product yield (i.e., the fraction of substrate that is incorporated into products). Whereas most traditional fermentation processes based on the conversion of 5- and 6-C sugars into fuels and biochemicals lose one third of feedstock carbon to pyruvate decarboxylation, recent studies on mixotrophic sugar consumption (Jones, Fast et al. 2016) and

non-oxidative glycolysis (Bogorad, Lin et al. 2013) have demonstrated the feasibility of complete conversion of a carbohydrate feedstock into useful products.

1.2 *Clostridium* organisms as a platform for biofuel and chemical production

Clostridium is a genus of Gram-positive anaerobic bacteria characterized by anaerobic non-sulfur-reducing metabolism and the ability to form endospores. *Clostridium* is a broad genus, containing more than 100 species, and *Clostridium* species are scientifically relevant for a wide variety of characteristics: the production of endotoxins that impact human health (e.g. *C. botulinum*, *C. difficile*, *C. perfringens*, *C. tetani*, and *C. sordellii*), the production of industrially important solvents (e.g. *C. acetobutylicum*, *C. beijerinkii*, and *C. pasteurianum*), the capability to break down and ferment cellulosic biomass (e.g. *C. thermocellum* and *C. cellulolyticum*), and the fixation of CO_2 (e.g. *C. ljungdahlii*, *C. autoethanogenum*, and *C. carboxidivorans*).

Because *Clostridium* is a broad genus that has evolved to live in a wide variety of native habitats, clostridia have one of the most wide-ranging toolkits for substrate utilization (Papoutsakis 2008, Tracy, Jones et al. 2012). Clostridia can utilize both simple and complex carbohydrates (e.g. cellulose, xylan, hemicellulose, virtually all 5- and 6-C sugars, starches, and pectin), glycerol, short-chain fatty acids, gases (CO_2, H_2, CO), alcohols (e.g. methanol, ethanol), and waste sludge (Jones and Woods 1986, Drake 1994, Kim, Shin et al. 2011, Tracy, Jones et al. 2012). They produce a broad range of native metabolites including acetate, butyrate, hexanoate, acetone, acetoin, ethanol, butanol, hexanol, and many others.

Clostridium acetobutylicum 824 is one of the best understood and the most widely studied among clostridia largely deriving from the fact that it was used to carry out the acetone-butanol-ethanol (ABE) fermentation. The ABE fermentation played an important role in the production of acetone, a key solvent used in gunpowder manufacturing, during the First and Second World Wars, but also for butanol production needed to manufacture car lacquers (Jones and Woods 1986). Fermentations of solventogenic clostridia continued to be a major source of acetone and butanol until the 1950s when petrochemical production replaced the fermentation

processes. The batch fermentation of *C. acetobutylicum* exhibits a two-phase fermentation profile, which is typical for the clostridial ABE production. During the initial growth phase (acidogenesis), hexose or pentose sugars are fermented to form acetate and butyrate which results in a decrease of the culture pH. As the culture enters stationary phase, the metabolism shifts into solventogenesis, in which acids are reassimilated, the solvents acetone, butanol, and ethanol are formed, and the culture pH rises. In *C. acetobutylicum*, the shift in fermentation from acidogenesis to solventogenesis is coupled to a shift in cellular morphology (Al-Hinai, Jones et al. 2015). The early vegetative cells divide symmetrically into a rod-shaped morphology. As the acid concentration increases and the medium pH decreases, the cells take on the cigar-shaped clostridial form and accumulate granulose. Towards the end of fermentation, accumulation of the toxic solvent butanol leads to the generation of endospores that are resistant to heat, chemical degradation, and radiation. When extracellular signals indicate the return of conditions conducive to growth, the spores germinate to form vegetative cells that can repeat the growth cycle.

The limited availability of genetic tools in clostridia has hindered both fundamental and applied research in the clostridial genus. While genetic engineering efforts in *C. acetobutylicum* have led to the development of basic genetic toolkit, the genetic capabilities in clostridia are not as well-developed when compared to other model organisms such as *Escherichia coli* or *Bacillus subtilis* (Pyne, Bruder et al. 2014). Genetic engineering in *C. acetobutylicum* was first enabled by the identification of the Type II restriction endonuclease Cac824I, which digests unprotected plasmid DNA and hindered the ability to electrotransform *C. acetobutylicum*. The development of a methylation system to protect plasmid DNA against Cac824I led to the first electroporation protocols in the early 1990s (Mermelstein and Papoutsakis 1993). The advent of efficient DNA transformation in *C. acetobutylicum* was followed by the creation of a gene reporter system (Tummala, Junne et al. 2003), antisense-RNA knockdown (Desai and Papoutsakis 1999), an inducible promoter-repressor system (Girbal, Mortier-Barriere et al. 2003), a lactose-inducible

promoter (Hartman, Liu et al. 2011), as well as its genome sequence (Nölling, Breton et al. 2001).

The lack of chromosomal manipulation systems hindered research into clostridial physiology until the application of group II intron technology in 2007 (Heap, Pennington et al. 2007). The group II intron approach utilizes retrohoming RNA molecules that splice into a targeted area on a host genome, thereby disrupting a gene of interest. Engineering a double disruption of the *pta* and *buk* genes from *C. acetobutylicum*, which are responsible for the production of acetate and butyrate, respectively, was shown to diminish the production of acids and allow for the direct production of solvents (Jang, Lee et al. 2012). The overexpression of $adhE1^{D485G}$ in this mutant strain led to the production of 18.9 g L^{-1} butanol in batch culture with a yield of 0.29 g/g glucose, which is the highest reported butanol titer from glucose for *C. acetobutylicum* batch culture.

The development of positive selection/counterselection systems in clostridia has enabled markerless knockout and integration through allelic exchange. The *pyrE/pyrF* system allows the antimetabolites 5-fluoroorotic acid or 5-fluorouracil to be used as counter-selection agents (Boeke, Trueheart et al. 1987); however, it requires the creation of uracil auxotrophic strains prior to the counterselection. The thermostability of 5-fluorooorotic acid allows for the use of *pyrE*/*pyrF* counterselection in thermophilic organisms such as *C. thermocellum (Tripathi, Olson et al. 2010)* and *M. thermoacetica (Kita, Iwasaki et al. 2013)*. The *mazF* counterselection system, first demonstrated in 2012, does not require the use of an auxotrophic host (Al-Hinai, Fast et al. 2012). Instead, a lactose-inducible promoter from *C. perfringens* was placed upstream of the *mazF* gene, which encodes an RNA interferase. Upon induction, MazF expression cleaves RNA at ACA sequences, resulting in growth arrest and cell death, which allows for the isolation of integration mutants while excluding plasmid background. The promoter hijacking technique, developed by Heap et al., allows for the creation of allelic exchange mutants without the need for counterselection by coupling the allelic exchange integration to the expression of a promoter-less antibiotic resistance marker whose integration locus is located downstream from a constitutively

expressed promoter (Heap, Ehsaan et al. 2012). An obvious drawback to promoter hijacking is that it restricts all integration and knockout events to chromosomal loci with strong promoters.

More recently, the application of CRISPR/Cas9-based editing techniques has allowed for the selective genome editing without the need for a counter-selection marker or an inducible promoter. Briefly, the CRISPR nuclease Cas9 can be targeted to a specific region on a chromosome using a synthetic single guide RNA (sgRNA). Once targeted, the Cas9 nuclease generates a double-stranded break in DNA, which leads to cell death. Thus, one can generate a chromosomal mutation through homologous recombination, and then one can screen for the deletion by selectively targeting the wild-type chromosome with the sgRNA. CRISPR/Cas9-based editing has recently been demonstrated in clostridial systems (Wang, Zhang et al. 2015, Pyne, Bruder et al. 2016) including clostridial acetogen *C. ljungdahlii*. It should be noted however, that the CRISPR/Cas9 system only facilitates DNA cutting or nicking but does not solve the serious problem of lack of an efficient system for recombination in Clostridium organisms. As was shown in these CRISPR/Cas9 reports, the efficiency is very low and comparable to previous methods as none resolves the issue of effective recombination.

1.3 Carbon fixation pathways

Six natural carbon fixation pathways are known so far, of which five are found to some extent in chemoautotrophs. The first autotrophic carbon fixation pathway, the Calvin-Benson-Bassham cycle or the reductive pentose phosphate cycle (rPP), is primarily found in plants, algae and cyanobacteria, which perform photosynthesis to power the rPP cycle. Additionally, many proteobacteria grow chemoautotrophically using the rPP pathway, including the hydrogen-oxidizing bacterium *Ralstonia eutropha* (Pohlmann, Fricke et al. 2006). The reverse tricarboxylic acid (rTCA) cycle was the second carbon fixation cycle to be proposed in 1966 (Evans, Buchanan et al. 1966). Most of the enzymes that catalyze the rTCA cycle are similar to those in the oxidative TCA cycle apart from three: an ATP-citrate lyase, a 2-oxoglutarate:ferredoxin oxidoreductase (OGOR), and a fumarate reductase. In the oxidative TCA cycle, these enzymes

catalyze energy-releasing, irreversible reactions, and therefore, separate enzymes are required for the forward and reverse directions.

The third carbon fixation pathway termed the Wood-Ljungdahl (WL) pathway, or reductive acetyl-CoA pathway, is only used for chemoautotrophic carbon fixation (Wood 1991). In the WL pathway, two molecules of carbon dioxide are directly reduced to form one molecule of acetate, in contrast to the other carbon fixation pathways that operate in a cyclical manner. The WL pathway occurs primarily in anaerobic bacteria (known as acetogens) and archaea (termed methanogens) of the phyla Firmicutes and Euarchaeota, respectively. The WLP consists of two branches: the methyl or eastern branch and the carbonyl or western branch (Ragsdale and Pierce 2008). In the methyl branch, CO_2 is reduced by two electrons to formate by formate dehydrogenase (FDH). An ATP-dependent formate-tetrahydrofolate ligase binds formate to tetrahydrofolate to form 10-formyltetrahydrofolate. Subsequent reduction and dehydration reactions consume an additional four electrons to reduce the 10-formyltetrahydrofolate to 5-methyltetrahydrofolate. In the carbonyl branch, a bifunctional CO dehydrogenase/acetyl-CoA synthase (CODH/ACS) reduces CO_2 to CO, which is condensed with the methyl-group from 5-methyltetrahydrofolate and coenzyme-A to form acetyl-CoA. The WL pathway operates strictly under anaerobic conditions due to its use of ferredoxins to drive reduction reactions and the extreme oxygen sensitivity of its main enzyme – the CO dehydrogenase/acetyl-CoA synthase.

Since 2002, three additional carbon fixation pathways have been elucidated. The first of these to be resolved was the 3-hydroxypropionate (3HP) cycle, a carbon fixation pathway that has been found exclusively in non-sulfur bacteria of the Chloroflexaceae family (Herter, Fuchs et al. 2002). The 3-hydroxypropionate/4-hydroxybutyrate (3HP/4HB) cycle and the dicarboxylate/4-hydroxybutyrate (DC/4HB) cycle are the fifth and sixth elucidated carbon fixation pathways, respectively (Berg, Kockelkorn et al. 2007, Huber, Gallenberger et al. 2008) . The 3HP/4HB pathway was found initially in the hyperthermophilic, aerobic archaeon *Metallosphaera sedula*, and genes of this pathway have since been identified in other aerobic archaea. The 3HP/4HB pathway has many metabolite intermediates in common with the 3HP

bicycle; however, differing enzymology between the two pathways suggests that they evolved independently (Alber, Olinger et al. 2006). The DC/4HB pathway is the most recently discovered carbon fixation pathway and is found in anaerobic archaea of the Thermoproteales and Desulfurococcales orders. The metabolic route of the DC/4HB pathway is very similar to that of the 3HP/4HB pathway and the rTCA cycle; however, the oxygen sensitivity of the enzymes in the DC/4HB cycle relegate it to strictly anaerobic environments.

1.3.1 Acetogens and the WL Pathway

Acetogens are defined as obligately anaerobic bacteria that can use the Wood-Ljungdahl pathway as the predominant mechanism for the reductive synthesis of acetyl-CoA and biomass from CO_2 (Drake 1994). Acetogens are a diverse group of bacteria. More than 100 species have been isolated so far across 22 genera, though most are in the class Clostridia and more specifically the *Clostridium* or *Acetobacterium* genera.

Acetogenesis was first reported in 1936 when the Dutch microbiologist K. T. Wieringa found that *C. aceticum* produced acetate through the reaction shown in Eq. 1.

$$4\ H_2 + 2\ CO_2 \rightarrow CH_3COOH + 2\ H_2O \qquad \text{(Eq. 1)}$$

Unfortunately, *C. aceticum* was lost and not recovered until the early 1980s. The model acetogen *Moorella thermoacetica* (formerly *C. thermoaceticum*; class Clostridia) was discovered in 1942 by Fontaine *et al.* Unlike *C. aceticum, M. thermoacetica* grew thermophilically and to high-densities, which gave biochemists large quantities of thermostable enzymes necessary to study the underlying enzymology of the WL pathway. The enzymes of *M. thermoacetica* were the subject of studies that elucidated the discovery of the tungsten-containing formate dehydrogenase (Ljungdahl and Andreesen 1975), the resolution of the tetrahydrofolate pathway (Ljungdahl 1986), the discovery and purification of the CO dehydrogenase (Ragsdale, Clark et al. 1983), and the mechanism of acetyl-CoA synthesis by the ACS (Ragsdale 1991).

Interestingly, it was not known until 1990 that *M. thermoacetica* could grow chemolithoautotrophically, i.e., in a defined medium with H_2/CO_2 or CO/CO_2 as a sole carbon sources (Daniel, Hsu et al. 1990).

Due to the unique 1-C metabolism of the WL pathway and the use of CO_2 as a terminal electron acceptor, acetogens can grow on a vast array of carbon sources beyond monosaccharides and disaccharides (i.e., glucose, fructose, and cellobiose) including but not limited to CO, H_2/CO_2, methanol, ethanol, glycerol, acetoin, formate, pyruvate, glyoxylate, and methoxylated aromatics(Drake 1994). Additionally, several acetogenic microbes have been shown to uptake electrons directly from an electrode for use in CO_2 fixation (Nevin, Hensley et al. 2011). The most common fermentative product of acetogenesis is acetate, for which the pathway is named. Additionally, lactate, ethanol (Phillips, Klasson et al. 1993), butyrate (Shen, Shieh et al. 1999), butanol (Kerby, Niemczura et al. 1983), hexanoate (Ramió-Pujol, Ganigué et al. 2015), hexanol (Ramió-Pujol, Ganigué et al. 2015), and 2,3-butanediol (Köpke, Mihalcea et al. 2011) have been observed in some acetogenic species.

The available tools for clostridial acetogens are far more limited and have only been demonstrated in a small subset of strains including *C. ljungdahlii* (Köpke, Held et al. 2010, Leang, Ueki et al. 2013, Tremblay, Zhang et al. 2013), *C. autoethanogenum* (Simpson, Köpke et al. 2011, Köpke, Simpson et al. 2012), *C. aceticum* (Lederle 2010), *A. woodii* (Strätz, Sauer et al. 1994, Straub, Demler et al. 2014), and *M. thermoacetica*. The most advanced genetic tools for an acetogen have been (Kita, Iwasaki et al. 2013) developed for *C. ljungdahlii*. The first acetogenic transformation was demonstrated in *C. ljungdahlii*, which was engineered with the butanol production pathway from *C. acetobutylicum* (Köpke, Held et al. 2010); however, no net butanol was produced under autotrophic conditions and very little (<10 mM) was produced under heterotrophic conditions due to competing reactions and unfavorable energetics. Recently the Lovley lab developed a robust electroporation protocol for introducing replicating plasmids and suicide vectors into *C. ljungdahlii* (Leang, Ueki et al. 2013). They demonstrated the function of four unique replicative origins for plasmid propagation, and they deleted several genes in the

chromosome via double-crossover homologous recombination with suicide vectors. Specifically, they deleted the *adhE1* and *adhE*2 genes individually and in combination to demonstrate the ability to redirect carbon and electron flow in this organism via gene disruptions, and also to determine which gene is most responsible for ethanol production. Thus, they witnessed that *adhE1*, but not *adhE2*, diminished ethanol production, and they could partially restore the wild-type phenotype through complementation. More recently, the same lab also demonstrated the utility of a lactose-inducible gene expression system in *C. ljungdahlii* (Banerjee, Leang et al. 2014)**.** Briefly, they adapted a lactose-inducible promoter and its divergent regulator (*bgaR*) from *C. perfringens* that was previously demonstrated to maintain tight gene control in *C. perfringens* (Hartman, Liu et al. 2011). They demonstrated the ability to control gene expression with a *gusA* reporter gene, and then showed the ability to affect carbon flux and increase ethanol production by inducing the over-expression of AdhE1.

A genetic transformation system has also been developed (although not reproduced in other labs) in the thermophilic acetogen *M. thermoacetica (Kita, Iwasaki et al. 2013)*. The lactate dehydrogenase gene from *Thermoanaerobacter pseudethanolicus* was inserted into the genome, resulting in the production of 6.8 mM lactate from fructose. The development of genetic tools for *M. thermoacetica* will not only allow for the development of this organism for industrial biotechnology but will also allow for genetic manipulation of the most studied Wood-Ljungdahl pathway genes, which will lead to a more fundamental understanding of Wood-Ljungdahl pathway biochemistry.

Acetone production pathways have been engineered in several acetogens including *C. aceticum (Lederle 2010, Schiel-Bengelsdorf and Dürre 2012)* and *A. woodii (Hoffmeister, Gerdom et al. 2016)*. The pathway was also added to *C. ljungdahlii* under the expression of an inducible promoter (Banerjee, Leang et al. 2014); however, others have questioned whether the reported acetone production was in fact isopropanol (Hoffmeister, Gerdom et al. 2016), due to the presence of a secondary alcohol dehydrogenase (SADH) that has high affinity towards acetone (Köpke, Mihalcea et al. 2011, Köpke, Gerth et al. 2014). In separate work, a SADH

knockout of *C. ljungdahlii* was constructed to prevent conversion of acetone to isopropanol, and the *C. ljungdahlii* (ΔSADH) was transformed with the engineered acetone production pathway, consisting of the thiolase gene from *C. kluyveri*, the CoA-transferase gene from *C. acetobutylicum*, and the acetoacetate decarboxylase gene from *C. acetobutylicum*. Under batch fermentation, the engineered *C. ljungdahlii* strain showed a total molar yield of 82%, with acetone as the primary metabolite.

1.4 Dissertation Aims and Outline

The aim of this dissertation is to study how CO_2 fixation can be integrated with traditional fermentation pathways to achieve greater yields of biofuels and chemicals from a given amount of feedstock.

Chapter 2 describes the six naturally-occurring carbon fixation pathways and how they might be implemented in a biochemical production process. Stoichiometric and energetic models were tested and used to assess the capacity of each of these pathways with respect to the maximum biological yield that can be achieved through chemoautotrophic fermentation. The results show that while the obligately-anaerobic WL pathway is energetically constrained by the lack of an oxidative electron transport chain to generate ATP, the low ATP requirements of the WL pathway make it much more efficient than the other pathways for the fixation of CO_2 into 2-carbon molecules (i.e. acetate and ethanol). The addition of sugars can alleviate the ATP limitation of the WL pathway and allow for the production of larger chemicals, such as butanol, as well.

The concept of mixotrophic fermentation, in which carbohydrates and CO_2 simultaneously fermented, is examined in Chapters 3 and 4. Stoichiometric models of heterotrophic, autotrophic, and mixotrophic fermentation were developed to compare the maximum biological yields for butanol production under these three fermentation schemes. These models identified that yield improvements could be achieved through the use of mixotrophic fermentation; however, less reduced metabolites, such as acetone or isopropanol,

showed a greater theoretical improvement in the mixotrophic case over the heterotrophic case than highly reduced metabolites, such as butanol.

In Chapter 4, we consider the growth of the native acetogens *C. ljungdahlii*, *Eubacterium limosum*, *M. thermoacetica*, and *C. autoethanogenum* in the presence of both a carbohydrate carbon source (i.e. fructose) and gaseous carbon sources (i.e. CO_2/CO/H_2) to determine whether carbon catabolite repression (CCR) plays a major role in the regulation of WL pathway genes.

In Chapter 5, we discuss the genetic engineering of a synthetic Wood-Ljungdahl pathway in the solventogenic *C. acetobutylicum*. Merely from the perspective of genetics, this was a significant challenge that required the development and implementation of new genetic techniques in *C. acetobutylicum*, specifically the co-expression of two plasmids as well as multiple sequential integrations of heterologous DNA, neither of which have been previously demonstrated in a clostridium organism.

The results of the expression of heterologous WL pathway genes in *C. acetobutylicum* is discussed in Chapter 6, where we assess the enzyme expression levels at the protein and mRNA levels. We also consider the protein activity of the heterologously expressed ACS/CODH enzyme both *in vitro* and *in vivo*.

Chapter 2

STOICHIOMETRIC AND ENERGETIC ANALYSES OF NON-PHOTOSYNTHETIC CO_2-FIXATION PATHWAYS TO SUPPORT THE PRODUCTION OF FUELS AND CHEMICALS

2.1 The importance of substrate cost and CO_2, H_2, and CO utilization for transformative biofuel- and chemical-production technologies

The major operating expenditure – frequently > 60% of the overall production cost (NRC-NAE, (U.S.). et al. 2009) – in biofuel and chemical production from renewable or waste carbon sources is substrate and substrate-related costs. Thus, platform organisms that can flexibly utilize a broad spectrum of renewable substrates, including waste materials and gases, with minimal pretreatment offer a major competitive advantage in the development of next-generation technologies to produce biofuels and chemicals. Many factors impact the costs associated with substrates and their utilization: substrate sourcing and availability; variability in substrate composition and purity; extent of necessary pretreatment; cellular flexibility in efficient and simultaneous utilization of various substrates; and complete substrate utilization. An associated issue is that of product yield, notably the fraction of carbon from the substrate that can be recovered as products. These issues, taken together, contribute to the "true product cost," which is beyond the cost of a single type or source of carbon (biomass, waste gases, or other), and the strain-development technologies to address the impact of the true product cost, in a holistic scale, have not been given the attention they deserve.

As part of optimizing for the cost of the substrate, engineering hosts to fix CO_2 while growing on conventional organic substrates has the potential to improve fermentation efficiencies. Of course, developing technologies based on purely chemoautotrophic organisms that utilize CO_2 and other waste gases for producing chemicals and fuels is not only desirable but surely one of the most challenging technological goals. Indeed, in the last few years, there has

been a large effort to identify, study, and explore natural and engineered organisms that utilize efficiently CO_2 or other waste gases/products aiming to identify and develop platform organisms suitable for engineering synthetic or semi-synthetic pathways to produce biofuels and chemicals (Hawkins, Han et al. 2011, Li, Opgenorth et al. 2012). The US Department of Energy, through its ARPA-E Division, has funded a substantial research effort for the development of the so-called electrofuels, namely the production of biofuel molecules from CO_2 and H_2 or electrons (Hawkins, Han et al. 2011, Li, Opgenorth et al. 2012). Several groups throughout the world, are working to engineer and improve organisms towards this goal.

This chapter will focus on the analysis of non-photosynthetic prokaryotic systems/programs from the point of view of the efficiency with which they fix CO_2. Specifically, stoichiometric analysis is used to assess their ATP and reducing energy (H_2 or equivalent electrons) requirements, and subsequently their expected capabilities to produce model biofuel molecules (acetate, ethanol and butanol) if these organisms were to be engineered to do so. The goal of this analysis is to provide a useful basis for developing synthetic biology strategies towards transformative technologies for the production of biofuels and chemicals. Almost 30 years ago, similar analyses of core primary metabolic pathways (Papoutsakis 1984, Papoutsakis and Meyer 1985) set the foundation for predicting the maximal yields of several important metabolites from the microbial utilization of carbohydrates. Those early analyses led to the development of genome scale models (Edwards 1999) and the foundation for the development, more recently, of metabolic and synthetic strategies (Jones, Paredes et al. 2008, Lutke-Eversloh and Bahl 2011, Tracy, Jones et al. 2012) to generate superior strains for the production of chemicals and fuels.

2.2 Natural non-photosynthetic carbon-fixation pathways

Six natural carbon fixation pathways are known so far, of which five are found to some extent in chemoautotrophs. The first autotrophic carbon fixation pathway (Fig. 1), the Calvin-Benson-Bassham cycle or the reductive pentose phosphate cycle (rPP), was discovered in the late

1940s through the use of early ^{14}C labeling studies (Calvin and Benson 1948). The majority of organisms using the rPP pathway, including plants, algae and cyanobacteria, perform photosynthesis to power the rPP cycle, which is reflected in its relatively high cost in terms of ATP hydrolysis. Nonetheless, many proteobacteria grow chemoautotrophically using the rPP pathway, including the hydrogen-oxidizing bacterium *Ralstonia eutropha* (Pohlmann, Fricke et al. 2006).

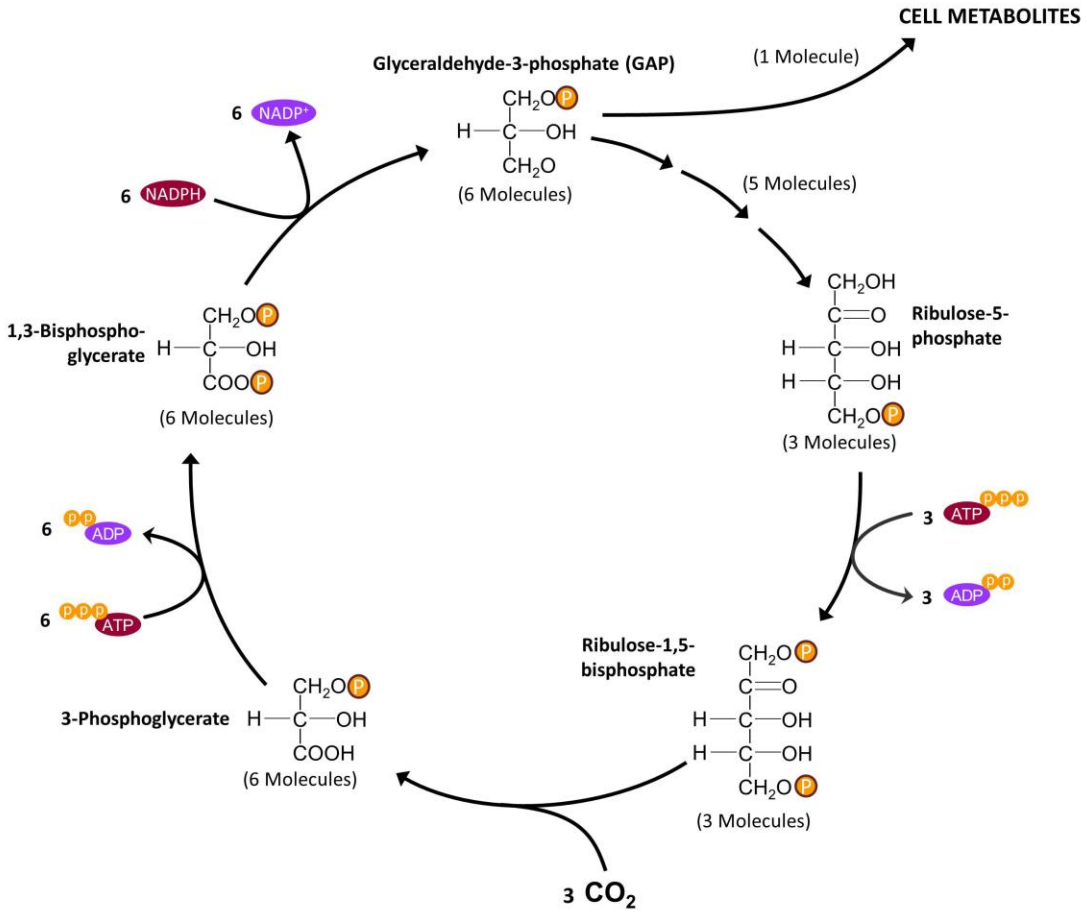

Figure 2.1: Reverse Pentose Phosphate Cycle. The rPP fixes CO_2 using the enzyme RuBP carboxylase/oxygenase (RuBisCO) which combines CO_2 with ribulose-1,5-bisphosphate. The resulting six-carbon sugar is unstable and immediately splits into two molecules of 3-phosphoglycerate. Further reduction and ATP activation steps convert the 3-phosphoglycerate to glyceraldehyde-3 phosphate that can be shuttled to regular metabolism or recycled to reform ribulose-5-phosphate.

The reverse tricarboxylic acid (rTCA) cycle (Fig. 2) was the second carbon fixation cycle to be proposed in 1966 (Evans, Buchanan et al. 1966). Most of the enzymes that catalyze the rTCA cycle are similar to those in the oxidative TCA cycle apart from three: an ATP-citrate lyase, a 2-oxoglutarate:ferredoxin oxidoreductase (OGOR), and a fumarate reductase. In the oxidative TCA cycle, these enzymes catalyze energy-releasing, irreversible reactions, and therefore, separate enzymes are required for the forward and reverse directions. Because the OGOR, the most important rTCA cycle enzyme, is somewhat oxygen sensitive, the rTCA cycle is primarily found in anaerobes/microaerobes including the anoxic phototrophic green sulfur bacteria (*Chlorobrium*) as well as many species of sulfur-reducing bacteria and archaea (Campbell, Engel et al. 2006). Interestingly, members of the phylum Aquifacae – most notably *Hydrogenobacter thermophilus* – oxidize hydrogen aerobically to drive the rTCA cycle (Arai, Kanbe et al. 2010).

The third carbon fixation pathway termed the Wood-Ljungdahl (WL) pathway, or reductive acetyl-CoA pathway (Fig. 3), is only used for chemoautotrophic carbon fixation (Wood 1991). In the WL pathway, two molecules of carbon dioxide are directly reduced to form one molecule of acetate, in contrast to the other carbon fixation pathways that operate in a cyclical manner. The WL pathway occurs primarily in anaerobic bacteria (known as acetogens) and archaea (termed methanogens) of the phyla Firmicutes and Euarchaeota, respectively. The WL pathway operates strictly under anaerobic conditions due to its use of ferredoxins to drive reduction reactions and the extreme oxygen sensitivity of its main enzyme – the CO dehydrogenase/acetyl-CoA synthase.

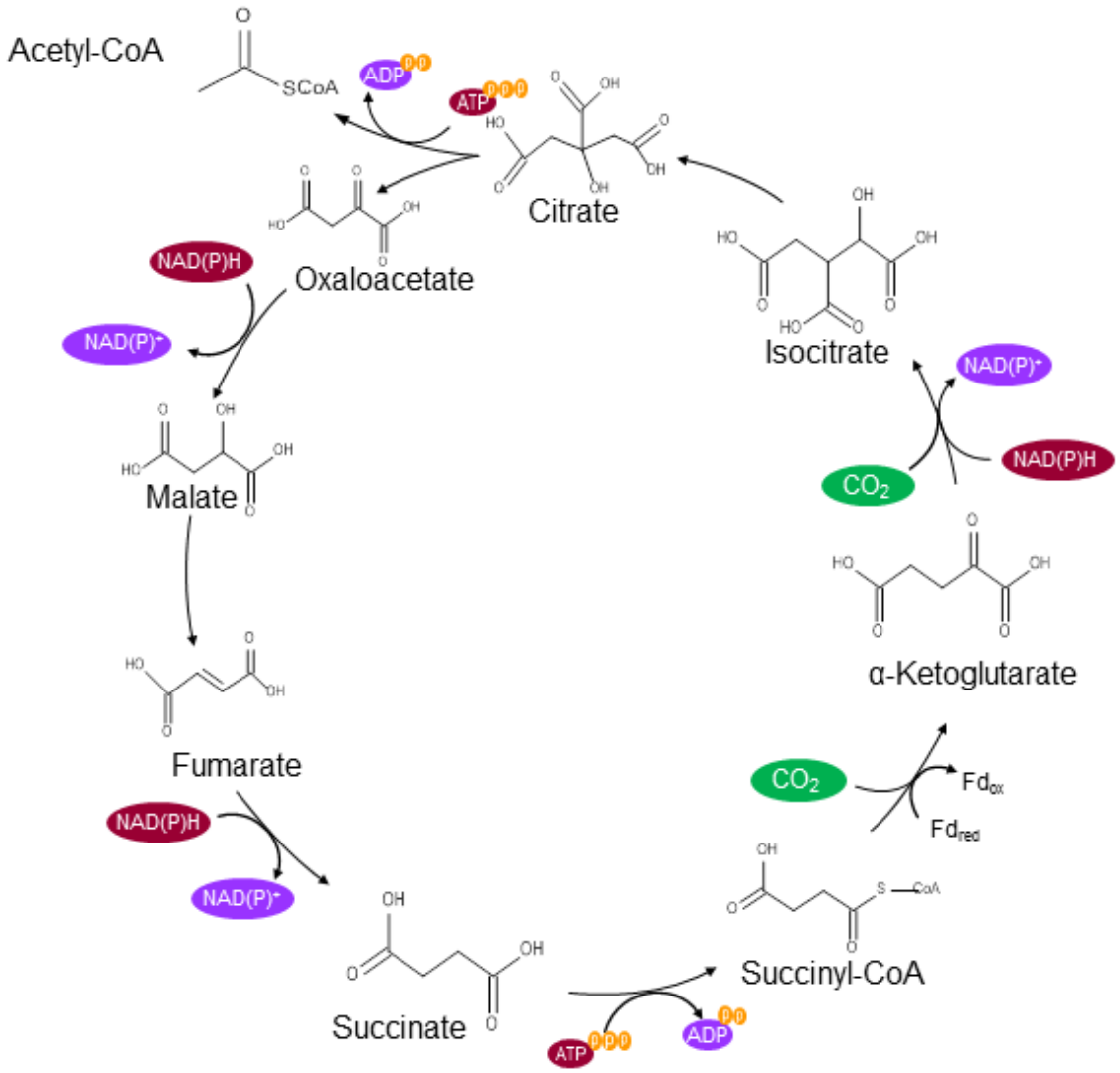

Figure 2.2: Reverse TCA Cycle. The rTCA cycle fixes CO_2 by operating in the opposite direction of the oxidative TCA cycle, using many of the same enzymes to produce acetyl-CoA from CO_2, NADH, and ATP.

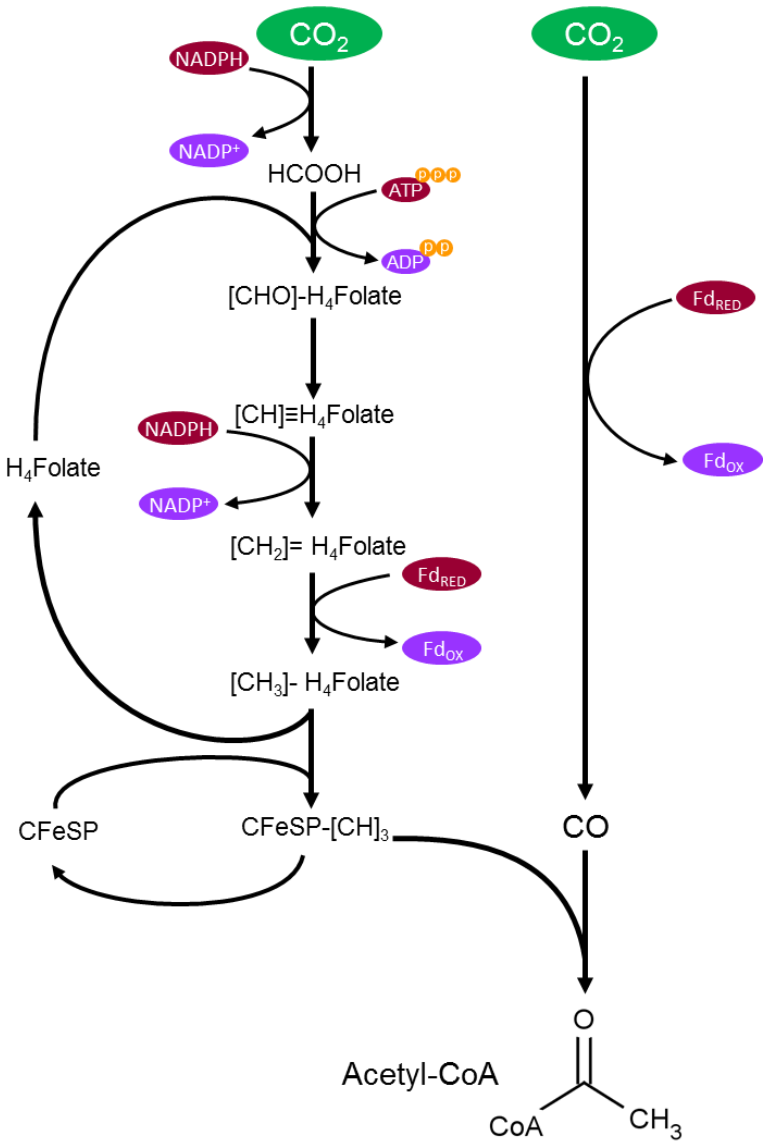

Figure 2.3: WL Pathway

In the last ten years, three additional carbon fixation pathways have been identified. The first of these to be resolved was the 3-hydroxypropionate (3HP) cycle, a carbon fixation pathway that has been found exclusively in non-sulfur bacteria of the Chloroflexaceae family (Herter, Fuchs et al. 2002). Because the 3HP cycle only occurs in photosynthetic organisms, it will not be considered in this review.

The 3-hydroxypropionate/4-hydroxybutyrate (3HP/4HB) cycle (Fig. 4) and the dicarboxylate/4-hydroxybutyrate (DC/4HB) cycle are the fifth and sixth elucidated carbon fixation pathways, respectively (Berg, Kockelkorn et al. 2007, Huber, Gallenberger et al. 2008) . The 3HP/4HB pathway was found initially in the hyperthermophilic, aerobic archaeon *Metallosphaera sedula*, and genes of this pathway have since been identified in other aerobic archaea. The 3HP/4HB pathway has many metabolite intermediates in common with the 3HP bicycle; however, differing enzymology between the two pathways suggests that they evolved independently (Alber, Olinger et al. 2006). The DC/4HB pathway is the most recently discovered carbon fixation pathway and is found in anaerobic archaea of the Thermoproteales and Desulfurococcales orders. The metabolic route of the DC/4HB pathway is very similar to that of the 3HP/4HB pathway and the rTCA cycle; however, the oxygen sensitivity of the enzymes in the DC/4HB cycle relegate it to strictly anaerobic environments. Additionally, organisms with the DC/4HB pathway require electron acceptors such as elemental sulfur (S^0) for anaerobic respiration, making the pathway non-ideal for use in industrial fuel production.

Table 2.1 presents a summary of the ATP and NAD(P)H (or equivalent) requirements as well as the number of enzymatic steps involved in the four non-photosynthetic, non-sulfur-reducing carbon fixation pathways. When comparing these pathways, many features stand out. First, the ATP efficiencies of the rTCA cycle and WL pathway are much higher than the other reaction pathways, perhaps reflecting their existence in highly reduced environments in which carbon reduction is more favorable. The net consumption of reducing equivalents, however, is equal across the pathways since electrons are conserved. The number of enzymes in each

pathway can be used as a first metric as to how straightforward or difficult each pathway would be to metabolically engineer or reconstruct in a non-native organism using synthetic-biology.

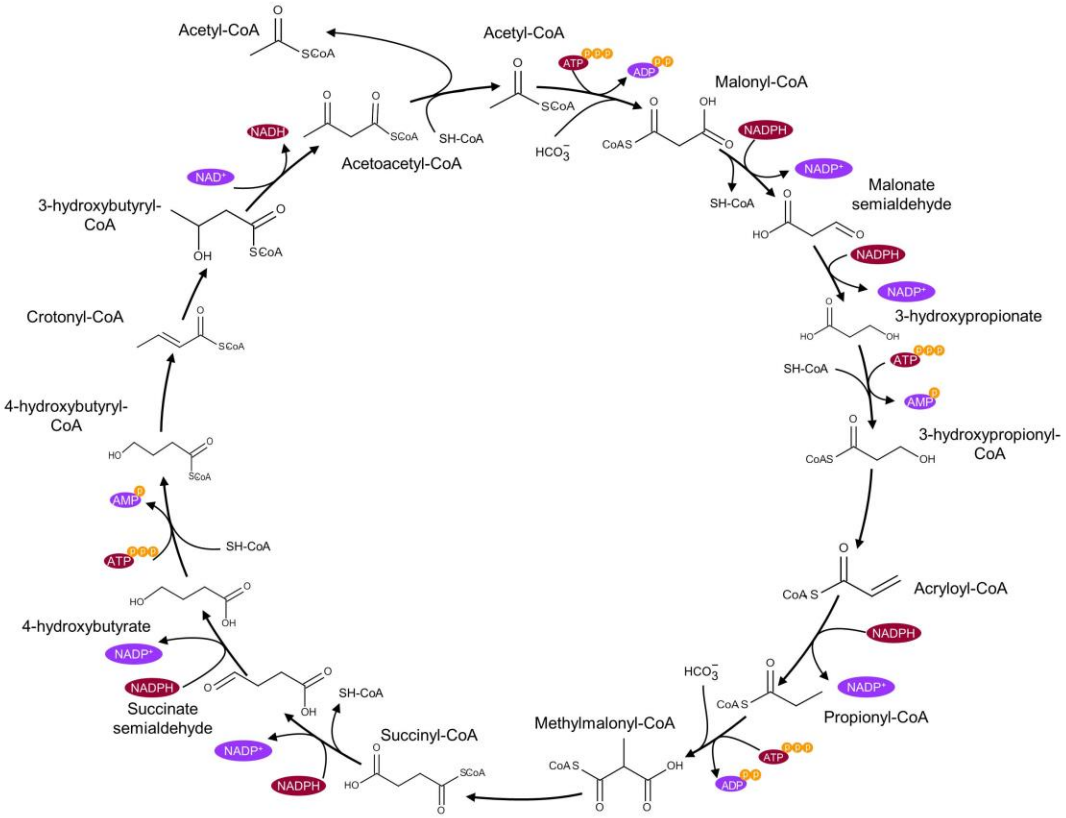

Figure 2.4: 3-Hydroxypropionate/4-Hydroxybutyrate Cycle

Table 2.1: Energetic requirements of carbon fixation for acetyl-CoA production

Pathway	Energetic and Electron Requirements to Fix One Mole of Acetyl-CoA			
	Mol NAD(P)H Equivalent	Mol ATP	Total Mol H_2 (for reducing equivalents and ATP)	Number of Enzymes
Reductive Pentose Phosphate	4	7	7.5	10
WL Pathway	4	< 1*	> 4†	8
3HP/4HB Cycle	4	6	7	13
Reductive TCA Cycle	4	2	5	8

*****Though one molecule of ATP is consumed in the WL pathway, some energy is conserved in the form of membrane gradients for ATP production. Thus, not quite one mole of ATP is consumed for every mole of acetyl-CoA that is produced. † In organisms with the WL pathway, H_2 cannot be directly oxidized to form additional ATP as shown in Eq. 2. Instead, a fermentation product (i.e., acetate or ethanol) is needed to recover the ATP deficit from acetyl-CoA production.

In 2011, Boyle and Morgan compared the thermodynamic efficiencies of all six carbon fixation pathways for the production of biomass using flux balance analysis and thermodynamic calculations targeting the maximum biomass production as the objective (Boyle and Morgan 2011). The study found that the photosynthetic pathways (i.e., the rPP pathway, the rTCA cycle, and the 3HP bicycle) are less efficient at producing biomass than the chemolithoautotrophic pathways; however, when one includes the energetic cost of hydrogen production in the analysis, the photoautotrophs come out ahead. Boyle and Morgan compared carbon fixation pathways by their efficiency in producing biomass. In microbial systems, unlike plants, biomass is not the intended product of industrial microbial carbon fixation. Instead, it is more logical to focus on the analysis of microbial carbon fixation for the formation of biofuels and biofuel precursors, such as lower alcohols and fatty acids. This is the focus of our analysis here.

2.3 Natural versus synthetic carbon-fixation pathways

In contemplating the introduction of a complete carbon fixation pathway into a prokaryotic host, there are two general options: introduce either a natural fixation pathway or a

synthetic one. Natural pathways seem advantageous because millions of years of evolution have engineered these pathways for fast kinetics and thermodynamic efficiency. On the other hand, natural pathways have been optimized for the survival and reproduction of their organisms, whereas a synthetic carbon fixation pathway could be engineered to accomplish other goals, namely fuel and chemical production.

In 2010, Bar-Even *et al.* developed an algorithm for finding synthetic carbon fixation cycles that are both thermodynamically feasible and kinetically fast (Milo, Bar-Even et al. 2010). To complete their analysis, the group collected a wide array of enzyme data, determined many potential reaction pathways, and analyzed these pathways for thermodynamic feasibility, energy efficiency (i.e., ATP and NAD(P)H usage), superior kinetics, and topological compatibility (i.e., sets of enzymes that operate effectively under similar conditions). Ultimately, they found a number of potential pathways that use the favorable carboxylating enzyme PEP carboxylase. Additionally, because the group was mostly considering agricultural applications, oxidative photosynthesis was used to model ATP and NADPH regeneration. This had two effects for the final pathway design. First, they could not compare the ferredoxin-oxidoreductase containing pathways because of oxygen sensitivity and a lack of kinetic data. Second, they placed very little emphasis on ATP and NADPH costs for their predicted cycles, as these cofactors are rarely limiting under light-saturated conditions. Obviously, neither of these conditions holds during non-photosynthetic carbon fixation, which is often ATP limited and depends on ferredoxin-oxidoreductase enzymes for all natural fixation pathways other than the rPP pathway and the 3-HP cycle. Though creating a synthetic pathway *in silico* may lead to a more efficient pathway, it will be important to tailor future models to microbial fuel production rather than photosynthesis.

2.4 Electron sources for non-photosynthetic carbon reduction

Without photosynthesis as a source of ATP and reducing equivalents, a reduced, energy-rich chemical species is necessary to drive the reduction of CO_2 and the formation of carbon-carbon bonds. Microbes in their natural settings have found numerous ways to extract electrons

and energy from non-biological, non-photosynthetic sources, including molecular hydrogen, reduced carbon (CO, formate, methanol), sulfur (H_2S, S), and nitrogen (NH_3) compounds (Berg, Kockelkorn et al. 2010). The electron source for pathway fermentation depends heavily on the practicality, cost and safety of a substrate. For instance, H_2 and CO have both been targeted as ideal electron sources for the production of biofuel from anaerobic acetogens, a subject of several recent reviews (Köpke, Mihalcea et al. 2011, Schiel-Bengelsdorf and Dürre 2012). However, the use of either H_2 or CO in aerobic fermentations is curtailed by flammability risks at a wide range of gas concentrations.

Additionally, a few acetogenic microbes have been shown to uptake electrons directly from an electrode for use in CO_2 fixation (Nevin, Hensley et al. 2011). This process, called electrosynthesis, is still in its nascent stages, with only a few confirmed examples of microbes accepting electrons from an anode. All of the organisms capable of producing acetate from CO_2 and electrons use the WL pathway for fixation; however, it may be possible to engineer these electron accepting organisms to produce biomolecules other than acetate.

Recent efforts by Li et al. demonstrate an alternative approach to microbial electrosynthesis, in which electrons are used indirectly to fix CO_2 (Li, Opgenorth et al. 2012). Inside a single reaction vessel, formate is continuously produced via electrolysis and then immediately consumed by Ralstonia eutropha H16 to ensure that minimal amounts of formate are decomposed at the anode. The NADH that Ralstonia generates from formate oxidation is used to fix CO_2 via the rPP pathway and to ultimately produce 3-methyl-1-butanol and isobutanol through engineered heterologous pathways.

2.5 Methodology for analysis

2.5.1 Stoichiometric modeling

To better understand the efficiency and efficacy of the non-photosynthetic carbon fixation pathways, we employ a stoichiometric analysis of the natural carbon fixation pathways

to identify their capacities for biofuel and biochemical production under autotrophic and mixotrophic fermentation conditions. Acetate, ethanol and butanol were chosen as target chemicals because of their growing importance to the renewable chemical and fuel market as well as to highlight the differing metabolic requirements of producing alcohols versus acids. Molecular H_2 was chosen as a source of reduction energy as it is common to all chemoautotrophic carbon fixation pathways and can readily be obtained from many sources (hydrolysis, gasification, etc.); however, similar results can be obtained from the use of another electron source, such as CO, formate, or methanol. For the mixotrophic analysis, glucose, metabolized via the Embden-Meyerhof-Parnas pathway of glycolysis, was used as a secondary carbon and energy source alongside CO_2 and H_2.

2.5.2 Common starting metabolite

As previously discussed, the computational analysis by Bar-Even *et al.* on the thermodynamics and kinetics of the six natural carbon fixation pathways as well as potential synthetic pathways for carbon fixation is tailored towards photosynthetic carbon fixation, in which ATP limitation does not play a large role (Bar-Even, Noor et al. 2010). When considering non-photosynthetic fermentation of H_2 and CO_2, the NAD(P)H and ATP efficiency of a pathway may have a drastic impact on the economics and feasibility of process scale-up (i.e., how much additional hydrogen will be needed to satisfy a cell's energy requirements). Additionally, Boyle *et al.* and Bar-Even *et al.* maximize as their objective functions biomass production and glyceraldehyde-3-phosphate (GAP) production, respectively (Bar-Even, Noor et al. 2010, Boyle and Morgan 2011). While these objective functions are indeed excellent choices for the analysis of pathways geared towards biomass production, when considering the energetics of non-photosynthetic carbon fixation for the direct production of biochemicals, it is apt to choose acetyl-CoA or pyruvate rather than GAP as a molecule for comparison, as they are common intermediates for the production of many biofuels and biochemicals (e.g., ethanol, acetate, butanol, etc.). Moreover, the use of GAP as a common metabolite for comparison, rather than

acetyl-CoA, places a penalty – in the form of ATP lost to gluconeogenesis – on those carbon fixation pathways that have either pyruvate or acetyl-CoA as a product, which include all of the natural carbon fixation pathways aside from the rPP pathway. Therefore, we use acetyl-CoA as a basis for assessing H_2 consumption during fermentation. The equation representing acetyl-CoA production by each the analyzed chemoautotrophic pathways is shown below with NAD(P)H representing a generic reducing equivalent. These equations can be derived from Figures 1-4.

rPP Cycle: 2 CO_2 + 7 ATP + 4 NAD(P)H → Acetyl-CoA (Eq. 1)

rTCA Cycle: 2 CO_2 + 2 ATP + 4 NAD(P)H → Acetyl-CoA (Eq. 2)

WL Pathway: 2 CO_2 + (1-n) ATP + 4 NAD(P)H → Acetyl-CoA (Eq. 3)

3HP/4HB Cycle: 2 CO_2 + 6 ATP + 4 NAD(P)H → Acetyl-CoA (Eq. 4)

As discussed in detail below, the coefficient *n* in WL pathway stoichiometry represents ATP generation deriving from membrane ion gradients

2.5.3 Biomass production

A model carbon-mole for cell biomass was calculated as $CH_{2.08}O_{0.53}N_{0.24}$ (M_{cell} = 26 g/mol) using previously described methods (Papoutsakis 1984). The precise composition of biomass has a small impact on the final calculations since we assume that only a small fraction of the carbon goes into biomass (see below). Therefore, even a 10-15% variation in the biomass composition will not alter our conclusions. The equation for biomass production from acetyl-CoA is summarized in Eq. 5.

1/2 Acetyl-CoA + (Mcell/YATP) * ATP + 0.3 NAD(P)H → C-mol Biomass (Eq. 5)

The NAD(P)H requirement of biomass production is calculated from the degree of reduction of acetyl-CoA (γ = 4) and of the biomass (γ =4.3), and the ATP requirement is calculated based on M_{cell} and the ATP yield coefficient, Y_{ATP} (g cells/mol ATP). In previous analysis of ATP conservation in acetogens (Tracy, Jones et al. 2012), an average ATP yield coefficient for anaerobic growth of 10.7 g cells/mol was used (Payne 1970). However, to better tailor these calculations to chemoautotrophs, the maximum Y_{ATP} for autotrophic growth on CO_2 of 6.5 g

biomass/mol (Thauer, Kaster et al. 2008) was used, a number which is consistent with other autotrophic Y_{ATP} calculations (Rose 1971, Fuchs 1986). We also assumed that 5% of carbon flux is directed to the production of biomass and 95% to products (Papoutsakis 1984). Again, this figure is consistent with many metabolite producing fermentations, including the acetogens' autotrophic anaerobic fermentations (Daniel, Hsu et al. 1990, Annous, Shieh et al. 1996).

2.5.4 ATP generation

As alluded to previously, one major consideration for non-photosynthetic microbial carbon fixation is the organism's method of ATP generation. While photosynthetic organisms are able to fulfill their ATP requirements through photophosphorylation, the generation of ATP for carbon fixation in chemoautotrophs varies from organism to organism. For the purposes of our analysis, we will exclude the 3-HP cycle, which is found exclusively in phototrophs, and the archaeal DC/4HB pathway, which requires elemental sulfur as an electron acceptor, making it an impractical pathway for use in a bioreactor.

The so-called Knallgas-bacteria such as *Ralstonia eutropha* and *Hydrogenobacter thermophiles*, which use the rPP pathway and the rTCA cycle for CO_2 fixation, respectively, oxidize H_2 and NADH through electron transport chains with O_2 as a terminal electron acceptor and use the resulting H^+ gradient to produce ATP (Pohlmann, Fricke et al. 2006, Hugler, Huber et al. 2007). Similarly, the archaeon *Metallosphaera sedula* synthesizes ATP for carbon fixation in the 3HP/4HB pathway by oxidizing hydrogen (Berg, Kockelkorn et al. 2007); however, the precise details of electron transport and ATP synthesis in *M. sedula* are still being studied (Auernik and Kelly 2008). Despite lingering questions regarding the mechanics and efficiency of oxidative phosphorylation in these three aerobic/microaerobic carbon fixation pathways, for the purpose of modeling ATP generation and consumption in a bioreactor, we will model the production of reducing equivalents from hydrogen and ATP generation through the electron transport chain as Eq. 6 and Eq. 7, respectively, below.

$$\text{Hydrogenase Reaction: } H_2 + NAD(P)+ \leftrightarrow NAD(P)H + H^+ \qquad \text{(Eq. 6)}$$

Electron Transport Chain: $1/2\ O_2 + NAD(P)H + H^+ \rightarrow (P/O) * ATP + H_2O$ (Eq. 7)

The P/O ratio, which can range from 1-3, is assumed to be 2 for the purpose of these calculations. In these equations NAD(P)H is used only to indicate a generic electron carrier, and it could be replaced with other electron carriers, including ferredoxin, NADH, and FAD.

In contrast to chemoautotrophs that use aerobic respiration, organisms that fix carbon with the WL pathway rely on oxygen sensitive enzymes for carbon fixation and, therefore, cannot use oxidative phosphorylation for the production of ATP. Therefore, autotrophic growth of acetogens and methanogens– the terms for bacteria and archaea, respectively, that use the WL pathway for carbon fixation – depends on the low ATP requirement of the WL pathway as well as the ability of acetogens and methanogens to conserve energy through the formation of membrane gradients. The mechanics of energy conservation in acetogens and methanogens has been reviewed elsewhere (Müller 2003, Thauer, Kaster et al. 2008). The WL pathway generates no net ATP from substrate-level phosphorylation. One molecule of ATP is formed in the conversion of acetyl-CoA to acetate but one molecule of ATP is consumed to form 10-formyltetrahydrofolate. Therefore, to grow as chemolithoautotrophs, acetogens must couple reactions within the WL pathway to the generation of transmembrane ion gradients, from which gradient-driven phosphorylation produces ATP. Two general mechanisms for gradient driven phosphorylation have been proposed (Müller 2003). First, a proton-gradient is generated by membrane-bound Rnf (which originally stood for Rhodobacter nitrogen fixation) complexes – as is the case for *C. ljungdahlii* (Köpke, Held et al. 2010) – or cytochromes, which are used by *M. thermoacetica* and *M. thermoautotrophica* (Das, Hugenholtz et al. 1989). Based on thermodynamic calculations, the reduction of 5,10-methylenetetrahydrofolate to 5-methyltetrahydrofolate has been proposed as the reaction that is coupled to proton gradient formation (Wohlfarth and Diekert 1991). Once a gradient is formed, a H+ F1F0 ATP synthase complex. The second proposed mechanism involves ATP generation through a Na+ gradient, which is how energy is conserved by the acetogen, Acetobacterium woodii (Müller, Schmidt et al. 2009). The thermodynamics of the WL-pathway overall reaction suggest that 1-2 mole

ATP/mole acetate could be formed when growing under H_2/CO_2 (ΔG = -95 kJ/mol) and 2-3 mol ATP/mol acetate could be formed when consuming CO alone (ΔG = -175 kJ/mol) (Phillips, Clausen et al. 1994). The amount of ATP generated from energy conservation pathways can be estimated using experimental data by dividing the WL pathway into three sub-reactions: Eq. 8) the ATP-dependent formation of acetyl-CoA from CO_2 and H_2, from which an unknown amount of ATP, represented by the coefficient n, is conserved using membrane gradients; Eq. 9) the formation of acetate from acetyl-CoA, regenerating ATP; Eq. 10) the creation of cellular material from acetyl-CoA and ATP via anabolism.

$$2\ CO_2 + 4\ H_2 + ATP \rightarrow \text{Acetyl-CoA} + 2\ H_2O + n\ ATP \qquad \text{(Eq. 8)}$$

$$\text{Acetyl-CoA} \rightarrow ATP + \text{Acetate} \qquad \text{(Eq. 9)}$$

$$\tfrac{1}{2}\ \text{Acetyl-CoA} + M_{cell}/Y_{ATP} * ATP \rightarrow \text{Cell } (CH_{2.08}O_{0.53}N_{0.24}) \qquad \text{(Eq. 10)}$$

The biomass molecular formula, $CH_{2.08}O_{0.53}N_{0.24}$ was used to calculate the molecular mass for Eq. 3 ($M_{cell} = 26.0 \frac{g\ cell}{C-mol\ cells}$). The dimensionless coefficient, $\frac{M_{cell}}{Y_{ATP}}$, was calculated using the average ATP yield (Y_{ATP} = 10.7 $\frac{g\ cell}{mol\ ATP}$). Combining Eqns. 8-10 after multiplying them by coefficients a, b, and c, respectively, yields:

$$2a\ CO_2 + 4a\ H_2 + (b+c/2)\ \text{Acetyl-CoA} + (a+c*(M_{cell}/Y_{ATP}))*ATP \rightarrow a*\text{Acetyl-CoA} + 2a*H_2O + (a*n+b)*ATP + b*\text{Acetate} + c*\text{Cell } (CH_{2.08}O_{0.53}N_{0.24}) \qquad \text{(Eq. 11)}$$

For no accumulation of acetyl-CoA and ATP (Papoutsakis 1984), one can calculate the coefficient n (Eq.12 and Table 2.2), the amount of ATP conserved via membrane gradients, from published cell yields for growth on H_2 and CO, $Y_{H2}\left(\frac{g\ cells}{mol\ H_2}\right)$ and $Y_{CO}\left(\frac{g\ cells}{mol\ CO}\right)$.

$$n = 2 * \frac{Y_{H_2}}{M_{cell}} + 4 * \frac{Y_{H_2}}{Y_{ATP}} = 2 * \frac{Y_{CO}}{M_{cell}} + 4 * \frac{Y_{CO}}{Y_{ATP}} \qquad \text{(Eq. 12)}$$

Table 2.2. Calculated ATP conservation coefficients derived from biomass yields

	Literature Values		Calculated ATP Conservation Coefficient (n)	
	Y_{H2}, $\frac{g\ cells}{mol\ H_2}$	Y_{CO}, $\frac{g\ cells}{mol\ CO}$	CO_2/H_2 growth	CO growth
*Acetobacterium woodii**	0.68		0.319	
*A. carbinolicum**	0.675		0.317	
*A. malicum**	1.17		0.549	
*A. kivui**	0.91		0.427	
*AOR**	0.28		0.131	
*Butyribacterium methylotrophicum**	1.7	3	0.797	1.407
C. ljungdahlii+	0.373	1.378	0.175	0.646
*M. thermoacetica**	0.46	1.28	0.216	0.6
*M. thermoautotrophica**	0.82	2.53	0.385	1.187
*Sporomusa termitid a**	0.5		0.235	

+ (Phillips, Clausen et al. 1994)
* (Daniel, Hsu et al. 1990)

For every case in which both sets of data were available, acetogen growth on CO alone gives a higher biomass/ATP yield than growth on CO_2/H_2.

2.5.5 Metabolite Production

We consider acetate, ethanol, butanol, butyrate and 2,3-butanediol (we include the last two for follow-up analysis on the capabilities of the WL pathway only) as potential pathway products that are produced from acetyl-CoA with the stoichiometries shown in Eq. 13-17, respectively.

Acetate: Acetyl-CoA → ATP + Acetate (Eq. 13)

Ethanol: Acetyl-CoA + 2 NAD(P)H → Ethanol (Eq. 14)

Butanol: 2 Acetyl-CoA + 4 NAD(P)H → Butanol (Eq. 15)

Butyrate: 2 Acetyl-CoA + 2 NAD(P)H → ATP + Butyrate (Eq. 16)

2,3-Butanediol: 2 Acetyl-CoA + 3 NAD(P)H → 2,3-Butanediol (Eq. 17)

Additionally, Köpke et al. (Köpke, Held et al. 2010) in their PNAS paper argue that the reduction of non-activated acetate by an aldehyde oxidoreductase (AOR) (Eq. 18), reducing acetate to

acetaldehyde without an ATP requirement. The acetaldehyde is further reduced to ethanol via an alcohol dehydrogenase reaction (Eq. 19) may be a method of ATP conservation for acetogenic ethanol production. The carboxylic reductase activity has been observed in whole cell experiments for a number of substrates (Simon, White et al. 1987) and in a number of acetogens (White and Simon 1992).

$$\text{AOR Acetaldehyde: Acetate} + Fd_{red} \rightarrow \text{Acetaldehyde} + Fd_{ox} \quad \text{(Eq. 18)}$$

$$\text{Alcohol Dehydrogenase: Acetaldehyde} + NAD(P)H \rightarrow \text{Ethanol} \quad \text{(Eq. 19)}$$

The AOR reaction was only included in the stoichiometric model of the WL pathway because the other pathways were modeled to use oxidative phosphorylation for ATP generation, and the AOR enzyme is highly sensitive to oxygen (Huber, Caldeira et al. 1994).

2.6 Results

2.6.1 Autotrophic ethanol and acetate production

Stoichiometric calculations for autotrophic acetate production are summarized in Table 2.3 A. Yields were calculated for maximum acetate production from 100 moles of CO_2 and also for production from 100 moles of H_2. A comparison of the pathways based on the most expensive substrate (H_2 or equivalent electrons) shows that the WL pathway is able to produce the most acetate (23.6 mol/100 mol H_2), followed by the rTCA cycle (20.0 mol/100 mol H_2), the 3HP/4HB cycle (14.1 mol/100 mol H_2), and the rPP pathway (13.1 mol/100 mol H_2). The results for autotrophic ethanol production (Table 2.3 B) follow the same trend as those for acetate, with the WL pathway showing the highest potential ethanol yield (16.0 mol EtOH/100 mol H_2) followed by the rTCA cycle, the 3HP/4HB, and the rPP pathway, in that order.

The maximum potential autotrophic acetate and ethanol yields for the four non-photosynthetic, non-sulfur pathways are a direct reflection of the ATP efficiency for each pathway. The WL pathway, which uses < 1 mole ATP for every two moles of CO_2 fixed to form acetyl-CoA, is able to produce the largest amount of acetate from the least amount of H_2 since no

H_2 is needed for ATP generation beyond what ATP is conserved during carbon fixation by transmembrane ion gradients (Schiel-Bengelsdorf and Dürre 2012, Tracy, Jones et al. 2012). The three pathways that are able to generate ATP using aerobic metabolism, however, are also less ATP efficient (Table 2.1) and must oxidize reducing equivalents to fulfill the energy requirements of carbon fixation. The rTCA cycle is the most ATP-efficient of the aerobic fixation pathways and, thus, achieves acetate and ethanol yields similar to those for the WL pathway. In contrast, the rPP and 3HP/4HB cycles oxidize 35-44% of the total H_2 for the production of ATP rather than for CO_2 reduction and product formation, making them less efficient, based on this analysis, when compared to the rTCA cycle or the WL pathway.

It is important to note that the inclusion of the AOR reaction (Eq. 18) in the WL pathway model was integral for autotrophic ethanol production. If the stoichiometric model only allowed for the production of ethanol from acetyl-CoA rather than from acetate directly, the WL pathway would be severely ATP limited and would be able to produce only limited quantities of ethanol. Under ATP-limited conditions the production of ethanol from acetyl-CoA using the alcohol/aldehyde dehydrogenase has a high ethanol- formation cost, since acetyl-CoA could also be used for the production of ATP through the formation of acetate. These energy considerations are consistent with the fact that all sequenced acetogens that produce ethanol (e.g., *C. ljungdahlii*, *C. carboxidivorans*) have annotated genes encoding AOR. One would suspect that this is the case for all acetogens currently engaged in industrial processes aiming to produce ethanol from waste gases (Köpke, Mihalcea et al. 2011).

Table 2.3: Stoichiometric calculations for the maximum potential production of acetate and ethanol

A	**Maximum Acetate Production** (mol/100 mol CO_2)				(mol/100 mol H_2)			
	WL	rPP	rTCA	3HP/4HB	WL	rPP	rTCA	3HP/4HB
ATP	1.0	0.0	0.0	0.0	0.5	0.0	0.0	0.0
ATP from Oxidative ETC	N/A	322.5	72.5	272.5	N/A	88.9	30.5	80.7
Cell (C-mole)	5.0	5.0	5.0	5.0	2.5	1.4	2.1	1.5
Butanol	--	--	--	--	--	--	--	--
Acetate	47.5	47.5	47.5	47.5	**23.6**	**13.1**	**20.0**	**14.1**
Ethanol	--	--	--	--	--	--	--	--
CO_2	-100.0	-100.0	-100.0	-100.0	-49.6	-27.6	-42.1	-29.6
H_2	**-201.5**	**-362.8**	**-237.7**	**-337.8**	-100.0	-100.0	-100.0	-100.0
B	**Maximum Ethanol Production** (mol/100 mol CO_2)				(mol/100 mol H_2)			
	WL	rPP	rTCA	3HP/4HB	WL	rPP	rTCA	3HP/4HB
ATP	1.0	0.0	0.0	0.0	0.3	0.0	0.0	0.0
ATP from Oxidative ETC	N/A	370.0	120.0	320.0	N/A	76.8	33.7	70.1
Cell (C-mole)	5.0	5.0	5.0	5.0	1.7	1.0	1.4	1.1
Butanol	--	--	--	--	--	--	--	--
Acetate	--	--	--	--	--	--	--	--
Ethanol	47.5	47.5	47.5	47.5	**16.0**	**9.9**	**13.3**	**10.4**
CO_2	-100.0	-100.0	-100.0	-100.0	-33.7	-20.8	-28.1	-21.9
H_2	**-296.5**	**-481.5**	**-356.5**	**-456.5**	-100.0	-100.0	-100.0	-100.0

2.6.2 Autotrophic butanol production

The calculated estimates for maximum autotrophic butanol production (Table 2.4 A) show that the rTCA cycle is capable of the highest butanol yield on H_2 (6.7 mol butanol/100 mol H_2) followed by the 3HP/4HB pathway (5.2 mol butanol/100 mol H_2) and the rPP pathway (4.9 mol butanol/100 mol H_2). The WL pathway calculations predict negligible butanol production under autotrophic conditions (0.2 mol butanol/100 mol H_2) due to ATP limitations. Although the production of acetate – or ethanol via the AOR reaction – results in the net production of ATP from the WL pathway, if acetyl-CoA flux is directed away from acetate and towards butyryl-CoA and butanol production, insufficient ATP will be produced to allow for continued carbon fixation, which highlights the challenge of using a strictly anaerobic carbon fixation pathway with limited means for autotrophic ATP generation. In an attempt to generate sufficient ATP for butanol production, the model predicts that the majority of carbon flux in the WL pathway will still be directed to acetate rather than to butanol. We will revisit the issue of butanol formation based on an acetogen platform, since this is an area of intense research activity in engineering acetogenic strains to produce butanol.

Table 2.4: Maximum butanol production from autotrophic and mixotrophic stoichiometric modeling

A	Maximum Autotrophic Butanol Production (mol/100 mol CO_2)				(mol/100 mol H_2)			
	WL	rPP	rTCA	3HP/4HB	WL	rPP	rTCA	3HP/4HB
ATP	0.0	0.0	0.0	0.0	0.0	0.0	0.0	0.0
ATP from Oxidative ETC	N/A	370.0	120.0	320.0	N/A	76.8	33.7	70.1
Cell	5.0	5.0	5.0	5.0	2.5	1.0	1.4	1.1
Butanol	0.5	23.8	23.8	23.8	**0.2**	**4.9**	**6.7**	**5.2**
Acetate	46.5	0.0	0.0	0.0	22.9	0.0	0.0	0.0
Ethanol	0.0	0.0	0.0	0.0	0.0	0.0	0.0	0.0
CO_2	-100.0	-100.0	-100.0	-100.0	-49.1	-20.8	-28.1	-21.9
H_2	**-203.5**	**-481.5**	**-356.5**	**-456.5**	-100.0	-100.0	-100.0	-100.0
B	Maximum Mixotrophic Butanol Production (mol/100 mol glucose + 500 mol H_2)				(mol/100 mol glucose + 800 mol H_2)			
	WL	rPP	rTCA	3HP/4HB	WL	rPP	rTCA	3HP/4HB
ATP	0.0	0.0	0.0	0.0	0.0	0.0	0.0	0.0
ATP from Oxidative ETC	N/A	316.2	58.8	313.3	N/A	543.7	154.3	523.5
Acetyl-CoA	0.0	0.0	0.0	0.0	0.0	0.0	0.0	0.0
Cell	38.9	36.1	38.3	36.1	46.2	39.3	42.5	39.4
Butanol	**133.4**	**121.6**	**131.9**	**121.7**	**134.1**	**136.5**	**152.1**	**137.3**
Acetate	2.5	0.0	0.0	0.0	71.0	0.0	0.0	0.0
Ethanol	0.0	0.0	0.0	0.0	0.0	0.0	0.0	0.0
Glucose	-100.0	-100.0	-100.0	-100.0	-100.0	-100.0	-100.0	-100.0
CO_2	22.6	77.6	34.2	77.1	-124.8	14.8	-50.9	11.4
H_2	-500.0	-500.0	-500.0	-500.0	-800.0	-800.0	-800.0	-800.0

2.6.3 Mixotrophic fermentations: the power of CO_2 fixation on improving the product yields of butanol for growth on carbohydrate substrates

In addition to providing routes towards autotrophically produced biochemicals, microbial carbon fixation pathways provide a means to improve yields for heterotrophic carbohydrate fermentations by recapturing CO_2 that is generally released during glycolysis, and/or exogenous CO_2 together with an electron source such as H_2, cathode-derived electrons, or CO. The potential mixotrophic butanol yields (Table 2.4 B) for each of the pathways were calculated for the fermentation of 100 moles of glucose supplemented with 500 moles of H_2 for the first case and 800 moles of H_2 for the second case. For fermentation of 100 mol of glucose supplemented with 500 mol of H_2 the stoichiometric model predicts that the WL pathway will produce the most butanol (133.4 mol butanol) followed by the rTCA cycle (131.9 mol butanol), the 3HP/4HB pathway (121.7 mol butanol), and the rPP pathway (121.6 mol butanol). For the fermentation of 100 moles of glucose supplemented with 800 moles of H_2, the maximum theoretical yields are 152.1 mol, 137.3 mol, 136.3 mol, and 134.1 mol for the rTCA cycle, 3HP/4HB cycle, the rPP pathway, and the WL pathway, respectively. As expected, the yield for each of the carbon fixation models was greater than the maximum predicted yield for butanol production from glucose without carbon fixation of 93.9 mol butanol (Papoutsakis 1984).

In practice, the question of catabolite repression may be an important factor in the success or failure of a given mixotrophic fermentation. Mixotrophic growth studies from Peters *et al.* (Peters, Janssen et al. 1998) confirm that acetogenic bacteria are able to simultaneously utilize H_2/CO_2 and organic substrates. In cases where catabolite repression are encountered, such as with the downregulation of hydrogenase in *C. aceticum* (Braun and Gottschalk 1981), the use of genetic tools to improve the expression of the downregulated carbon fixation genes would become necessary.

2.6.4 The dependence of metabolite yields from acetogens on the efficiency of membrane-driven ATP production

Although the WL pathway was the best performing pathway for acetate and ethanol production, ATP limitation is shown to decrease the level of butanol production in both autotrophic and mixotrophic growth. The primary assumption that determines to what extent the WL pathway is ATP limited is the choice of the ATP conservation coefficient, *n*, in Eq. 3. Table 2.5 shows improvements in the theoretical butanol yield for growth on 100 moles H_2 given increased ATP conservation. ATP conservation in acetogens is dependent on a number of factors, mainly the mechanism of membrane gradient generation, the substrate used but also the growth conditions (Daniel, Hsu et al. 1990, Tracy, Jones et al. 2012). Interestingly, the choice of electron source has a major impact on the cellular yield, and thus the calculated *n*-value. Specifically, acetogens grown on CO/CO_2 rather than H_2/CO_2 had consistently higher cell yields and thus consistently higher n values – typically 1.5-3 times higher than those calculated from the cell yield on H_2. For instance, *Butyribacterium methylotrophicum* exhibits high biomass yields when growing autotrophically on CO alone (Y_{CO} = 3 g biomass/mol CO) versus on a H_2/CO_2 mixture (Y_{H2} = 1.7 g cells/mol H_2) (Daniel, Hsu et al. 1990). The *n* values can be calculated from these yields using previously described methodology (Tracy, Jones et al. 2012). One finds that for Y_{ATP}=6.5 g biomass/mol ATP and M_{cell}=26 g biomass/mol, the *n* values are 1.18 and 2.08 for CO_2/H_2 growth and CO growth, respectively. Considering the calculations in Table 2.5, these n-values suggest that significant autotrophic butanol production through the WL pathway is possible if one chooses appropriately the organism and feedstock. We note here that that for *n* values > 2, butanol formation is no longer ATP limited, making the process more efficient than in any other pathway (compare yields in Tables 2.5 and 2.4 A).

Table 2.5: WL pathway butanol production with various ATP conservation using A) the butanol/butyraldehyde dehydrogenase route to butanol formation (Eq. 11) or B) the hypothetical AOR route to butanol formation (Eq. 14)

A	Butanol produced from butyryl-CoA using butanol/butyraldehyde dehydrogenase				
	mol/100 mol H_2				
	n = 0.47	0.6	0.8	1	2
CO_2	-49.1	-46.2	-42.3	-39.0	-33.7
ATP	0.0	0.0	0.0	0.0	10.1
Cell	2.5	2.3	2.1	1.9	1.7
H_2 (or CO)	-100.0	-100.0	-100.0	-100.0	-100.0
Acetate	22.9	18.5	12.7	7.8	0.0
Butanol	**0.2**	**1.7**	**3.7**	**5.4**	**8.0**
B	Butanol produced from butyrate using AOR				
	mol/100 mol H_2				
	n = 0.47	0.6	0.8	1	2
CO_2	-48.7	-43.2	-36.8	-33.7	-33.7
ATP	0.0	0.0	0.0	1.3	18.1
Cell	2.4	2.2	1.8	1.7	1.7
H_2 (or CO)	-100.0	-100.0	-100.0	-100.0	-100.0
Acetate	22.1	14.0	4.6	0.0	0.0
Butanol	**0.5**	**3.2**	**6.4**	**8.0**	**8.0**

There are several recorded instances of acetogenic butanol production through both native (Grethlein, Worden et al. 1991, Bruant, Lévesque et al. 2010) and engineered (Köpke, Held et al. 2010) butanol pathways. In a *C. carboxidivorans* batch culture (Bruant, Lévesque et al. 2010), 36.45 mmol butyrate, 8.91 mmol butanol, 56.58 mmol acetate and 38.21 mmol ethanol can be produced per mole of CO (CO is equivalent to H_2 for the purposes of our model). This experimental butanol yield is within the range of potential yields reported in Table 2.5, which suggests that our predictions are sound and realistic. Furthermore, the minimum *n* value for this fermentation can be calculated (Table 2.6) by setting each of the metabolite concentrations in the model and solving for the minimum *n* that yields a non-negative coefficient for ATP production. This calculated coefficient of $n = 0.75$ corresponds to a Y_{CO} of 1.08 g cells/mol CO, which is

consistent with other Y_{CO} estimates (Daniel, Hsu et al. 1990). Low butanol formation yields, consistent with our predictions, were also reported for an engineered *C. ljungdahlii* strain (Köpke, Held et al. 2010). Under conditions of continuous culture with cell recycle, butanol titers of 36.4 mM and a yield of 3.7 mol butanol per 100 mol CO were observed; these are lower than the max yield of 8 shown in Table 2.4, again showing that our maximal yield calculation is realistic.

Table 2.6: Comparison of experimental yields (Bruant, Lévesque et al. 2010) from *C. carboxidivorans* to model generated yields

	Experimental data from *C. carboxidivorans* (mol/100 mol CO)	Calculated (mol/100 mol CO)
n =	N/A	0.75
CO_2	N/A	-40
Cell (C-mol)	N/A	2
CO	-100	-100
NAD(P)H	N/A	0.0
ATP	N/A	0.0
Acetyl-CoA	N/A	0.0
Butanol	**0.9**	**0.9**
Acetate	**5.7**	**5.7**
Butyrate	**3.6**	**3.7**
Ethanol	**3.8**	**3.8**

1.6 DISCUSSION

1.6.1 Acetogens as platform organisms for fuel and chemical production

The overall efficiency of the WL pathway shows that it has great potential for development of commercial technologies, which is already occurring for a number of chemicals (Schiel-Bengelsdorf and Dürre 2012). One significant advantage to working with the WL pathway in industrial settings is that it can only operate in anaerobic environments, circumventing any safety challenges, as previously discussed, that may be encountered for H_2 or CO fermentation in

aerobic organisms. Additionally, the lack of an oxygen-dependent electron transport system ensures that all of the cellular electron flow will be directed to CO_2 fixation rather than oxidative phosphorylation.

As previously mentioned, the reduction of acetate to acetaldehyde by the enzyme AOR likely plays a key role in ATP conservation in acetogens that produce ethanol. Whole cell studies suggest that this enzyme could also be used for the production of butanal directly from butyrate (Simon, White et al. 1987), thereby decreasing the net ATP cost of butanol production as ATP is generated from the hydrolysis of butyryl-CoA to butyrate and coenzyme A (Eqs. 20-21).

$$\text{AOR Butanal: Butyrate} + Fd_{red} \rightarrow \text{Butanal} + Fd_{ox} \qquad \text{(Eq. 20)}$$

$$\text{Alcohol Dehydrogenase: Butanal} + \text{NAD(P)H} \rightarrow \text{Butanol} \qquad \text{(Eq. 21)}$$

A summary of maximal butanol production yields using the AOR enzyme and a range of *n* is summarized in Table 2.5 B. Under ATP limited conditions the AOR reaction allows for 1.5-2 times more butanol production per 100 moles H_2. For high *n* values ($n > 1$), butanol production is limited by reduction energy rather than ATP, such that the AOR reaction does not provide an advantage over the butyraldehyde/butanol dehydrogenase pathway.

In addition to the native production of butanol, acetogens have been shown to produce butyrate (Bruant, Lévesque et al. 2010) and 2,3-butanediol (23BD) (Köpke, Mihalcea et al. 2011), two important industrial chemicals and a precursor (butyrate) to biofuel production by chemical means (Papoutsakis 2008, Ji, Huang et al. 2011). Eqs. 20 and 21 summarize the biochemical route to the production of butyrate and 23BD. The maximum autotrophic and mixotrophic yields for these chemicals were calculated for the WL pathway, with the results shown in Table 2.7. The maximum yields for 23BD via the WL pathway are only slightly higher than those for butanol (Table 2.5), despite butanol production requiring more NAD(P)H

equivalent than 23BD. Though 23BD is in fact energetically cheaper, only small difference in potential yield is predicted because under ATP limited conditions the predominant cost of autotrophic production via the WL pathway is not the reduction of acetyl-CoA to butanol or 23BD, but rather the reduction of CO_2 to acetate in order to generate ATP. Thus, one would expect increased 23BD production, as well as increased differential production with respect to butanol, if a higher *n* value were used. Likewise, the maximum autotrophic yields of butyrate and butanol from the AOR pathway (Table 4B, n=0.47) – the two pathways differ by two reducing equivalents per molecule – are influenced primarily by the large amount of reduction energy needed to produce acetate for ATP production. However, the difference in NAD(P)H cost is influential for mixotrophic growth (100 mol glucose + 500 mol H_2), when ATP is not a limiting factor. Thus, the maximum calculated mixotrophic butyrate yield from Table 6 is 159.84 mol, while the mixotrophic butanol (via AOR pathway) would be 134.23 mol (data not shown).

Though acetogens are capable of producing many useful short-chain chemicals as has already been discussed, production of longer-chain carbon molecules for use in biodiesel or jet fuels is outside the metabolic capacity of acetogenic bacteria on their own due to ATP limitations. To address the need for renewably-produced long-chain fatty acids, the concept of combining an acetogen fermentation with an aerobic fermentation has been proposed (Stephanopoulos 2011). In such a scheme, CO_2 and H_2 are used to feed an acetogen in order to produce acetate, which is then fed to an oleaginous microbe, housed in a separate aerobic reactor, thus enabling the production of biodiesel entirely from CO_2 and H_2. Through analogous schemes, one could envision the use of autotrophic carbon fixation to produce a vast number of chemicals.

Table 2.7: Potential production of 2,3-butanediol and butyrate from autotrophic and mixotrophic WL pathway fermentation

	2,3-Butanediol Production by WL pathway (n=0.46)		**Butyrate production by WL pathway (n = 0.46)**	
	Autotrophic (mol/100 mol H_2)	Mixotrophic (mol/100 mol glucose + 500 mol H_2)	Autotrophic (mol/100 mol H_2)	Mixotrophic (mol/100 mol glucose + 500 mol H_2)
Cell (C-mol)	2.5	42.2	2.5	44.2
Excess ATP	0.0	0.0	0.0	108.0
Acetate	22.9	33.0	22.4	0.0
Ethanol	0.0	0.0	0.0	0.0
Butanol	0.0	0.0	0.0	0.0
Butyrate	0.0	0.0	0.5	159.8
Butanediol	0.3	133.7	0.0	0.0
Glucose	0.00	-100.0	0.0	-100.0
CO_2	-49.3	-43.1	-49.1	-83.5
H_2	-100.00	-500.00	-100.0	-500.0

2.6.5 Application of synthetic biology to CO_2 fixation

Our analysis suggests great opportunities for using synthetic-biology approaches to create strains that utilize H_2, CO or other electron sources to fix CO_2. As is clear from the pathways discussed here, carbon fixation requires a relatively large set of genes, most of which involve complex, largely unexplored regulation (Kusian and Bowien 1997), as well as specialized and demanding biophysical cellular environments. For desirable metabolites, even simple ones like butanol, an additional set of metabolic genes must be engineered, and several other genes that lead to competing reactions must be inactivated. Once a proof of concept has been demonstrated, optimizing these pathways (e.g., by removing carbon-catabolite repression, achieving coordinated gene/protein expression for the desired pathway fluxes, etc.) will remain a great challenge for major pathway engineering. An additional complexity here is that several of these pathways require complex physicochemical cellular environments, such as anaerobic or microaerobic conditions, suitable redox environments, specialized metals chaperones, and membrane systems for ATP coupling, such as the energy generation systems in the WL pathway of acetogens (Köpke, Held et al. 2010, Schiel-Bengelsdorf and Dürre 2012, Tracy, Jones et al. 2012). Thus, suitable design and coordinated expression of these complex metabolic pathways are a challenge and a great opportunity. These and many other cellular programs are frequently coded in clusters with complex regulations (Fischbach and Voigt 2010), which hinders efforts to effectively engineer them. Thus, de novo engineering of such programs without the complex regulation is a synthetic biology strategy to overcome this problem, although such synthetic programs have to be well balanced in order to effectively operate (Farmer and Liao 2000, Lee, Park et al. 2007, Lutke-Eversloh and Stephanopoulos 2008, Leonard, Ajikumar et al. 2010).

Synthetic biology tools have been used to alter gene expression at the genome scale, thus frequently referred to as genome engineering (Boyle and Gill). Synthetic promoters were tested in *Lactococcus lactis*, whereby consensus sequences were maintained but the spacer sequence was altered for tuning gene expression(Jensen and Hammer 1998). Ribosome binding sites

(RBS) are well-suited targets and can be engineered by random libraries (Pfleger, Pitera et al. 2006) or through a rational design approach (Salis, Mirsky et al. 2009), resulting in a wide dynamic range of expression. Similarly, libraries with tunable intergenic regions (TIGRs) can be used to modify the expression from entire operons, allowing for the simultaneous optimization of multiple genes (Pfleger, Pitera et al. 2006). As the cost of DNA synthesis decreases, and novel molecular biology techniques such as Gibson assembly are developed (Gibson, Young et al. 2009), complex libraries utilizing TIGRs can be readily constructed to optimize expression of entire pathways. In addition, expression of multiple genes in various locations on the chromosome can be altered and optimized using multiplex automated genome engineering (MAGE)(Wang, Isaacs et al. 2009), which utilizes synthetic oligonucleotides inserted into target regions across the chromosome to increase genomic diversity and modulate gene expression. Similarly, synthetic cassettes can be inserted in the *E. coli* genome alongside molecular barcodes, which alter gene expression and can be evaluated on a genome scale using trackable multiplex recombineering (TRMR) (Warner, Reeder et al. 2010). Other approaches have also been used to engineer whole cellular programs. For instance, simultaneous and tuned overexpression of multiple heat shock proteins (HSPs) has been used to engineer increased protein solubility in strains of *E. coli* producing high concentrations of recombinant proteins (de Marco 2007, de Marco, Deuerling et al. 2007). Several HSPs were overexpressed using a multiplasmid system to regulate their expression to stoichiometrically appropriate levels using inducible promoters and tunable plasmid copy numbers. Similar approaches can be used to express tunable sets of HSPs in bacteria in order to generate strains that tolerate high levels of metabolite stress (Nicolaou, Gaida et al. 2010). Other approaches employed RNA molecules, which play important role in post-transcription regulation of expression by various mechanisms, ranging from structural composition of the mRNA transcript itself (hairpins in mRNA molecules (Kozak 2005)) to *trans*-acting RNAs (Gottesman 2004) or RNA molecules with catalytic activity (Serganov and Patel 2007) (riboswitches). Small non-coding RNAs are also attracting a lot of attention as a means of generating desirable complex phenotypes by virtue of their ability to regulate a large set of genes

or programs at the same time (Borden, Jones et al. 2010, Nicolaou, Gaida et al. 2011). Identifying such small RNAs that act alone or in combination with other RNAs or proteins will also require powerful library-screening capabilities (Borden and Papoutsakis 2007, Borden, Jones et al. 2010). Eventually, it is the applications of such powerful tools in hosts that provide the suitable metabolic environment for engineering CO_2/CO fixation pathways in tandem with the desirable metabolite producing pathways that will exceed the current limits of synthetic biology and metabolic engineering. Great challenges remain, yet even greater opportunities in this emerging field.

Chapter 3

USING ACETOGENIC MIXOTROPHY TO IMPROVE PRODUCT YIELDS FOR THE PRODUCTION OF BIOFUEL MOLECULES AND CHEMICALS FROM GASES AND CARBOHYDRATES

(Bryan Tracy, Shawn Jones, and Ellinor Schmidt contributed to this chapter, which was published in Current Opinions in Biotechnology (Fast, Schmidt et al. 2015). Specifically, Bryan contributed to the introduction and the discussion of genetic tools, and all three contributed edits to the other sections.)

3.1 CO_2 lost during glycolysis leads to low yields in the production of chemicals and biofuels from biomass carbohydrates

In order to commercialize next-generation biofuels and commodity chemicals at large scale, the combined costs of production must be low enough and provide sufficient co-product revenue to allow bio-based fuels to be sold at prices competitive with the oil-derived fuels they replace. The wholesale price of gasoline averaged $2.43 during 2015 (US Energy Information Administration), making it difficult to develop cost-competitive second-generation biofuels. Currently, cellulosic-biofuel production in the US lags behind projections, the previous 2013 cellulosic biofuel mandate was six million gallons, but production only reached 800,000 gallons by 2015 (Service 2014, Klein-Marcuschamer and Blanch 2015, Papoutsakis 2015). One of the primary factors affecting the economic viability of next generation biofuel processes is the cost of feedstock and feedstock pretreatment, which can exceed 50% of total operating expenditure (Gnansounou and Dauriat 2010, Klein-Marcuschamer, Oleskowicz-Popiel et al. 2012). One way to mitigate high feedstock costs is by maximizing feedstock conversion to the product of interest. The ability to achieve high mass yields from carbohydrate fermentations, however, is impeded by CO_2 loss during classical Embden-Meyerhof-Parnas (EMP) glycolysis. Due to the

decarboxylation of pyruvate when forming acetyl-CoA, one third of hexose carbons cannot be recovered as useful products. In practice, this means that the theoretical maximum mass yields for gasoline replacements range from 33% for 3-methyl-1-butanol to 51% for ethanol (Rude and Schirmer 2009). For diesel replacements, the maximum mass recovery from hexose is even lower, with theoretical yields ranging from 29% in the case of farnesene to 35% for ethyl hexadecanoate, and for biocrudes, the theoretical yields are the lowest at 25% for squalene to 30% for hentriacontene (Rude and Schirmer 2009).

In response, there have been efforts based on biological approaches to minimize or ideally eliminate CO_2 loses, as this could theoretically result in complete conversion of carbohydrate sources to acetyl-CoA (Fast and Papoutsakis 2012, Tracy, Jones et al. 2012, Bogorad, Lin et al. 2013), a central building block of metabolism. Two different methods for mitigating carbon loss from glycolysis have been suggested. The first is a recently-developed, synthetic pathway, termed non-oxidative glycolysis (NOG), which can theoretically enable the stoichiometric conversion of carbohydrate feedstocks into acetyl-CoA (i.e., 2.5 to 3 moles of acetyl-CoA per mole of pentose and hexose sugar, respectively) (Bogorad, Lin et al. 2013). An engineered NOG pathway was demonstrated both in vitro and in vivo using Escherichia coli as a host. However, NOG does not generate adenosine triphosphate (ATP) without converting acetyl-CoA into acetate and consumes all reducing equivalents (i.e., NAD(P)H) that are produced from hexose sugars. Consequently, NOG-based product yields are limited by both ATP and NAD(P)H when producing metabolites that are more reduced, on a carbon basis (i.e., carbon degree of reduction), than the feedstock consumed.

A second proposed approach to improve carbon yields from carbohydrate fermentation is to genetically engineer and metabolically enhance acetogenic mixotrophic fermentation (Braun and Gottschalk 1981, Fast and Papoutsakis 2012), whereby CO_2 evolved during EMP glycolysis is reassimilated into biomass and fermentation products by a carbon fixation pathway. Here I carried out analysis of a specific version of acetogenic mixotrophic fermentations aiming to

define the potential and limits of the concept, assess its metabolic advantages, and discuss its potential in a number of host organisms.

3.2 Anaerobic, Non-Photosynthetic (ANP) mixotrophic fermentation

The focus of this chapter is on mixotrophy based on acetogenic bacteria, which are the anaerobic, non-photosynthetic bacteria that concurrently utilize organic and inorganic (i.e., CO_2/H_2, CO, formate, methanol, etc.) substrates for growth and metabolism (Fast and Papoutsakis 2012). This form of mixotrophy is in contrast to the well-documented mixotrophic growth of photosynthetic cyanobacteria and microalgae (Brennan and Owende 2010, Subashchandrabose, Ramakrishnan et al. 2013). As mentioned, the major motivation behind utilizing mixotrophy is to reassimilate the CO_2 and H_2 evolved during glycolysis in order to produce additional acetyl-CoA. While any of the six known natural carbon fixation pathways could be used to re-capture CO_2, as discussed in Chapter 2, only the bacteria that use the Wood-Ljungdahl carbon fixation pathway (WLP), termed acetogens, are natively capable of performing the stoichiometric conversion of one mole of glucose or an assortment of six carbon sugars into three moles of acetate. This ability to stoichiometrically convert sugar to acetate is well known (Fontaine, Peterson et al. 1942), and companies are exploring the commercial potential to produce acetic acid and then catalytically convert it into other industrial chemicals. However, the potential to directly convert sugars stoichiometrically to desirable biofuels and longer chain chemicals is far less explored.

As discussed in Chapter 2, acetogens are capable of carbon conservation from glucose to acetate due to the low ATP cost (*i.e.*, <1 mole ATP per mole of acetyl-CoA produced) of the WLP, which allows the excess NADH produced during glycolysis to be used for CO_2 fixation. The other five carbon fixation pathways – namely, the reductive pentose phosphate cycle, the reverse tricarboxylic acid cycle, the 3-hydroxypropionate pathway, the 3-hydroxypropionate/4-hydroxybutyrate pathway, and the dicarboxylate/4-hydroxybutyrate pathway – all have higher ATP costs than the WLP. To generate the ATP required for CO_2 fixation, the organisms with

these pathways either utilize photosynthesis or an electron transport chain that oxidizes reducing equivalents using terminal electron acceptors, such as O_2 or oxidized sulfur compounds. Both methods of ATP generation are undesirable for a bioprocess, as they increase the cost and complexity of fermentation. Moreover, the oxidation of reducing equivalents to generate ATP decreases the reducing pool that could otherwise be used for biosynthesis or biochemical production (Fast and Papoutsakis 2012). For these reasons, this analysis will focus on mixotrophic fermentation using the WLP.

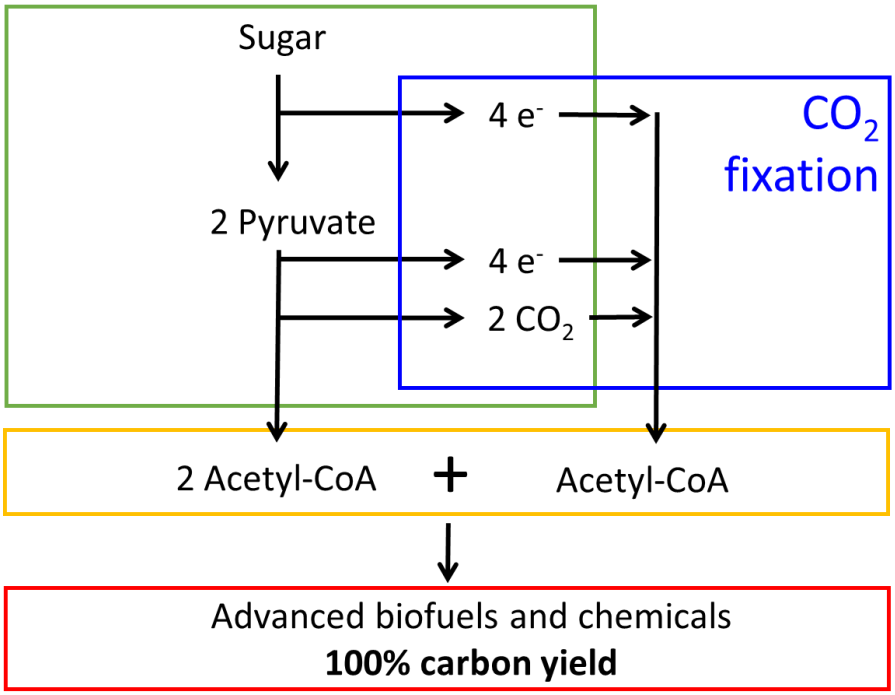

Figure 3.1: The concept for ANP mixotrophy relies on recapturing the 8 electrons and 2 molecules of CO_2 that are lost during glycolysis using the WLP, which increases the overall acetyl-CoA yield from 2 mol/mol glucose to 3 mol/mol glucose.

Figure 3.1 presents the overall concept of ANP mixotrophic fermentation, whereby glycolysis and the WLP are combined to generate pyruvate and acetyl-CoA, respectively, which

serve as intermediates for the production of potential biofuels. During glycolysis, two moles of pyruvate, two moles of ATP, and four electrons are generated per mole of hexose sugar (e.g., glucose). For most biofuel production pathways (discussed below), the two molecules of pyruvate are converted to acetyl-CoA by a pyruvate synthase or pyruvate:ferredoxin oxidoreductase, which results in the release of two moles of CO_2 and four additional electrons per mole of glucose. Overall, the glycolysis yields two moles of acetyl-CoA, two moles of ATP, two moles of CO_2, and eight electrons from each mole of glucose. Without a mechanism for CO_2 reassimilation, CO_2 is lost, and much of the reducing equivalent pool is oxidized by hydrogenase activity to release H_2.

The WLP consists of two branches: the methyl or eastern branch and the carbonyl or western branch (Ragsdale and Pierce 2008). In the methyl branch, CO_2 is reduced by two electrons to formate by formate dehydrogenase (FDH). An ATP-dependent formate-tetrahydrofolate ligase binds formate to tetrahydrofolate to form 10-formyltetrahydrofolate. Subsequent reduction and dehydration reactions consume an additional four electrons to reduce the 10-formyltetrahydrofolate to 5-methyltetrahydrofolate. In the carbonyl branch, a bifunctional CO dehydrogenase/acetyl-CoA synthase (CODH/ACS) reduces CO_2 to CO, which is condensed with the methyl-group from 5-methyltetrahydrofolate and coenzyme-A to form acetyl-CoA. In summary, glycolysis and the WLP are complementary in that the two molecules of CO_2 and eight electrons generated from glycolysis can be fully utilized by the WLP to produce an additional acetyl-CoA, thereby increasing the acetyl-CoA yield by 50% as compared to standard EMP glycolysis.

3.3 Potential metabolic and economic advantages of ANP mixotrophy for n-butanol production

In order to broadly compare the potential benefits of ANP mixotrophic fermentation, one must first consider the requirements for acetyl-CoA production from four pathways – namely, EMP glycolysis, the WLP, NOG, and ANP mixotrophic fermentation. The comparison is based

on the net consumption or production of ATP, CO_2, and reduced electron carriers (Table 3.1). Acetyl-CoA was used as a common metabolite due to its importance in the production of many advanced biofuels of interest (as shown in Figure 1) as well as in many cellular biosynthesis processes. The ideal fuel production pathway would maximize acetyl-CoA generation, minimize CO_2 evolution, and produce excess ATP in order to create and maintain biomass. As shown in Table 3.1, the ANP mixotrophic fermentation is the only approach that produces acetyl-CoA, does not evolve CO_2, and produces excess ATP. EMP glycolysis on its own generates excess ATP, but $CO_2$is evolved. The WLP converts $CO_2$to acetyl-CoA, but the pathway is ATP consuming. The NOG pathway is a viable approach for complete carbon conversion from sugar to acetyl-CoA, but the pathway consumes one mole of ATP for every mole of hexose sugar consumed. Both the NOG and WLP have a negative ATP yield when producing acetyl-CoA. Therefore, in order to balance ATP requirements, both the NOG and WLP must either produce acetate as a byproduct to generate ATP through substrate-level phosphorylation or, in the case of the acetogens, couple the WLP to energy conserving membrane reactions.

Table 3.1. Comparison of ATP, CO_2 evolved or consumed, and acetyl-CoA generation between four different fermentation strategies.

	Feedstock	**Net ATP**	**CO_2 evolved**	**Acetyl-CoA**
Glycolysis	Hexose	2	2	2
WLP	$CO_2 + H_2$	Less than 1	-2	1
ANP Mixotrophy	Hexose	1	0	3
NOG	Hexose	-1	0	3

Glycolysis refers to EMP glycolysis. WLP refers to Wood-Ljungdahl Pathway of carbon fixation. NOG is referring to Non-Oxidative Glycolysis. The feedstock for each strategy is identified in the second column. Negative values for ATP and CO_2 imply consumption.

For a more comprehensive analysis of ANP mixotrophic potential, the outcomes for n-butanol production were quantified. From here on, n-butanol will be referred to simply as butanol, unless a different isomer is being referred to. Butanol is used in this analysis, because it

is desirable biofuel that compliments or even exceeds the potential of ethanol. Butanol exhibits favorable energy density and physical properties for blending into gasoline (Szulczyk 2010), which may allow for higher than 10% (v/v) gasoline blends and potentially mitigate the United States' ethanol blending wall. Additionally, butanol production highlights the differences in limited and supplemented mixotrophic fermentation, as detailed below.

Accordingly, a stoichiometric and energetic model was created similar to the one described in Chapter 2, and the potential butanol production with biomass formation was calculated under four different culture scenarios: 1) glucose only (i.e., heterotrophic), 2) gas only (i.e., autotrophic), 3) glucose and gases derived directly from glycolysis (i.e., limited mixotrophic), and 4) glucose with CO_2 evolved from glycolysis and exogenous hydrogen (i.e., supplemented mixotrophic). All calculations were performed using 100 moles of glucose as substrate. Calculations for autotrophic growth using only the WLP were performed assuming 700 moles of H_2 consumption with the necessary CO_2 as the carbon source. In the supplemental mixotrophic case, an additional 600 moles of molecular hydrogen per 100 moles of glucose were added to the model.

Briefly, regarding the model, ATP and acetyl-CoA production were considered according to equations 1 and 4. Equation 1 describes CO_2 fixation via the WLP. Included in Equation 1 is an ATP conservation coefficient (n), which accounts for ATP generated through membrane-bound ATPases, driven by cytochrome- or Rnf-created H+ or Na+ membrane gradients. Outcomes of autotrophic fermentation were evaluated for the three different ATP conservation coefficients (n = 0.4, 0.7, and 1). As previously reviewed (Tracy, Jones et al. 2012), n ranges from 0.2 – 0.77 when cultures are grown on CO_2 and H_2 only, but can be higher when grown on CO. Therefore, n = 1 may be unrealistic, but represents the alleviation of ATP constraints for biomass formation via the WLP alone.

Equation 4 represents the production of ATP, acetyl-CoA, CO_2 and reducing equivalents from glycolysis of hexose sugar to acetyl-CoA. Cell production was defined according to Equation 2, and approximately 5% of carbon flux was directed to biomass formation, as

previously discussed by Fast and Papoutsakis (Fast and Papoutsakis 2012). Reducing equivalent production from hydrogen was modeled according to Equation 3. Finally, butanol production was modeled according to Equation 5.

$$\text{WLP: } 2\ CO_2 + 4\ H_2 + ATP \rightarrow \text{Acetyl-CoA} + 2\ H_2O + nATP \qquad \text{(Eq. 1)}$$

$$\text{Biomass: } \tfrac{1}{2}\ \text{Acetyl-CoA} + (M_{cell}/Y_{ATP})*ATP + 0.3\ NAD(P)H \rightarrow \text{C-mole Biomass } (CH_{2.08}O_{0.53}N_{0.24}) \qquad \text{(Eq. 2)}$$

$$\text{Hydrogenase: } H_2 + NAD(P)+ \leftrightarrow NAD(P)H + H+ \qquad \text{(Eq. 3)}$$

$$\text{Glycolysis: Hexose} \rightarrow 2\ \text{Acetyl-CoA} + 2\ CO_2 + 2\ ATP + 4\ NAD(P)H \qquad \text{(Eq. 4)}$$

$$\text{Butanol: } 2\ \text{Acetyl-CoA} + 4\ NAD(P)H \rightarrow \text{Butanol} \qquad \text{(Eq. 5)}$$

Results shown in Table 3.2 suggest that supplemented mixotrophic fermentation has the highest carbon efficiency and butanol mass yield. It is important to note that when producing highly reduced molecules such as butanol the limited mixotrophic pathway without H_2 supplementation does not generate excess reducing equivalents, thus the evolved CO_2 cannot be fixed via the WLP. Accordingly, the outcomes from hexose alone and hexose + gas evolved are identical. For the case of autotrophic growth (i.e., H_2 and CO_2 alone) using the WLP, increasing the value of the ATP conservation coefficient, *n*, results in improved butanol yields. This outcome is expected because the previous model (Fast and Papoutsakis 2012) showed that autotrophic butanol production via the WLP is an ATP-limited process. Therefore, since *n* is a measurement of the number of ATP molecules that can be generated per CO_2 consumed via ATPase-enabled ion pumping and the associated ion gradient generated by the either cytochromes or an Rnf complex in native acetogens, increasing *n* results in greater butanol production. Even at high

values for *n* (i.e., 1) that are not observed in acetogens growing on H_2/CO_2 (Tracy, Jones et al. 2012), acetate still must be formed to generate ATP for biomass production. Mixotrophic fermentation alleviates the ATP constraint due to the large amount of ATP produced by glycolysis and, depending upon the amount of biomass generated, can actually result in an excess of ATP, as shown in Table 3.2. In the presence of exogenous hydrogen, all carbon from hexose can theoretically be converted into butanol resulting in a near 100% carbon efficiency. This results in a mass yield of 58.3% on glucose, which is a 53% increase over what is possible using EMP glycolysis alone. Using a conservative estimate of sugar cost being 50% of total advanced biofuel operating expenditure (OPEX) a 53% increase in mass yield decreases total OPEX by more than 17%. If one assumes sugar cost to be upwards of 75% of total OPEX, which has been reported in some cases (Gnansounou and Dauriat 2010), this mass yield benefit would reduce total OPEX by more than 25%.

Table 3.2. Stoichiometric calculations to determine the maximum yield of n-butanol using glycolysis, the WLP, and ANP mixotrophic fermentation.

Substrate or metabolite	**Heterotrophic**	**Autotrophic**			**Limited Mixotrophic**	**Supplemented Mixotrophic**
	Hexose	**Gas (0.4 ATP)**	**Gas (0.7 ATP)**	**Gas (1 ATP)**	**Hexose + Gas evolved**	**Hexose + Gas evolved+ H_2**
ATP Cons.	N/A	0.4	0.7	1	0.4	0.4
Substrate						
CO_2	200.0	-320.7	-282.0	-249.7	193.0	-11.2
H_2	21.0	-700.0	-700.0	-700.0	0.0	-600.0
Hexose	-100.0	0.0	0.0	0.0	-100.0	-100.0
Metabolite						
Cell	30.0	8.0	7.0	6.2	30.2	35.3
ATP	80.0	0.0	0.0	0.0	77.2	0.0
Acetate	0.0	128.3	70.5	25.2	0.0	4.5
n-BuOH	92.5	14.0	33.5	48.7	94.2	141.7
Output						
Carbon effic.	61.7%	17.5%	47.5%	78.0%	62.8%	94.5%
***n*-BuOH mass yield**	38.1%	7.4%	20.0%	32.8%	38.8%	58.3%
Hydrogen effic.*	N/A	2.0%	4.8%	7.0%	N/A	8.2%

* Hydrogen efficiency is calculated as the ratio of butanol produced per mole hydrogen for autotrophic cases (mol butanol/mol H_2) and as additional moles butanol produced per mole hydrogen for the supplemented mixotrophic case ((mol $butanol_{supp\ mixo}$ – mol $butanol_{hetero}$)/mol H_2).

3.4 The benefits of limited ANP mixotrophy beyond butanol production

As shown in Table 3.2, the limited mixotrophic production of butanol provides little benefit over the heterotrophic case because all of the electrons from glucose are consumed in the production of butanol, leaving no excess electrons for CO_2 fixation. However, limited mixotrophic fermentation provides a tangible yield improvement over heterotrophic fermentation when considering the production of less reduced chemicals, such as organic acids as well as alcohols with lower electron requirements. To demonstrate this feature of limited mixotrophic fermentation, we modeled the production of ethanol, acetate, butyrate, isopropanol, and 2-pentanol using equations 6-10 for both heterotrophic and limited mixotrophic conditions.

$$\text{Ethanol: Acetyl-CoA} + 2\ \text{NAD(P)H} \rightarrow \text{Ethanol} \qquad \text{(Eq. 6)}$$

$$\text{Acetate: Acetyl-CoA} \rightarrow \text{ATP} + \text{Acetate} \qquad \text{(Eq. 7)}$$

$$\text{Butyrate: 2 Acetyl-CoA} + 2\ \text{NAD(P)H} \rightarrow \text{ATP} + \text{Butyrate} \qquad \text{(Eq. 8)}$$

$$\text{Isopropanol: 2 Acetyl-CoA} + 1\ \text{NAD(P)H} \rightarrow \text{Isopropanol} + CO_2 \qquad \text{(Eq. 9)}$$

$$\text{2-Pentanol: 3 Acetyl-CoA} + 3\ \text{NAD(P)H} \rightarrow \text{2-Pentanol} + CO_2 \qquad \text{(Eq. 10)}$$

A comparison between the potential mass yields from heterotrophic fermentation and mixotrophic fermentation are shown in Table 3.3. Like butanol, ethanol production from glucose is not improved by limited mixotrophic fermentation, as nearly all the reducing equivalents produced from glycolysis are used to reduce acetyl-CoA to ethanol. In contrast, the production of carboxylic acids such acetic and butyric acid provides a large excess of electrons that can be used for fixing CO_2 and generating additional product. Consequently, the mass yields of acetate and

butyrate can be improved in limited mixotrophic fermentation by 51% and 22% over heterotrophic fermentation, respectively. The secondary alcohols, isopropanol and 2-pentanol, are produced through a decarboxylation reaction, rather than a stepwise reduction of the carboxyl-group using NAD(P)H. Due to the lower NAD(P)H requirement, isopropanol and 2-pentanol show improved yields under the limited mixotrophic condition of 35% and 22%, respectively. Ultimately, the potential benefit of limited mixotrophic fermentation is directly correlated to the ratio of NAD(P)H to acetyl-CoA required to produce a given chemical. Ethanol and butanol, which have a 2:1 NAD(P)H to acetyl-CoA ratio, show little improvement in the limited mixotrophic case, whereas the other molecules shown in Table 3.3 all have lower NAD(P)H to acetyl-CoA ratios that allow the excess reducing equivalents to be used for CO_2 fixation.

Table 3.3. Potential mass yields of different chemicals and biofuels from heterotrophic and mixotrophic fermentations.

Potential Yield from Heterotrophic and Mixotrophic Fermentation				
	Heterotrophic (mol/100 mol glucose)	Limited Mixotrophic (mol/100 mol glucose)	Yield Increase (%)	NAD(P)H to Acetyl-CoA Ratio
Ethanol	185.0	188.4	2%	2
n-Butanol	92.5	94.2	2%	2
Acetate	185.0	279.9	51%	0
Butyrate	92.5	112.6	22%	1
Isopropanol	92.5	124.8	35%	0.5
2-Pentanol	61.7	75.1	22%	1

3.5 Viability of ANP mixotrophy in acetogenic bacteria

A major concern in the implementation of ANP mixotrophic fermentation is how the consumption of sugars will affect carbon fixation via the WLP and vice versa. One concern is that carbon catabolite repression (CCR), a regulatory mechanism by which bacteria repress the consumption of secondary carbon sources in the presence of a preferred carbon or energy source (Stülke and Hillen 1999), may cause WLP genes to be downregulated in the presence of sugars. A separate concern is that the kinetics of the WLP and glycolysis will be incompatible in a way that impedes the complete consumption of CO_2 by the WLP. Below, we review some of the questions surrounding CCR and pathway kinetics. Additionally, we discuss recent accomplishments in our understanding of energy conservation and electron bifurcation mechanisms that are essential for acetogenic growth, and presumably also for mixotrophic growth.

3.5.1 Differential Regulation and Carbon Catabolite Repression.

For 70 years, there has been evidence for co-utilization of the glycolysis and the WLP which was first observed in a *Moorella thermoacetica* (f. *Clostridium thermoaceticum*) culture that could produce 2.5 moles of acetate per mole of glucose (Fontaine, Peterson et al. 1942). While there are limited data on the co-utilization of syngas mixtures alongside carbohydrates, it appears that differential regulation of the WLP genes in response to carbohydrate carbon sources varies between species and culture conditions. In some cases, catabolite repression of the WLP genes is clearly observed in the presence of carbohydrate sources. In an early study by Braun and Gottschalk, the ability of *C. aceticum* to consume CO_2/H_2 was tested in both the presence and absence of sugars (Braun and Gottschalk 1981). While *C. aceticum* readily consumes H_2/CO_2 in the absence of fructose, only small amounts of H_2/CO_2 consumption were observed in the presence of fructose. It was also shown that cell extracts of mixotrophically-grown *C. aceticum* had much lower hydrogenase activity than extracts from *C. aceticum* grown on H_2/CO_2. Though Braun and Gottschalk only tested for the downregulation of hydrogenase activity, it is possible

that other WLP genes were also repressed in the presence of fructose. Hexose-dependent hydrogenase regulation was also recently shown to occur in *M. thermoacetica*. *M. thermoacetica* cell extracts from glucose-grown cells were tested for hydrogenase activity, and it was found that both the NADP-dependent hydrogenase and the electron bifurcating hydrogenase were downregulated 100-fold and 3-fold, respectively, compared to H_2/CO_2-grown cell extracts (Huang, Wang et al. 2012). Cultures of *Eubacterium limosum* when consuming mixtures of glucose and methanol – which is metabolized through the WLP like other one-carbon substrates – exhibits a diauxic growth profile that is characteristic of CCR. In one study, *E. limosum* was inoculated into media containing equimolar carbon mixture of glucose and methanol (50 mM methanol and 8.3 mM glucose) (Loubière, Gros et al. 1992). During early stages of culture, only glucose is consumed; however, once glucose is depleted to 6 mM, the cells began to consume methanol and glucose simultaneously during a short period of mixotrophy. Interestingly, once glucose is completely depleted, *E. limosum* undergoes a lag phase for ~12 hours before resuming the consumption of methanol. The precise mechanism that governs the diauxic growth of *E. limosum* has not yet been investigated.

Despite the evidence for the downregulation of WLP genes in the presence of sugars, many organisms seem to be able to use gases and carbohydrates simultaneously without any signs of WLP inhibition. The aforementioned Braun and Gottshalk study on *C. aceticum*, for instance, also tested the ability of *Acetobacterium woodii* to grow on CO_2/H_2 in the presence of fructose, glucose, and lactate (Braun and Gottschalk 1981). In all three cases, A. woodii readily consumed both the gaseous and organic substrates, resulting in the production of higher yields of acetate than could be produced using the organic substrates alone. Furthermore, they measured the hydrogenase activity of *A. woodii* and found that it was not differentially regulated in the presence of fructose, in contrast to the hydrogenase of *C. aceticum*. Butyribacterium methylotrophicum, a close relative of *E. limosum*, has been shown to co-utilize 1-carbon substrates and sugars. One study showed that a CO-adapted strain of *B. methylotrophicium* could consume both glucose and CO/CO_2 simultaneously (Shen, Shieh et al. 1999). However, due to

saturation of the ferredoxin pool with electrons from CO and pyruvate:ferredoxin oxidoreductase, pyruvate overflow and lactate production were observed. The addition of the artificial electron carrier neutral red alleviated the over-reduction of the ferredoxin pool, allowing for redirection of carbon flux from pyruvate and lactate to acetate and butyrate.

Since the publication of the *Clostridium ljungdahlii* genome sequence (Köpke, Held et al. 2010), a number of studies have examined the transcriptomic response of *C. ljungdahlii* to the presence of carbohydrates. An RNA-seq based study from Tan *et al.* collected transcriptomic data on *C. ljungdahlii* cells grown autotrophically on a CO/CO_2 mixture as well as *C. ljungdahlii* grown on 5 g/L fructose (Tan, Liu et al. 2013). Their results showed a number of carbon fixation genes were upregulated under autotrophic growth conditions, including genes encoding both the methyl- and carbonyl- branches of the WLP, which suggests that the WLP may be repressed in the presence of sugar (Tan, Liu et al. 2013). In a separate study from Nagarajan *et al*., total RNA was collected from *C. ljungdahlii* cells grown heterotrophically on fructose and autotrophically on H_2/CO_2. In this case, transcriptomic analysis via RNA-seq showed no differential expression of WLP genes. The authors postulated that the disparate finding was due to a different gas composition for their autotrophic study (CO/CO_2 for the study showing differential regulation and H_2/CO_2 for the study that showed similar expression levels for both autotrophic and chemotrophic growth). However, both transcriptomic studies found no significant up or down regulation of the Rnf genes between the autotrophic and heterotrophic conditions. In another study that established the importance of the ATP-conserving Rnf complex in the autotrophic growth of *C. ljungdahlii*, which will be discussed below, using quantitative reverse transcription PCR (qRT-PCR), they showed that transcription from the Rnf operon was significantly higher in cells grown on H_2/CO_2 as compared to transcription in cells grown on fructose (Tremblay, Zhang et al. 2013). Given the conflicting transcriptional analyses, it is clear that further experiments need to be conducted to clearly establish evidence for catabolite repression, and that more –omics tools need to be applied to elucidate the mechanisms involved. Furthermore, the inclusion of mixotrophic growth conditions in future studies would provide additional insight as to

whether downregulation of the WLP – if it occurs – is triggered by the absence of gases or the presence of sugars.

3.5.2 Electron Bifurcation for Energy Conservation.

Reduced ferredoxin is required to drive many steps in acetogenic metabolism, including the reduction of CO_2 to CO, the synthesis of pyruvate from acetyl-CoA, and the proposed direct reduction of acetate to acetaldehyde via aldehyde:ferredoxin oxidoreductase (AOR). In addition, the aforementioned Rnf complexes of *A. woodii* and *C. ljungdahlii* require high-energy electrons from reduced ferredoxin ($E^{o'}$~ -500 mV) to drive ion translocation across the cell membrane (Hess, Schuchmann et al. 2013, Tremblay, Zhang et al. 2013). To generate the low-potential reduced ferredoxin required for the WLP, acetogens have evolved unique systems for producing highly reduced electron carriers from less reduced sources. When cells are grown with H_2 as an electron source, the redox potential of H_2 ($E^{o'}$= -414 mM) is not sufficiently low to reduce ferredoxin directly. Therefore, electron bifurcation – a recently discovered mechanism (Li, Hinderberger et al. 2008) in which an "uphill," endergonic reduction is coupled to a "downhill," exergonic reduction – is required to generate the reduced ferredoxin necessary for CO_2 fixation and ATP generation via the Rnf complex. Electron bifurcating hydrogenases catalyze the oxidation of two molecules of H_2 to form Fd_{red} and NADH ($E^{o'}$ = -320 mV). Because the reduction of NADH with H_2 is exergonic, the excess energy is used to enable the unfavorable reduction of Fd_{red} from H_2. NAD-specific electron-bifurcating hydrogenases were first isolated from *M. thermoacetica* and *A. woodii* (Schuchmann and Müller 2012, Wang, Huang et al. 2013); *C. autoethanogenum* was shown to contain an NADP-specific electron-bifurcating hydrogenase (Wang, Huang et al. 2013). The NADP-specific hydrogenase from *C. autoethanogenum* forms a complex with formate dehydrogenase, allowing for the reduction of two molecules of CO_2 to formate using high-energy electrons from Fd_{red} and low-energy electrons from NADPH. The same genes are also found in *C. ljungdahlii*. Furthermore, *A. woodii* was recently discovered to contain a hydrogenase which forms a complex with formate dehydrogenase as well

(Schuchmann and Müller 2013). Considering the many hydrogenase genes contained within acetogens, we can postulate that many more reactions proceeding in an electron-bifurcating manner will be discovered in the future. Electron bifurcation serves a second purpose in acetogens to correct cofactor imbalances that arise during mixotrophic growth. In *M. thermoacetica* for instance, two of the CO_2 reduction reactions in the WLP require the use of a NADPH cofactor, but glycolysis exclusively produces reducing equivalents in the form of NADH and Fd_{red}. To adjust the available co-factor pool, *M. thermoacetica* uses an electron bifurcating NADH-dependent reduced ferredoxin:$NADP^+$ oxidoreductase (NfnAB), which reduces two molecules of $NADP^+$ using NADH and Fd_{red} (Huang, Wang et al. 2012). By transferring electrons between reduced co-factors, *M. thermoacetica* enables the simultaneous utilization of glycolysis and the WLP. The same NfnAB genes are present in *C. ljungdahlii*, although they are expressed as a fusion gene previously annotated as glutamate synthase, and are predicted to have similar function for interconversion between NADPH and NADH during autotrophic growth (Nagarajan, Sahin et al. 2013). The role of electron bifurcation in biofuel production has yet to be explored. But since electron-bifurcation plays such a large role in the conservation, conversion and efficient utilization of reducing power, electron-bifurcation will likely play a larger role for understanding electron fluxes involved in the production of more reduced products. Due to the fact that the ANP mixotrophic model for butanol production requires electron supplementation in the form of H_2 to achieve the desired yields, electron bifurcation mechanisms could be used to shift electrons from Fd_{red} and NADPH to NADH, which is the most important cofactor required for alcohol fermentation. As more data becomes available regarding electron bifurcation in acetogens, metabolic engineers will potentially be able to leverage the energy conservation and cofactor balancing utility of electron bifurcation to achieve higher product yields in acetogen fermentation processes.

3.6 Studies needed to advance the concept

As discussed, one of the major challenges facing the realization of ANP mixotrophic fermentation is the lack of data on how acetogenic organisms regulate metabolism in the presence of gaseous and carbohydrate substrates. With the rise of 'omics' analysis, the collection large datasets on the transcriptional, translational, and metabolic flux changes that occur under differing acetogenic culture conditions will become simpler and more cost effective. Additionally, computational techniques, such as the recent construction of a genome-scale model of *C. ljungdahlii* (Tremblay, Zhang et al. 2013), are going to play a larger role in the identification of gene-targets for engineering. Still, knowledge surrounding many of the underlying mechanisms that enable acetogenic fermentation – including ion translocation, electron bifurcation, and the role of AOR in alcohol production – are not fully understood, and to a large degree, a better understanding of these mechanisms can only be achieved through enzyme purification, characterization, and other basic science tools. One certainty in the development of ANP mixotrophic fermentation is the need for genetic engineering techniques. Given that few acetogens produce biofuels of interest as sole fermentation products (Table 3.4), any process will require the ability to add new biosynthesis pathways to and knockout competing reactions from any acetogenic host.

Table 3.4. Potential host organisms for ANP mixotrophic processes. This list of acetogens, while by no means exhaustive, provides some examples for good hosts for ANP mixotrophic fermentations

Name	Carbon Sources					Native Fermentation Products	Genome Available	Genetic Tools
	H_2/CO_2	CO/CO_2	C5 Sugars	C6 Sugars	Methanol			
A. woodii	X	X		X	X	acetate, ethanol	Yes	Yes (Strätz, Sauer et al. 1994)
B. methylotrophicum	X	X	X	X	X	acetate, ethanol, butyrate, butanol, lactate	No	No
C. aceticum	X	X	X	X		acetate	No	Yes (Lederle 2010)
C. carboxidivorans P7T	X	X	X	X		acetate, ethanol, butyrate, butanol, hexanol	Yes*	No
C. ljungdahlii	X	X	X	X		acetate, ethanol, 2,3-butanediol, lactate	Yes	Yes (Köpke, Held et al. 2010, Leang, Ueki et al. 2013)
C. autoethanogenum	X	X	X	X		acetate, ethanol, 2,3-butanediol, lactate	Yes	Yes (Simpson, Köpke et al. 2011)
E. limosum	X	X	X	X	X	acetate, butyrate, caproate, lactate	Yes	No
M. thermoacetica	X	X	X	X	X	acetate	Yes	No

* The genome sequence for *C. carboxidivorans* exists only as a draft.

In the past two decades, genetic tools for clostridia species have considerably improved, as recently reviewed (Pyne, Bruder et al. 2014). Advancements include broad host range multi-copy plasmid gene expression, dual plasmid gene expression, antisense RNA down-regulation of genes, homologous recombination based gene disruption and deletion, iterative gene disruption/deletion, transposon based gene disruption, Group II Intron based gene disruption (Kuehne, Heap et al. 2011), negative selection systems for chromosomal manipulations (Fast and Papoutsakis 2012, Heap, Ehsaan et al. 2012), RecT based recombineering strategies (Dong, Tao et al. 2014), and CRISPR-Cas9 genome editing (Huang, Chai et al. 2016). However, the majority of these genetic engineering technologies has been developed and demonstrated only in solventogenic, pathogenic, cellulolytic, acidogenic and/or thermophilic strains of clostridia. The available tools for clostridial acetogens are far more limited, and as indicated in Table 2.4, have only been demonstrated in four strains, *C. ljungdahlii* (Köpke, Held et al. 2010, Leang, Ueki et al. 2013, Tremblay, Zhang et al. 2013), *C. autoethanogenum* (Simpson, Köpke et al. 2011, Köpke, Simpson et al. 2012), *C. aceticum* (Lederle 2010) and *A. woodii* (Strätz, Sauer et al. 1994, Straub, Demler et al. 2014). The most advanced genetic tools for an acetogen have been demonstrated in *C. ljungdahlii*. Recently the Lovley lab developed a robust electroporation protocol for introducing replicating plasmids and suicide vectors into *C. ljungdahlii* (Leang, Ueki et al. 2013). They demonstrated the function of four unique replicative origins for plasmid propagation, and they deleted several genes in the chromosome via double-crossover homologous recombination with suicide vectors. Specifically, they deleted the *adhE1* and *adhE*2 genes individually and in combination to demonstrate the ability to redirect carbon and electron flow in this organism via gene disruptions, and also to

determine which gene is most responsible for ethanol production. As a result, they witnessed that *adhE1*, but not *adhE2*, diminished ethanol production, and they could partially restore the wild-type phenotype through complementation. More recently, the same lab also demonstrated the utility of a lactose-inducible gene expression system in *C. ljungdahlii* (Banerjee, Leang et al. 2014)**.** Briefly, they adapted a lactose-inducible promoter and its divergent regulator (*bgaR*) from *C. perfringens* that was previously demonstrated to maintain tight gene control in *C. perfringens* (Hartman, Liu et al. 2011). They demonstrated the ability to control gene expression with a *gusA* reporter gene, and then showed the ability to affect carbon flux and increase ethanol production by inducing the over-expression of AdhE1.

CRISPR/Cas9-based editing techniques in acetogens could allow for the selective genome editing without the need for a counter-selection marker or an inducible promoter. Briefly, the CRISPR nuclease Cas9 can be targeted to a specific region on a chromosome using a synthetic single guide RNA (sgRNA). Once targeted, the Cas9 nuclease generates a double-stranded break in DNA, which leads to cell death. Thus, one can generate a chromosomal mutation through homologous recombination, and then one can screen for the deletion by selectively targeting the wild-type chromosome with the sgRNA. CRISPR/Cas9-based editing has recently been demonstrated in clostridial systems (Wang, Zhang et al. 2015, Pyne, Bruder et al. 2016), and recently CRISPR/Cas9-based genome editing was also demonstrated in acetogenic clostridia, whereby Huang *et al* constructed knockout mutants of *pta*, *adhE1*, *ctf*, and *pyrE* in *C. ljungdahlii* (Huang, Chai et al. 2016).

Given the recent increase in interest, it is likely a short matter of time until more advanced genetic tools available for solventogenic and pathogenic clostridia are

adapted to acetogens. Through the coupling of ‘omics’ datasets, directed genetic engineering studies and consorted commitments by academia and industry, we believe that ANP mixotrophy can have a tremendous positive impact on industrial biofuel and renewable chemical production.

Chapter 4

NATIVE MIXOTROPHY IN ACETOGENS AND ITS USE FOR IMPROVING METABOLITE YIELDS

PREFACE: This chapter was completed as part of an STTR project with White Dog Labs. Fermentation experiments and metabolite analysis were conducted as a collaboration between Shawn Jones, Alan Fast, and Ellinor Carlson. For q-RT-PCR experiments, RNA was from *Clostridium ljungdahlii* samples collected by both Alan Fast and Ellinor Carlson. The q-RT-PCR was performed and analyzed by Alan Fast.

4.1 Introduction

4.1.1 CO_2 lost during glycolysis leads to low yields in the production of chemicals and biofuels from biomass carbohydrates

The mass yield for fermentative production of fuels and chemicals from hexose sugars is severely limited by the fact that desired metabolites are commonly more reduced than the sugar consumed. In the particular case of biofuels and commodity chemicals, standard, anaerobic fermentation requires first the partial oxidation of feedstock (e.g., glucose) to form the intermediate acetyl-CoA, and then the subsequent reduction to produce either primary or secondary alcohols and other reduced metabolites. The partial oxidation of glucose – more specifically the decarboxylation of pyruvate to acetyl-CoA – results in low product mass yields due to the release of

CO_2, which hinders the industrial application of biological fermentations (Figure 4.1). As a result of hexose decarboxylation, only two thirds of the feedstock carbon can in theory be recovered in products, although quite often the actual mass yield is much lower. Given the impact of substrate costs on overall process viability (Papoutsakis 2015), recovering the CO_2 lost from glycolysis and fixing that CO_2 into useful products is a major step towards bioprocess feasibility.

While some have suggested that the yield from sugars could be improved through the use of non-oxidative glycolysis (Bogorad, Lin et al. 2013), a synthetic pathway that allows for the stoichiometric conversion of sugars to products, the energetic limitations – the pathway requires net ATP consumption to produce acetyl-CoA – of non-oxidative glycolysis constrain the potential applications of this pathway (Figure 4.1). Additionally, the NOG pathway does not produce excess reducing equivalents when converting sugars to acetyl-CoA, therefore an exogenous electron source would need to be added to allow for the production of reduced products such as alcohols or even four carbon carboxylic acids, such as butyrate.

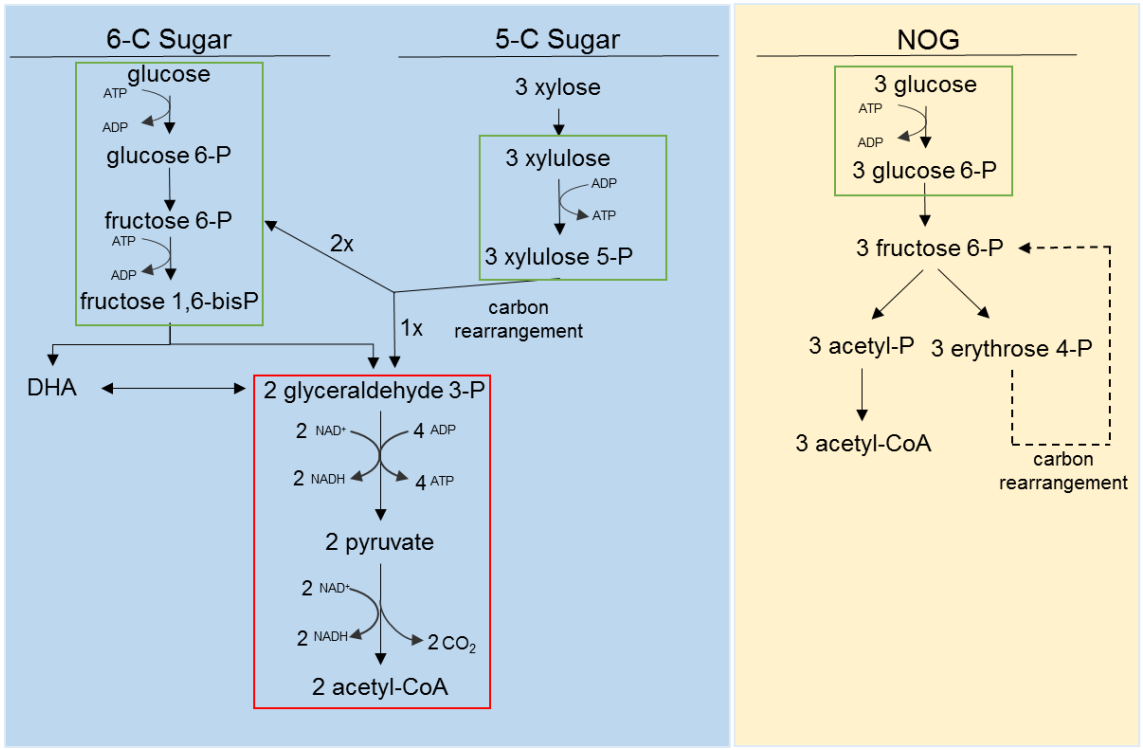

Figure 4.1. Comparison of the five and six carbon sugar glycolysis pathways (blue highlight) and the non-oxidative glycolysis (NOG) pathway (yellow highlight). All three pathways begin with a preparatory phase in which ATP is consumed to activate the sugar molecule (green box). The oxidative glycolysis pathways produce ATP as well as NADH in the payoff phase from glyceraldehyde-3-phosphate to acetyl-CoA (red box). In NOG, there is no ATP or NADH generation, leading to an ATP deficit.

One alternative that simultaneously improves glycolytic mass yields while allowing for the production of a wide range of fuels and chemicals is anaerobic, non-photosynthetic (ANP) mixotrophic fermentation – hereafter referred to as simply mixotrophic fermentation – in which the carbon dioxide released through glycolysis is reassimilated through carbon fixation and converted into useful products (Figure 4.2). Mixotrophy is defined as the concurrent utilization of organic substrates (i.e., carbohydrates) and inorganic substrates (e.g., CO_2, CO, H_2, and methanol). One prominent class of carbon fixing bacteria, termed acetogens, are particularly well-suited to the mixotrophic conversion of sugars to fuels and chemicals due to their use of the Wood-Ljungdahl pathway (WLP) for carbon fixation. The WLP has a low ATP requirement relative to other carbon fixation pathways (Bar-Even, Noor et al. 2010), which allows for a larger portion of carbon to be converted to products, since yields from CO_2 fixing pathways in non-photosynthetic organisms are constrained by ATP (Fast and Papoutsakis 2012). Furthermore, glycolysis generates precisely enough excess NAD(P)H to recapture the CO_2 released during glycolysis, thereby forming an additional molecule of acetyl-CoA per molecule of glucose consumed (Figure 4.2B). In addition to improving yields on hexose alone, mixotrophy could allow for the supplementation of hexose fermentation using gases to improve product yields.

To frame the discussion of mixotrophy, we define four distinct fermentation schemes (Figure 4.2A). In heterotrophy (Case I), sugar is consumed to produce CO_2, a fermentation metabolite (e.g., acetate, ethanol, or butanol) and – depending on the overall electron balance – H_2. For mixotrophy (Case II), sugar is consumed to produce a fermentation metabolite and a portion of the CO_2 is recaptured through carbon fixation using excess reducing equivalents. Under H_2-enhanced mixotrophy (Case III),

sugar is consumed, and CO_2 is fully reassimilated into products using electrons from exogenously added H_2. For syngas-enhanced mixotrophy, both sugar and syngas are consumed simultaneously resulting in metabolite production as well as CO_2 production, depending on syngas composition.

In this chapter, it is demonstrated that *C. ljungdahlii* as well as a broad range of acetogenic bacteria can grow mixotrophically without carbon catabolite repression (CCR), which enables the conversion of sugar into metabolites at higher yields than are possible through heterotrophic fermentation. Under mixotrophic conditions it is shown that as much as 83% of carbon from sugars can be recovered in products without the addition of additional reducing equivalents, and under syngas-enhanced mixotrophy, where acetogens are grown under a pressurized syngas (i.e., CO_2/CO/H_2) headspace, all carbon from sugars are recovered in metabolites.

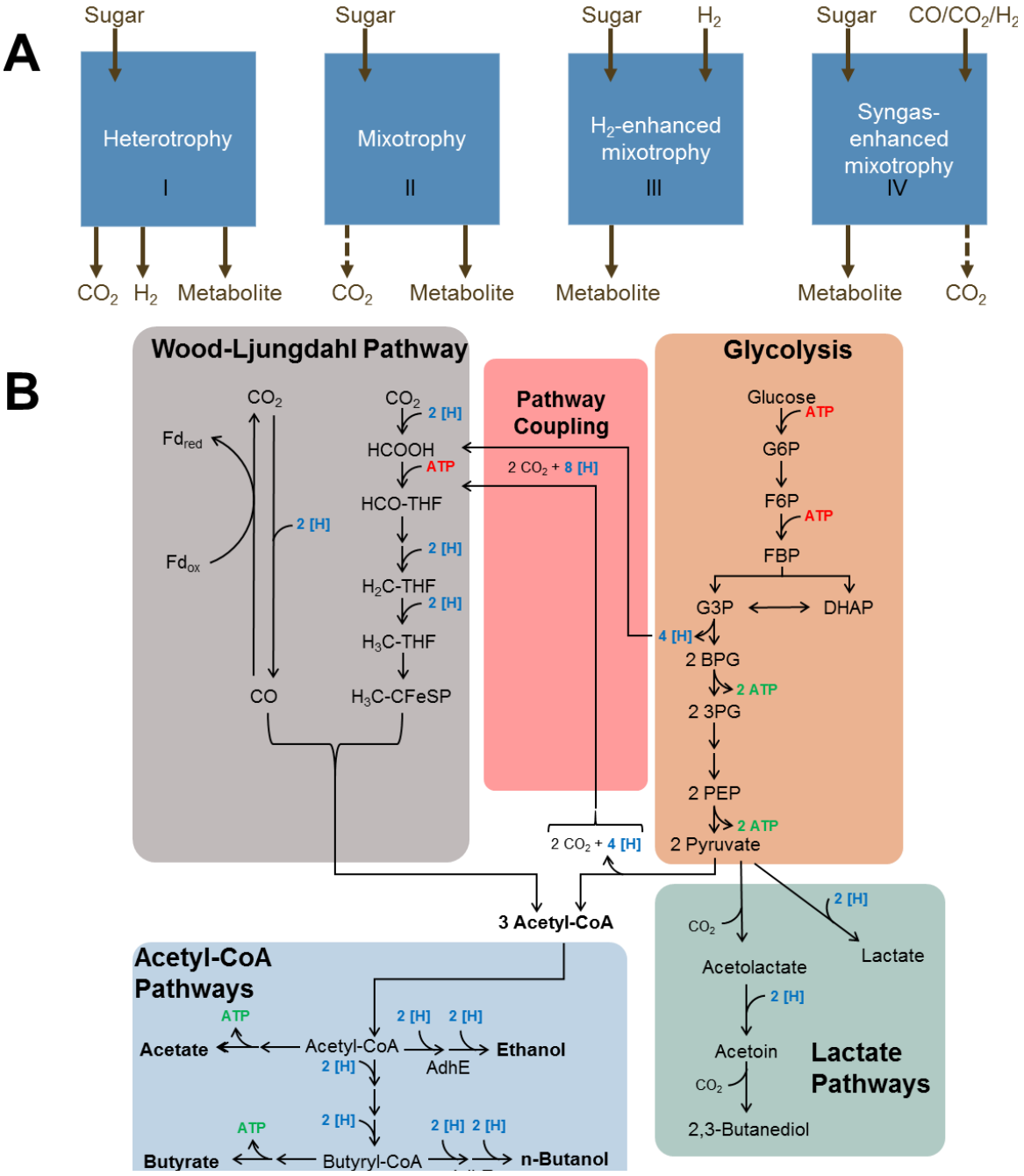
A
Sugar
Heterotrophy
I
CO2 H2 Metabolite
Sugar
Mixotrophy
II
CO2 Metabolite
Sugar H2
H2-enhanced mixotrophy
III
Metabolite
Sugar CO/CO2/H2
Syngas-enhanced mixotrophy
IV
Metabolite CO2
B
Wood-Ljungdahl Pathway
CO2
Fdred
Fdox
2 [H]
CO
CO2
2 [H]
HCOOH
ATP
HCO-THF
2 [H]
H2C-THF
2 [H]
H3C-THF
H3C-CFeSP
Pathway Coupling
2 CO2 + 8 [H]
2 CO2 + 4 [H]
Glycolysis
Glucose
ATP
G6P
F6P
ATP
FBP
G3P
DHAP
4 [H]
2 BPG
2 ATP
2 3PG
2 PEP
2 ATP
2 Pyruvate
3 Acetyl-CoA
Acetyl-CoA Pathways
ATP
Acetate
Acetyl-CoA
2 [H] 2 [H]
Ethanol
AdhE
2 [H]
2 [H]
ATP
Butyrate
Butyryl-CoA
2 [H] 2 [H]
n-Butanol
CO2
2 [H]
Acetolactate
Lactate
2 [H]
Acetoin
CO2
2,3-Butanediol
Lactate Pathways

Figure 4.2. A conceptual framework for heterotrophy, mixotrophy, and enhanced mixotrophy and the corresponding metabolic network (adapted from (Fast, Schmidt et al. 2015)). A) Heterotrophy (case I): hexose is consumed without CO_2 fixation producing metabolites, CO_2, and potentially H_2 Mixotrophy (case II): hexose is consumed, and excess reducing equivalents fix endogenously produced CO_2 into metabolites. H_2-enhanced mixotrophy (case III): Hexose and H_2 are co-utilized allowing for all endogenous CO_2 to be fixed. Syngas-enhanced mixotrophy (case IV): Hexose and syngas (CO_2/H_2/CO) are fed resulting in metabolite production as well as some CO_2 production, depending on the metabolite of interest and the composition of the syngas. B) Mixotrophic fermentation pathways. Glycolysis generates reducing equivalents and CO_2 along with acetyl-CoA, and the WLP reassimilates CO_2 using the excess reducing equivalents to generate additional acetyl-CoA.

4.2 Materials and Methods

4.2.1 Strains and Growth Conditions

C. ljungdahlii DSM-13528 (CLJ), *C. autoethanogenum* DSM-10061 (CAU), *Eubacterium limosum* DSM-20543), and *Moorella thermoacetica* DSM-521 (MTA) were obtained from DSMZ (Braunschweig, Germany). All cultures were grown anaerobically in sealed serum bottles (Wheaton) in a shaking incubator (150 r.p.m) at 37 ºC, except for MTA which was cultured at 55 ºC. All cultures were cultivated in American Type Culture Collection (ATCC) medium 1754, with the exception of *E. limosum* which was grown in a modified ATCC medium 1754 (supplemented with 20g/L MES). Growth was monitored by measuring the optical density at 600 nm (OD_{600nm}). A 5% inoculum of mid-exponential phase (OD_{600nm} of 0.8-1.5) was used to inoculate 160ml serum bottles (Wheaton), with 50ml of culture media and 110 ml of gas headspace. For autotrophic and mixotrophic cultures, the headspace was pressurized to 30 psig with syngas ($CO:CO_2:H_2:N_2$, 55:10:20:15), except for *E.*

limosum which was pressurized to 20 psig. *M. thermoacetica* was grown in a mixture without CO (CO_2:H_2, 80:20). Heterotrophic cultures were pressurized to 20 psig with N_2. Culture pH was monitored and kept between 5.0-6.5 by adding 4M NH_4OH. Metabolites were quantified on an Agilent 1200 HPLC equipped with a Bio-Rad Aminex HPX 87H column using a 5 mM H_2SO_4 mobile phase (Buday, Linden et al. 1990).

4.2.2 ^{13}C Metabolite Labeling

CLJ was grown as described above, but the media was buffered with 20 g/L MES to allow for growth on CO and 5 g/L of ^{12}C-fructose was used instead of 10 g/L. The CO-enhanced mixotrophic and autotrophic cultures were pressurized with ^{13}CO in the headspace. Culture bottles were first flushed with ^{12}CO at ambient pressure and subsequently pressurized with ^{13}CO to 30 psig resulting in a gas mixture with a ^{12}CO:^{13}CO ratio of ~ 1:2. Samples were taken at early, mid, and late exponential phase and metabolites and biomass were analyzed for ^{13}C content. Gas chromatography-mass spectrometry analysis of ^{13}C-labeling was performed on an Agilent 7890A GC system equipped with a DB-5 MS capillary column connected to a Waters Quattro Micro Tandem Mass Spectrometer operating under ionization by electron impact at 70 eV (Au, Choi et al. 2014).

4.2.3 RNA Isolation and Quantitative Real-Time PCR

RNA was extracted using the RNEasy Kit (Qiagen, Hilden, Germany) with a modified protocol as follows: Cells were thawed on ice and washed and resuspended in 220 µl RNase-free SET Buffer + 20 µl Proteinase K. Samples were sonicated for 10 minutes using 15 seconds pulse on/off at 40% amplitude using a Sonic Dismembrator

ultrasonic processor FB-505 (Thermo Fisher Scientific, Waltham, MA) with a 3” cup horn attachment (Qsonica, Newtown, CT). 1 ml of Trizol was added to each sample, split in two and another 400 µl Trizol was added to a final volume of 1 ml. 200 ul of ice-cold chloroform was added and vigorously mixed for 15 seconds, then incubated at room temperature for 3 minutes. Samples were spun at <12000 rpm for 15 minutes at 4°C. Upper aqueous phase was mixed with 500 µl of 70% ethanol and RNEasy protocol was followed per manual. Sample concentration was determined using a Nanodrop ND-3300 spectrophotometer (Thermo Fisher Scientific, Waltham, MA). Concentrations ranged from ~50 ng/µl – 500 ng/µl depending on sample.

cDNA was synthesized using a high-capacity cDNA reverse transcription kit (Applied Biosystems), and resultant cDNA was used for qRT-PCR with the iQ SYBR Green Supermix (BioRad). Each sample was tested with three technical replicates and two biological replicates. CLJ_c13280 (*recA*) was used as a housekeeping gene (Banerjee, Leang et al. 2014).

Table 4.1. List of Q-RT-PCR Primers

Primer Name	**Sequence (5'- 3')**	**Gene Target**
c37550 RT F	GGA CTT GAC CTC AGG GTT ATT C	ACS Alpha
c37550 RT R	TGC ACC TGC TGA AAC TAC AA	ACS Alpha
c37670 RT F	GGG TCG AAA CAG TTT GGG ATA G	ACS Beta
c37670 RT R	GTA CCT GCT GCA ACC ATT CT	ACS Beta
c37570 RT F	TGC AAG AGC ACT TCC TCT TTA T	CFeSP Alpha
c37570 RT R	CCT GCA TCT GGT ATA ACC ATC C	CFeSP Alpha
c37580 RT F	GTA GGA GCT GCA GGT GTA ATG	CFeSP Beta
c37580 RT R	GCT GCA AGC TTT ACT CTGTCT A	CFeSP Beta
c07070 RT F	GTA TGT ATA CCG GTG CAG GAA C	FeFe Hydrogenase
c07070 RT R	TAA GCC GGA AAC TAC TCC TAC T	FeFe Hydrogenase
c20040 RT F	ATGCGAAGTGACCCTGATATAAA	FDH A
c20040 RT R	GGC TCT ACA GGC TTA CGA ATA C	FDH A
c37220 RT F	CCT CTG TGT ATG GAA GAG GAT TT	Putative Hydrogenase
c37220 RT R	CCT TCA CAC ATC ATT CCC TCT AT	Putative Hydrogenase
c09090 RT F	TCC ACA AAG TAC TTG AGG GAA G	Accessory CODH
c09090 RT R	GAG GAA GCA CCA GAA GCT ATA A	Accessory CODH
c23590 RT F	CTT GCA GGT AAT GCC GTA ATT G	Accessory CODH
c23590 RT R	GCC GAT TCC GTT TCC ATT TG	Accessory CODH
c09340 RT F	CTG CTA TAG ACA AGG GCG TAA A	Pyruvate:Ferredoxin Oxidoreductase

c09340 RT R	CTG CTG GGA ATG TAC CAT CTT	Pyruvate:Ferredoxin Oxidoreductase
c40770 RT F	AGG ATT CTT CTT TCT TCC CTT CC	rpoA
c40770 RT R	CAA CAA CTT CTC CTG GTC CTT	rpoA
c08930 RT F	CTG CTA TGG GCA GAA CAA ATG	Non-Seleno FDH
c08930 RT R	GCG CCA TAC TTG TCT CTT ATT TC	Non-Seleno FDH
c28660 RT F	TCT ATG GAA GTA GGA CCT CTA GC	Hydrogenase hyaB
c28660 RT R	AAT CCT GCA CCA AAT GCT TTA TC	Hydrogenase hyaB
c37610 RT F	GGC CTG TGT TAC ACC TAG ATA TG	MethyleneTHFR
c37610 RT R	TTT AGC CAT ACC AGC TGA CTT T	MethyleneTHFR
c11360 RT F	AGA TGT AGG TGC GGT TGT TC	RnfC
c11360 RT R	GGT TCC TCC TTA AAT CCT CCA C	RnfC
c29340 RT F	CAG ATG TTG CAG CTG TTT ATC C	Pyruvate:Ferredoxin Oxidoreductase
c29340 RT R	TCC TTG TGA AGC AGT GTA TGT	Pyruvate:Ferredoxin Oxidoreductase

4.2.4 Stoichiometric and energetic model

A stoichiometric and energetic model was created for combined glycolysis and WLP that maximizes the production of a specific metabolite, while assuming 5% of all carbon goes towards biomass formation, as described in Chapter 2 and the publication (Fast and Papoutsakis 2012) based on that chapter. Briefly, the model considers ATP and acetyl-CoA production according to equations 1 and 2. Equation 1 describes CO_2 fixation via the WLP. Included in equation 1 is an ATP conservation coefficient (n), which accounts for ATP generated through membrane-bound ATPases, driven by

cytochrome- or RNF-created H^+ or Na^+ membrane gradients. For the calculations presented here, n = 0.9. Equation 4 represents ATP, acetyl-CoA, CO_2, and reducing equivalent production from glycolysis of hexose sugars to acetyl-CoA. Cell production was modeled according to equation 2. Reducing equivalent production from hydrogen was modeled according to equation 3.

$$2CO_2 + 4H_2 + ATP \rightarrow \text{Acetyl-CoA} + 2\ H_2O + n\text{ATP} \quad \text{(Eq. 1)}$$

$$\tfrac{1}{2}\ \text{Acetyl-CoA} + (M_{cell}/Y_{ATP})\ ATP + 0.3\ NAD(P)H \rightarrow \text{Biomass} \quad \text{(Eq. 2)}$$

$$H_2 + NAD(P)^+ \rightarrow NAD(P)H + H^+ \quad \text{(Eq. 3)}$$

$$\text{Hexose} \rightarrow 2\ \text{Acetyl-CoA} + 2\ CO_2 + 2\ ATP + 4\ NAD(P)H \quad \text{(Eq. 4)}$$

4.3 Results

4.3.1 ^{13}C-labeling shows *C. ljungdahlii* utilizes gaseous and carbohydrate substrates simultaneously

An essential concern regarding the feasibility of mixotrophic fermentation is the possibility of carbon catabolite repression (CCR) that could downregulate the expression of enzymes required for WLP functionality in the presence of a 'preferred' substrate such as glucose or fructose (Gorke and Stulke 2008). For instance, *C. aceticum* has been shown to downregulate hydrogenase genes in the presence of fructose, so that it is unable to utilize CO_2/H_2 mixtures when fructose is available (Braun and Gottschalk 1981). The acetogen *E. limosum* exhibits the diauxic growth profile that is characteristic of CCR when grown on mixtures of hexose and methanol

(Loubière, Gros et al. 1992). The question of how CLJ WLP genes are regulated when cells are grown on sugars and gases has been a contentious topic in recent years. Some researchers have shown widespread upregulation of WLP genes when cells are grown under autotrophic conditions as compared to cells grown on sugars alone (Tan, Liu et al. 2013). Others have found no CCR differential regulation regardless of growth substrate (Nagarajan, Sahin et al. 2013). Whereas the mechanisms for CCR have been characterized in model organisms such as *Escherichia coli*, there is much less information on the metabolic regulation of the clostridial acetogens. For Firmicutes in general, *Bacillus subtilis* serves as the model organism for CCR (Singh, Schmalisch et al. 2008). In *B. subtilis*, CCR is accomplished by the transcription regulator CcpA, which is governed by the presence of the phosphorylated cofactors HPr and Crh. CcpA has also been shown to regulate cellulosome expression in *Clostridium cellulolyticum* (Abdou, Boileau et al. 2008). Analysis of the CLJ genome identified orthologs to the *B. subtilis* CcpA (c01900) as well as the HPr (c13350).

To determine whether CCR has a similar effect on the metabolism of CLJ, we tested for utilization of ^{13}CO under autotrophic (i.e., CO only) and CO-enhanced mixotrophic (i.e., CO and fructose) conditions. The CO in the headspace had a severe, negative impact on growth. Autotrophic and CO-enhanced mixotrophic cultures exhibited lag phases of 73 hrs and 49 hrs, respectively, before growth was observed. After the lengthy lag phase, however, both the autotrophic and CO-enhanced mixotrophic cultures exhibited typical growth profiles (Figure 4.3). For the autotrophic case, between 42% and 63% of acetate, the primary metabolite, exhibited ^{13}C labeling over the course of the fermentation.

The CO-enhanced mixotrophic fermentation completely consumed 5 g/l fructose after 70 hrs and continued to produce metabolites until the end of the fermentation at 113 hrs. Between 23% and 52% of the acetate exhibited labeling over the course of the fermentation, and importantly, even early time points, during which fructose was not yet depleted, showed between 23% and 30% of acetate labeled. At the time of fructose depletion, 40% of acetate was labeled, which clearly indicates that the WLP is active in the presence of fructose for CLJ.

Despite ^{13}CO being the only carbon source under autotrophic conditions, it is not surprising that < 100% of acetate is labeled for two reasons. First, the headspace of the cultures was flushed with ^{12}CO before being pressurized with ^{13}CO resulting in a headspace gas composition that was only ~ 2/3 labeled. Second, the autotrophic cultures started with 4 mM unlabeled acetate that was carried over from the preculture. This affected the labeling data at early time points, for which the initial unlabeled acetate concentration made up 21% and 11% of the total acetate pool for the 48 hr and 63 hr samples, respectively.

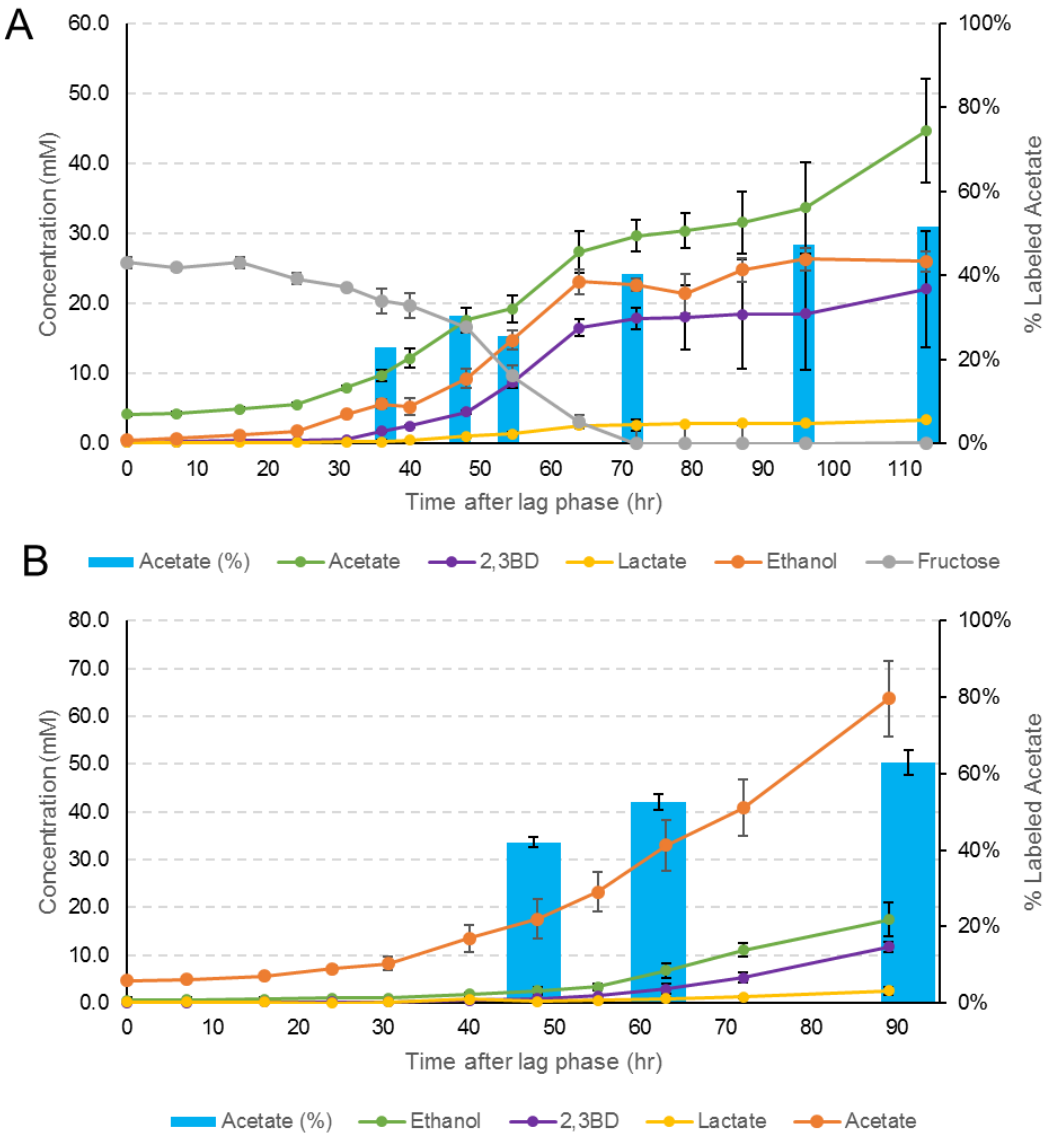

Figure 4.3. Metabolic and ^{13}C labeling profiles of *C. ljungdahlii* fermentation for CO-enhanced mixotrophic (A) and autotrophic (B) conditions. To remove long lag phases, the CO-enhanced mixotrophic and autotrophic profiles were time-shifted by 49 hrs and 73 hrs, respectively (n=3).

The long lag phase observed for these cultures can be attributed to CO inhibition. similar observations of CO inhibition in acetogens have been reported in the literature (Genthner and Bryant 1982, Savage, Wu et al. 1987, Mörsdorf, Frunzke et al. 1992). At high CO concentrations – and therefore, low CO_2 concentrations – there is no available electron acceptor for the initial oxidation of CO to CO_2. Without available CO_2, there is no substrate for the WLP to reduce to form acetyl-CoA, which results in growth inhibition.

In addition to creating a large lag phase, an increase in headspace CO concentration causes a drastic shift in product profiles towards more reduced metabolites (Figure 4.4). Under syngas-enhanced mixotrophy, CLJ predominantly produced acetate, which made up > 80% of total metabolite carbon, along with smaller amounts of 2,3-butanediol, lactate, and ethanol, which is similar to the metabolite profile observed for CLJ growing on syngas alone (Köpke, Mihalcea et al. 2011). For CO-enhanced mixotrophy, CLJ produces some acetate (~35% of total metabolite carbon), but produces large amounts of reduced metabolites, most notably 2,3-butanediol (>35% of total metabolite carbon) and ethanol (>30% of total metabolite carbon). While the metabolite profile for CLJ grown solely under a CO headspace has not previously been reported, a similar shift in product profiles was observed when *Butyribacterium methylotrophicum* was grown on glucose in the presence of CO, resulting in the production of pyruvate and lactate and decreased production of acetate and butyrate (Shen, Shieh et al. 1999). The net effect of this metabolite shift is that average degree of reduction for products from syngas-enhanced mixotrophy (γ_{syngas}) is 4.3, while the average degree of reduction for products from CO-enhanced mixotrophy (γ_{CO}) is 5.0. The shifted metabolite profile for CO-enhanced mixotrophy indicates that

the cells have an overabundance of electrons and have insufficient electron acceptors available to proceed through glycolysis to form acetyl-CoA from pyruvate, which requires free NAD^+ or oxidized ferredoxin (Fd_{ox}). Ultimately, this electron overabundance is due to CO inhibiting hydrogenase activity. Like other clostridia (Meyer, Roos et al. 1986), acetogens have been shown to produce hydrogen as a byproduct of carbohydrate consumption (Shen, Shieh et al. 1999). Under normal fermentation conditions, the decarboxylation of pyruvate is coupled to the production of reduced ferredoxin (Fd_{red}). The Fd_{ox} pool is then regenerated either through the Fd_{red}-dependent production of H_2 or through the transfer of electrons from Fd_{red} to NADH by an NADH-ferredoxin oxidoreductase. With a 100% CO atmosphere, H_2 production has been shown to be completely abolished, thereby increasing the ratio of Fd_{red} to Fd_{ox}, decreasing the favorability of pyruvate decarboxylation, and increasing the production of pyruvate by-products, such as lactate and 2,3-butanediol.

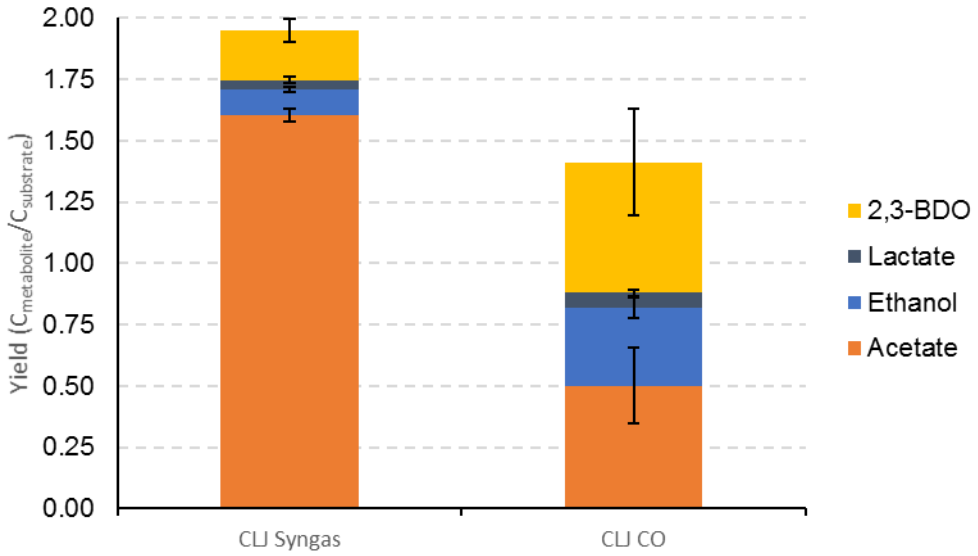

Figure 4.4. Product profiles of *C. ljungdahlii* when grown under syngas-enhanced mixotrophy (left) and CO-enhanced mixotrophy (right). The standard deviation of three biological replicates is shown in the black bars

4.3.2 *C. ljungdahlii* does not exhibit differential regulation of key WLP genes at the mRNA level in the presence of fructose

The mRNA levels of four key genes in the WLP were examined to determine whether any CCR could be detected on an mRNA level (Figure 4.5). Downregulation of these genes with respect to autotrophic conditions was not observed under either mixotrophic conditions (i.e., fructose only) or syngas-enhanced mixotrophic conditions (i.e., fructose + CO_2/CO/H_2).

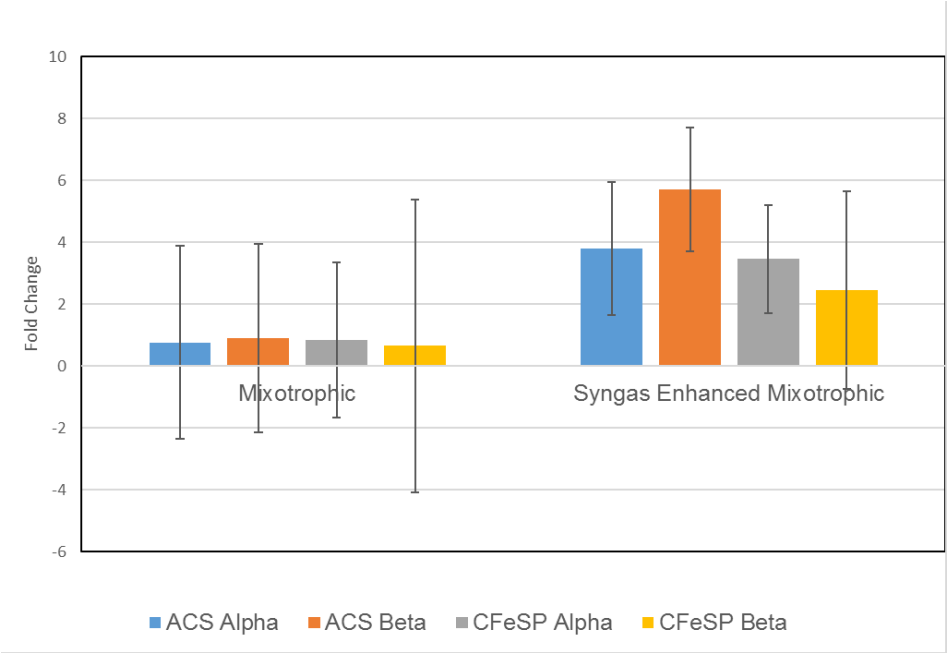

Figure 4.5. qRT-PCR for the subunits of the ACS and CFeSP. The relative expression of the ACS genes and CFeSP genes under mixotrophic and syngas-enhanced mixotrophic conditions was determined with respect to an autotrophic control. None of the genes in the mixotrophic case showed statistically significant differences compared to the autotrophic control.

Sixteen other WLP genes were also tested for mRNA downregulation under autotrophic conditions as compared to mixotrophic conditions and the resulting ΔC_t

values are shown in Table 4.2 with lower ΔC_t indicating higher expression. The comparison of autotrophic and mixotrophic gene expression reveals that most of the WLP genes tested were expressed at similar levels under both growth conditions. The most highly expressed genes in both cases were the ACS Alpha/Beta, CFeSP Alpha/Beta, pyruvate ferredoxin oxidoreductase (PFOR), RNF complex (subunit C), and the methylene tetrahydrofolate reductase (MTHF Reductase), all of which were expressed at levels higher than *rpoA* as indicated by the negative ΔC_t values. These data also show that several genes that have previously been suggested to play a role in the CLJ WLP functionality based on their annotation are in fact expressed at low levels, even during autotrophic fermentation. For instance, c23590, which is annotated as an accessory CODH is expressed ~1000x lower than ACS/CODH complex. Similarly, the annotated hydrogenase genes c17280, c20290, and c28660 are also expressed at low levels relative to the housekeeping gene. Additionally, both of the selenocysteine-containing FDH genes (c06990 and c20040) are expressed at higher levels than the non-seleno c08930, suggesting that the two seleno-proteins play a more significant role in WLP functionality.

Table 4.2. Relative expression of WLP genes in autotrophic, mixotrophic, and supplemented mixotrophic conditions as represented by ΔCt values relative to the housekeeping gene rpoA (n=2, ± SD)

Gene	**Gene ID**	**Autotrophic ΔC_t**	**Mixotrophic ΔC_t**
Accessory CODH	c09090	1.1 ± 4.2	3.2 ± 2.6
Accessory CODH	c23590	9.6 ± 1.4	9.3 ± 0.5
ACS Alpha	c37550	-2.7 ± 1.3	-2.3 ± 0.7
ACS Beta	c37670	-2.0 ± 1.3	-1.9 ± 0.7
CFeSP Alpha	c37570	-2.1 ± 0.7	-1.9 ± 0.7
CFeSP Beta	c37580	-2.4 ± 1.1	-1.8 ± 0.7
Formate DH	c06990	0.7 ± 1.5	-0.1 ± 0.4
Formate DH	c08930	6.5 ± 1.0	4.5 ± 3.0
Formate DH	c20040	2.2 ± 1.5	2.6 ± 0.9
Hydrogenase	c07070	0.8 ± 1.3	1.0 ± 0.2
Hydrogenase	c17280	7.7 ± 1.2	7.4 ± 0.3
Hydrogenase	c20290	7.1 ± 1.1	6.8 ± 0.2
Hydrogenase	c28660	11.1 ± 2.0	10.8 ± 0.6
Hydrogenase	c37220	1.4 ± 1.8	1.9 ± 0.5
PFOR	c09340	-1.4 ± 1.2	-1.0 ± 0.6
RNF Complex (C subunit)	c11360	-1.3 ± 1.0	-1.2 ± 0.5
MTHF Reductase	c37610	-3.5 ± 0.9	-3.1 ± 0.5

4.3.3 Mixotrophy is a capability of a broad range of acetogens

Upon confirmation of mixotrophic capabilities in CLJ, we sought to examine whether this mixotrophic behavior was a trait shared by a broader group of acetogens. Thus, we expanded our study to include *C. autoethanogenum* (CAU), *E. limosum* (ELM), and *M. thermoacetica* (MTA). All four strains were cultured under mixotrophic and syngas-enhanced mixotrophic conditions. Additionally, the solventogenic *C. acetobutylicum*, which is related to many acetogens but does not contain a native carbon fixation pathway, was included as a negative control. Under mixotrophic conditions, all four acetogens displayed carbon yields greater than the theoretical maximum that could be achieved in the absence of carbon fixation (Figure 4.6). CLJ exhibited the highest carbon yield, recovering 83% of the carbon from fructose in metabolites. MTA had a mixotrophic carbon yield of 78%, and both CAU and ELM exhibited mixotrophic carbon yields of 72%. The lower yields from CAU and ELM are due to the fact they produce reduced larger amounts of reduced products, ethanol and butyrate, respectively, compared to CLJ and MTA, and in producing reduced products, there are fewer electrons available to fix CO_2 (Figure 4.7 A). With the addition of syngas to the headspace, the apparent carbon yield from sugar increased beyond that of the mixotrophic case for all four strains (Figure 4.6). Both MTA and ELM were unable to grow with 30 psig of the syngas-mixture in the headspace, likely due to CO toxicity (Kerby and Zeikus 1983, Mörsdorf, Frunzke et al. 1992). We were able to culture ELM if the syngas headspace was pressurized to just 20 psig; however, MTA will not grow at high CO concentrations without adaptation, so we cultured MTA under a CO_2/H_2 headspace instead.

The addition of syngas enabled complete CO_2 assimilation for CLJ, CAU, and MTA and decreased the amount of CO_2 evolved from the ELM cultures (Figure 4.7

B). As expected, the headspace composition had an effect on the endpoint metabolite profile, with the addition of syngas leading to the production of more reduced products. For CLJ and CAU, we observe an increase in the amount of 2,3-butanediol produced, and MTA and ELM produce more lactate and butyrate, respectively.

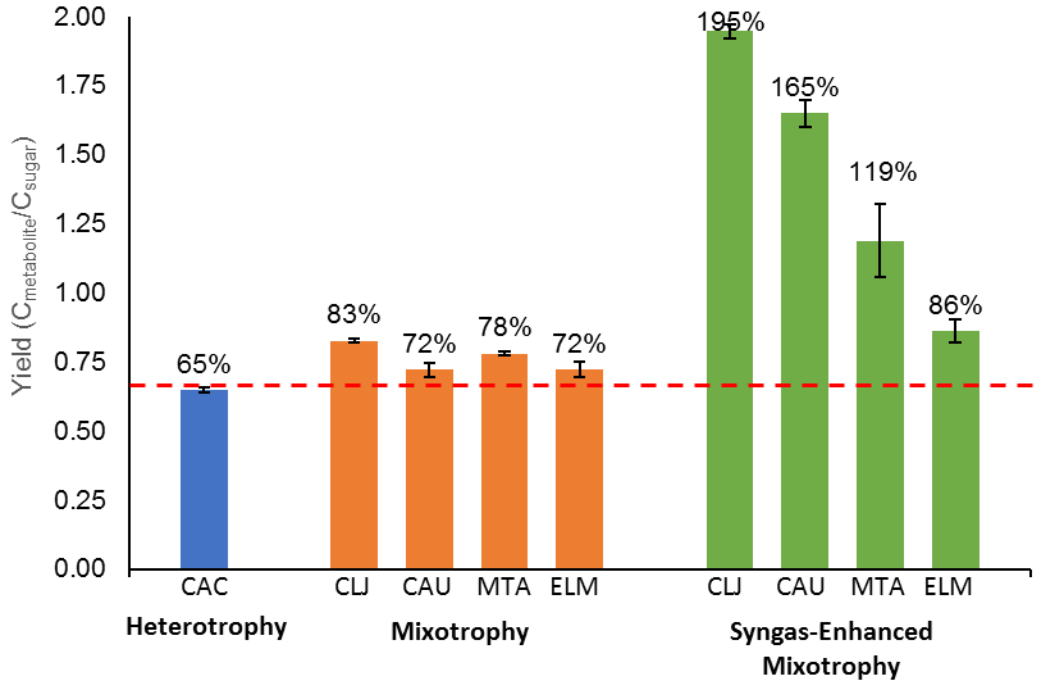

Figure 4.6. Carbon molar yields ($C_{metabolites}/C_{sugars}$), which is the carbon moles of metabolite produced divided by the carbon moles of sugar consumed, for *C. acetobutylicum* (CAC), *C. ljungdahlii* (CLJ), *C. autoethanogenum* (CAU), *M. thermoacetica* (MTA), and *E. limosum* (ELM). Cultures for heterotrophy and mixotrophy were grown on 10 g/L fructose with a N_2 headspace. For syngas-enhanced mixotrophy, cultures were grown on 10 g/L fructose with a syngas ($CO:CO_2:H_2:N_2$, 55:10:20:15) headspace, except for MTA, which was grown under a H_2/CO_2 mixture ($CO_2:H_2$, 80:20) to avoid CO toxicity. A dashed line is drawn at a carbon yield of 67%, which is the maximum carbon yield of acetate from sugars under heterotrophy. (n = 3, error bars are s.d.)

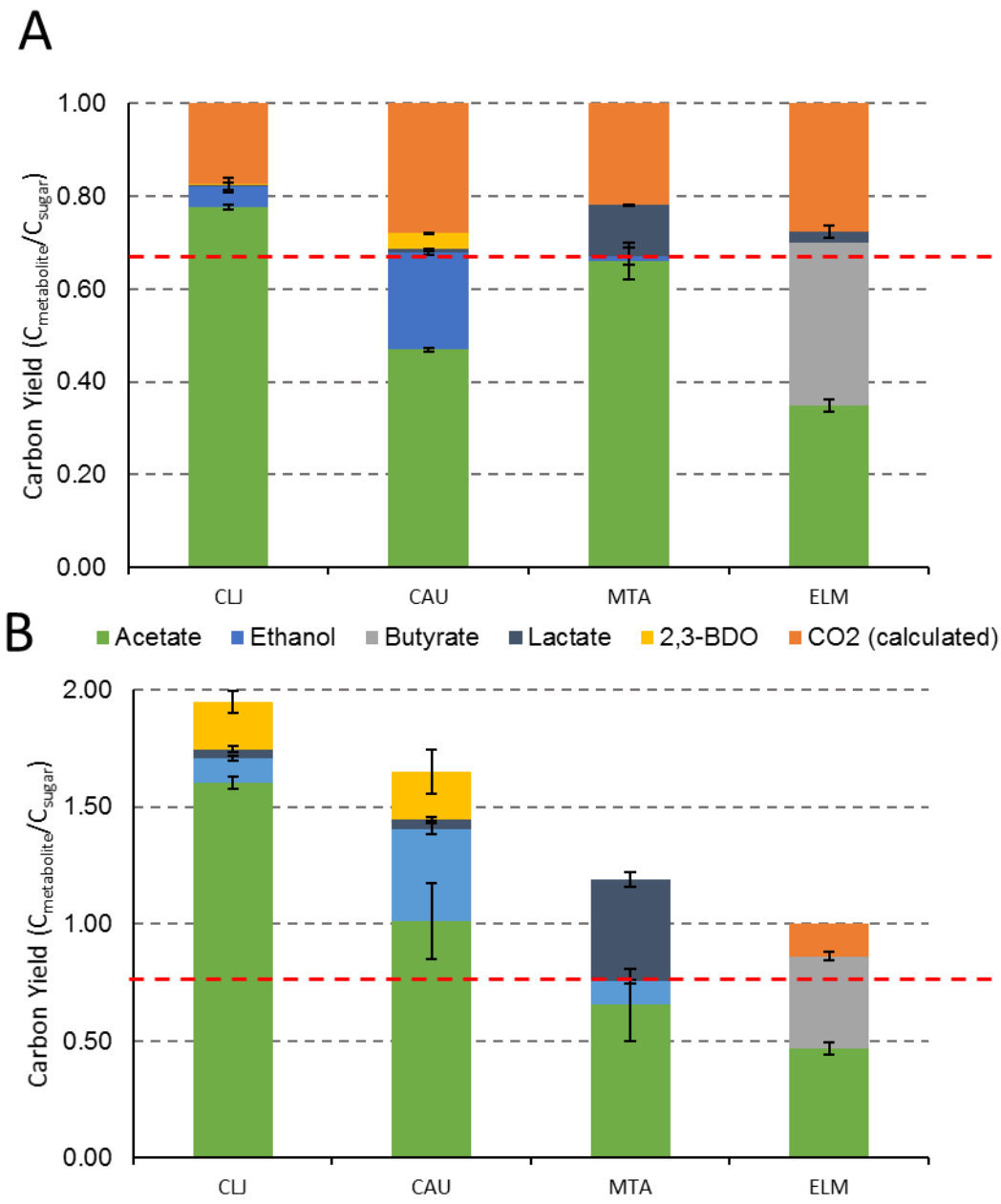

Figure 4.7. Endpoint metabolite distribution for CLJ, CAU, MTA, and ELM under mixotrophic (A) and syngas-enhanced mixotrophic conditions (B). The CO_2 was not directly measured, but was calculated from the difference in sugar carbon consumed and metabolite carbon produced. (n = 3, error bars are s.d.)

4.3.4 The applicability of mixotrophy to other metabolites

To demonstrate how mixotrophy could be applied to improve yields across a broad range of target chemicals, the maximum theoretical yield was calculated for heterotrophy, mixotrophy with no exogenous gas, and H_2-enhanced mixotrophy, in which the model supplies sufficient H_2 to recapture the carbon emitted from glycolysis decarboxylation (Figure 4.8). For highly reduced products, such as ethanol, n-butanol, and propionate, the yield improvement from mixotrophy alone is modest because the excess reducing equivalents from glycolysis are used to reduce acetyl-CoA rather than fix CO_2. For less reduced products, such as acetate, acetone, and 3-hydroxybutyrate, there are excess electrons available from glycolysis that can be used to fix CO_2 and increase the theoretical mixotrophic yield. Ultimately, one can determine the potential yield improvement from mixotrophic fermentation based on the ratio of NAD(P)H required to reduce acetyl-CoA to the desired product to the amount of acetyl-CoA required to produce the desired product (Table 4.2).

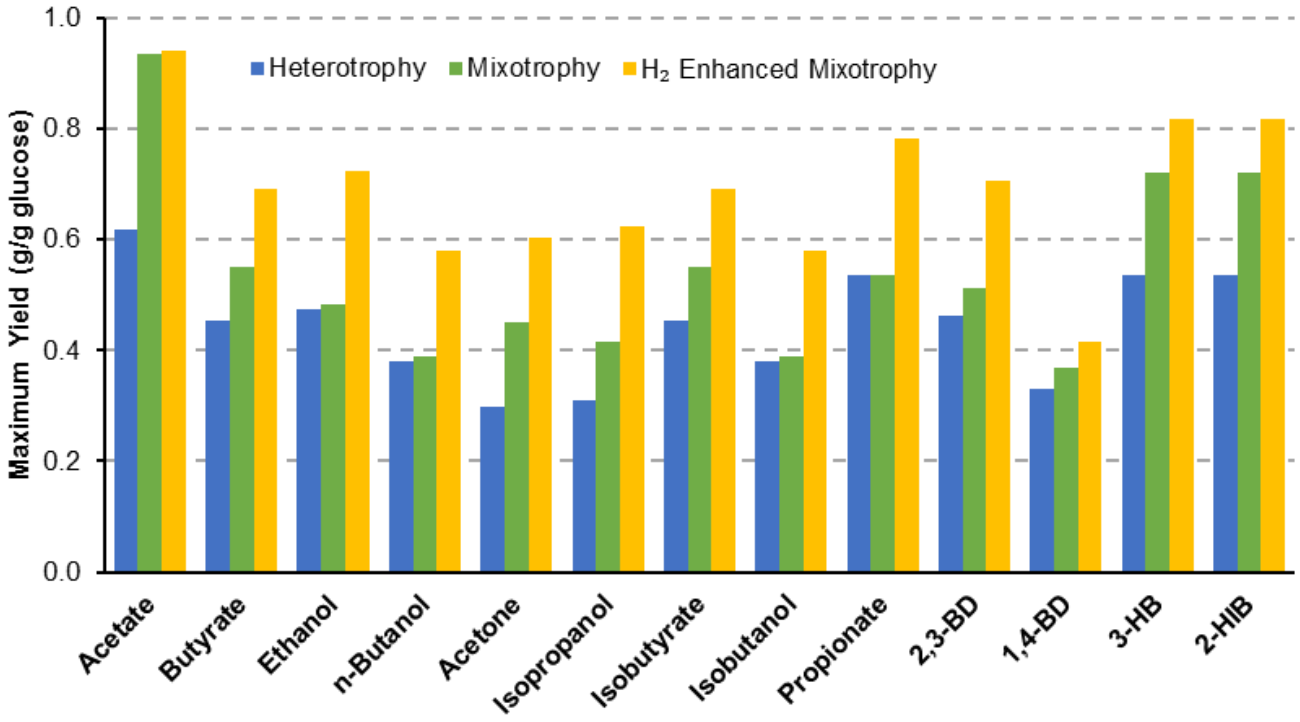

Figure 4.8. Maximum theoretical yields calculated for heterotrophic, mixotrophic, and H_2-supplemented mixotrophic conditions. Abbreviations: 2,3-butanediol (2,3-BD), 1,4-butanediol (1,4-BD), 3-hydroxybutyrate (3-HB), 2-hydroxyisobutyrate (2-HIB).

Table 4.3. The NAD(P)H/Acetyl-CoA ratio directly correlates to the increase in yield for mixotrophy over heterotrophy with high ratios resulting in very little yield improvement and low ratios resulting in yield improvement up to 51%.

	Acetate	Butyrate	Ethanol	n-Butanol	Acetone	Isopropanol	Isobutyrate	Isobutanol	Propionate	2,3-BD[1]	1,4-BD[1]	3-HB[1]	2-HIB[1]
NAD(P)H/ Acetyl-CoA ratio	0	1	2	2	0	0.5	1	2	3	1.5	1.5 or 7[2]	0.5	0.5
Increase in yield of mixotrophy over heterotrophy	51%	22%	2%	2%	51%	35%	22%	2%	0%	11%	11%	35%	35%

1 2,3-butanediol (2,3-BD); 1,4-butanediol (1,4-BD); 3-hydroxybutyrate (3-HB); 2-hydroxyisobutyrate (2-HIB)
2 1,4-BD can be produced either through the carboxylation of pyruvate or through the rearrangement of two pyruvate molecules. Thus, the NAD(P)H/Acetyl-CoA ratio can be written as either 1.5 or 7. Given that the WLP can fix carbon to produce one molecule of acetyl-CoA from the four molecules of NAD(P)H, 1.5 and 7 are equivalent in our system.

In the end, electron restraints can be removed through supplementation with H_2. While the relatively oxidized chemicals, such as acetate, that showed large yield improvements from mixotrophy over heterotrophy receive little additional benefit from H_2 supplementation. However, the highly reduced chemicals, such as ethanol, butanol, isobutanol, show marked yield improvements with H_2 supplementation. Importantly, the improved yields from H_2-enhanced mixotrophy come at the cost of H_2, and the more reduced chemicals that stand the most to benefit from H_2 supplementation accordingly require the most H_2 to achieve their maximum theoretical yield. Ultimately, producers will have to weigh the cost of supplementing fermentations with H_2 against the potential yield improvement from a given amount of hexose.

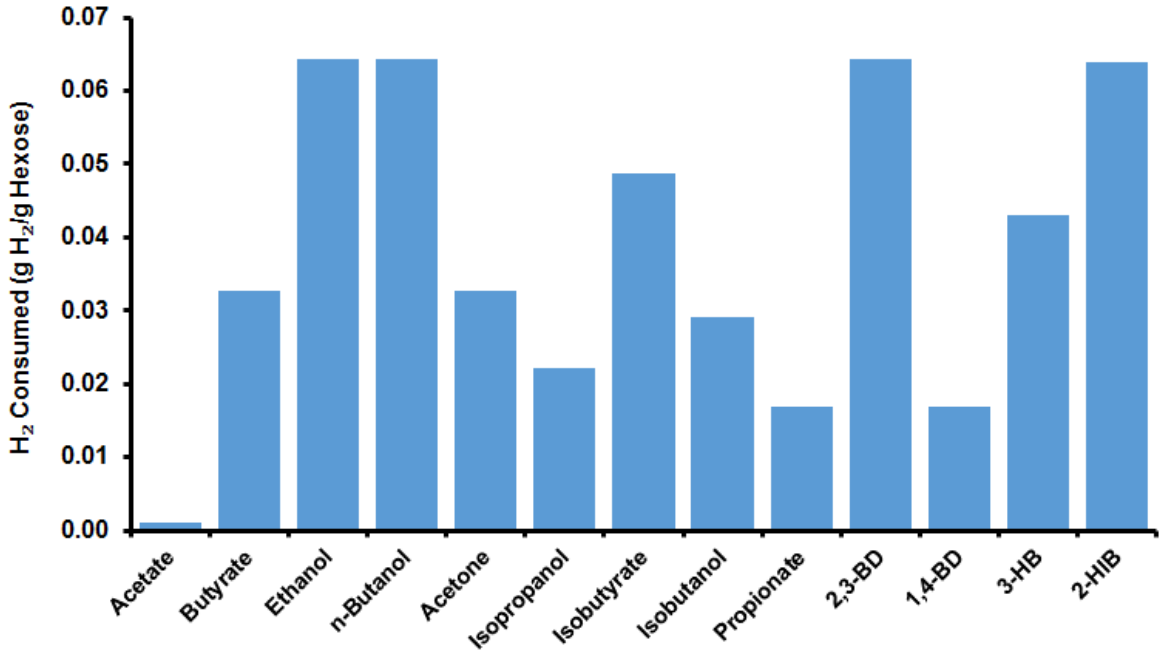

Figure 4.9. Amount of H_2 required to recapture CO_2 lost to glycolysis and maximize target metabolite production from Figure 4.7.

4.4 Discussion

Mixotrophy has been previously demonstrated in the thermophilic acetogen *M. thermoacetica* when producing acetate from glucose as well as in *Acetobacterium woodii* and when grown on mixtures of sugars and H_2/CO_2 (Fontaine, Peterson et al. 1942, Braun and Gottschalk 1981). However, it had remained unclear whether mixotrophy was a generalized phenomenon in acetogens and moreover, whether the relative rates of sugar and gas consumption were comparable, a necessity if mixotrophy were to be used to recapture CO_2 from industrial fermentation processes. In this Chapter, we showed through ^{13}C labeling that, in the case of CLJ, gas incorporation occurs concurrently with sugar consumption and that the relative rates of gas and sugar production allow for more than 40% of acetate to be derived from the WLP rather than glycolysis. The mRNA expression data from *C. ljungdahlii* confirmed that the WLP is not downregulated at an mRNA level even when sugars are present, and the relative expression of several WLP genes that have multiple paralogs in *C. ljungdahlii* such as the hydrogenase genes, the accessory CODH genes, and the three formate dehydrogenase genes indicates that some are expressed at low levels, even during autotrophic growth, indicating that these paralogs are not in fact important for WLP functionality.

We also showed that mixotrophy is a wide spread phenomenon across all four acetogens that we tested. CLJ, CAU, ELM, and MTA all demonstrated the capability to simultaneously consume sugars and gases by producing metabolites at yields higher than that which could be achieved through heterotrophic fermentation alone. However, the amount of CO_2 from glucose that could be reassimilated into metabolites differed between the four organisms, with the organisms that produced more reduced metabolites such as ethanol and butyrate also fixing less CO_2 over the course of the

fermentation. While the impact of metabolite reduction played a role in how much CO_2 could be reassimilated, we also showed that the gas composition in syngas-enhanced mixotrophic cultures and CO-enhanced mixotrophic cultures had an impact on the degree of reduction of the metabolites produced. The presence of syngas in the headspace allowed for the complete reassimilation of glucose carbon in three out of four acetogens tested, and the product profiles of these acetogens in the presence of syngas was shifted to more reduced products. The most dramatic shift in response to the headspace gas was observed for the CLJ cultures that were grown under a 100% CO headspace, which drove the production of pyruvate-derived fermentation products such as lactate and 2,3-butanediol due to the inhibition of hydrogenase and pyruvate decarboxylation, a phenomenon that has been observed to some extent in other acetogens (Shen, Shieh et al. 1999) and other clostridia (Meyer, Roos et al. 1986).

In the end, the goal of mixotrophic fermentation is to improve the product yields for industrially relevant fermentation products. In the recently published work in part based on this chapter (Jones, Fast et al. 2016), CLJ was engineered to produce acetone. Acetone was selected as the target molecule because the conversion of acetyl-CoA to acetone requires no NADH, thereby allowing all of the reducing energy to be used for CO_2 fixation. Batch fermentation of the acetone strain (CLJ ΔSADH (pTCtA) on fructose resulted in a 34wt% acetone yield which is greater than the theoretical maximum for heterotrophic fermentation of 32wt%. Under high cell density continuous fermentation, the total acetone yield was increased to as high as 44.6wt%. Given this proof of concept, it seems clear that the benefits of mixotrophic fermentation could be expanded to other products and/or organisms. The choice of a target fermentation product, however, should be made based on where the greatest

mixotrophic gains can be achieved (Figure 4.8). Due to their low requirements of exogenous reducing energy acetone, isopropanol, and various carboxylic acids seem to be good first targets for engineered mixotrophy. While CLJ seems to be the most likely host for initial studies due the availability of genetic techniques (Molitor, Kirchner et al. 2016), as more genetic tools are made available other acetogens may become more suitable targets for engineering mixotrophic fermentation.

Chapter 5

DEVELOPMENT AND DEMONSTRATION OF GENETIC TOOLS IN PURSUIT OF A FUNCTIONAL WOOD-LJUNGDAHL PATHWAY IN CLOSTRIDIUM ACETOBUTYLICUM

5.1 Introduction

The microbial production of biofuels and commodity chemicals from renewable feedstocks is vital to reducing global dependence on fossil fuels and decreasing greenhouse gas emissions. Currently, the majority of domestic biofuel production comes from the fermentation of corn mash (Fairley 2011). However, recent rises in global food and energy prices highlight the need for feedstocks that do not directly compete with the food supply, such as cellulosic biomass. Non-photosynthetic microbial carbon dioxide fixation is a promising method for the production of biofuels from a wide range of feedstocks. The most prominent non-photosynthetic carbon fixation pathway is the Wood-Ljungdahl (WLP) reaction pathway, in which two moles of CO_2 are reduced to produce one mole of acetyl-CoA – an important biological intermediate that is used for many cellular processes including biomass production and solvent/acid generation – with CO or H_2 being used to generate reducing equivalents (Ragsdale 1997). Because synthesis gas – a mixture consisting of CO, H_2, H_2O and CO_2 – can be generated from many different feedstocks, including cellulosic biomass and municipal solid wastes, a functional WL pathway allows an organism to utilize any substrate that can be gasified. Furthermore, the anaerobic bacteria that contain the

WL pathway, termed acetogens, can utilize carbon atoms and reducing equivalents that are generally lost during fermentation to CO_2 and H_2 off-gas when fermenting sugars. This enables many acetogens to stoichiometrically convert one mole of glucose (6 carbons) to three moles of acetate (6 carbons) (Drake and Daniel 2004). These capabilities make the WL pathway a desirable addition to anaerobic industrial organisms, such as *C. acetobutylicum*, to expand substrate range and improve carbon yield.

The WL pathway is found in over 100 species of anaerobic bacteria, many of which are in the class Clostridium, including the recently sequenced *Moorella thermoacetica, Clostridium carboxidivorans, Clostridium difficile,* and *Clostridium ljungdahlii (CLJ)* (Parkhill, Sebaihia et al. 2006, Ragsdale, Pierce et al. 2008, Köpke, Held et al. 2010, Paul, Austin et al. 2010). *C. acetobutylicum* – another clostridium, though without a native WLP – is a Gram-positive obligate anaerobe, which is well-known industrially for its ability to produce commodity chemicals (i.e., butyrate, acetate, acetoin, and acetone) and biofuels (i.e., butanol and ethanol) (Papoutsakis 2008). Although *C. acetobutylicum* does not express the full WLP, the enzymes that catalyze the reduction of 10-formyltetrahydrofolate to 5-methyltetrahydrofolate, as well as a ferredoxin hydrogenase, are found in the *C. acetobutylicum* genome (Nölling, Breton et al. 2001). Therefore, due to the close relation of *C. acetobutylicum* to other acetogens and the native expression of many of the WL enzymes, it is proposed to express heterologous genes from the WLP in *C. acetobutylicum* to allow it metabolize CO_2 as a carbon source for the production of chemicals and biofuels.

While genetic tools have been available since the development of a methylation system and electroporation protocols in the early 1990s (Mermelstein and

Papoutsakis 1993), the integration of significant amounts of genetic material has been hindered by the lack of robust, repeatable integration techniques. In this chapter, we demonstrate how an inducible MazF counterselection marker (Al-Hinai, Fast et al. 2012) can be used for multiple, sequential integrations of genetic material, allowing for the engineering of entire genetic pathways.

5.2 Materials and Methods

5.2.1 Bacterial strains, media, and growth conditions

The bacterial strains and plasmids used in this work are listed in Table 5.1. *Escherichia coli* strains were grown aerobically at 37º C and 250 rpm in liquid LB media or solid LB with agar (1.5%) media supplemented with the appropriate antibiotics (ampicillin at 100 µg/mL, chloramphenicol at 35 µg/mL, or kanamycin 25 µg/mL). *E. coli* strains were stored at -85 ºC in 15% glycerol. *C. acetobutylicum* ATCC 824, *C. acetobutylicum* M5, and knockout/integration strains were grown anaerobically in liquid clostridial growth media (CGM), liquid 2x yeast-tryptone-glucose (pH 5.2) (2xYTG), and solid 2xYTG media at 37º C. Plasmid-containing and knockout/integration strains were grown with appropriate antibiotics (erythromycin at 100 µg/mL and thiamphenicol at 10 µg/mL). For spore forming strains, colonies were grown on 2xYTG for at least 5 days and heat shocked for 10 minutes at 80º C prior to growth, which serves to kill vegetative cells and ensure the presence of the megaplasmid pSOL1. Growth was monitored by measuring the optical density at 600 nm (OD_{600nm}).

Table 5.1 Strains and plasmids

Bacterial strain or plasmid	**Relevant Characteristics**	**Source or Reference**
E. coli strains		
ER2275	*hsdR mcrA recA1 endA1*	NEB
Turbo	F' *proA*$^{+}$*B*$^{+}$ *lacI*^{q} Δ*lacZM15 / fhuA2* Δ*(lac-proAB) glnV galK16 galE15 R(zgb-210::Tn10)*Tet^{S} *endA1 thi-1* Δ*(hsdS-mcrB)5*	NEB
C. acetobutylicum strains		
ATCC 824	Wild-type strain	ATCC
M5	ATCC 824; pSOL1 negative	ATCC
M5 *sigK::fdh*	*fdh* (c08930) integrated in the *sigK* locus; Th^{r}	(Al-Hinai, Fast et al. 2012)
M5 *sigK::fdh_um*	*fdh* integrated in the *sigK* locus with excised Th^{r} gene	(Al-Hinai, Fast et al. 2012)
824 *sigF::fdh*	*fdh* (c08930) integrated in the *sigF* locus; Th^{r}	This study
824 *sigF::fdh_um*	*fdh* integrated in the *sigF* locus with excised Th^{r} gene	This study
824 *sigF::fdh_um sigG::FeS/MTR/Gly*	*fdh* at the *sigF* locus and *FeS/MTR/Gly* integrated at the *sigG* locus; Th^{r}	This study
824 *sigF::fdh_um sigG::FeS/MTR/Gly_um*	*fdh* at the *sigF* locus and *FeS/MTR/Gly* integrated at the *sigG* locus; Th^{r} excised	This study
Plasmids		
pAN1	Cm^{r}; Φ3T I gene; p15A origin	(Mermelstein and Papoutsakis 1993)

pAN2	Amp^r; Φ3T I gene; p15A origin	(Mermelstein and Papoutsakis 1993)
pAN3	Km^r; Φ3T I gene; p15A origin	(Al-Hinai, Fast et al. 2012)
p94MCS	Amp^r MLS^r; RepL; *ptb* promoter; MCS	(Al-Hinai, Fast et al. 2012)
p95MCS	Amp^r MLS^r; RepL; *thl* promoter; MCS	This study
p95ACS	Amp^r MLS^r; RepL; *thl* promoter; *acsA, acsB, cooC2, meTr*	This study
p95ACS_MetF	Amp^r MLS^r; RepL; *thl* promoter; *acsA, acsB, cooC2, meTr, metF*	This study
pJIR750	Cm/Th^r; pIP404; *lac* promoter	(Bannam and Rood 1993)
pJIR750_pta	Cm/Th^r; pIP404; *pta* promoter	This study
pJIR750_CFeSP	Cm/Th^r; pIP404; *pta* promoter; *acsC, acsD, cooC1*	This study
p94FLP_asRepL	MLS^r; flippase (flp): *ptb* promoter; *bgaR* and P_{pgaL} upstream of asRNA to the *repL* origin	(Al-Hinai, Fast et al. 2012)
pKISIGK::FDH_mazF	Th^r-FRT; MLS^r; *recU repL*; ori; *bgaR* and P_{bgaL} upstream of *mazF*; Th^r and *fdh* flanked by *sigK* homology regions	(Al-Hinai, Fast et al. 2012)
pKOSIGF_mazF	Th^r-FRT; MLS^r; *recU repL*; ori; *bgaR* and P_{bgaL} upstream of *mazF*; Th^r flanked by *sigF* homology regions	(Al-Hinai, Fast et al. 2012)
pKISIGF::FDH_MazF	Th^r-FRT; MLS^r; *recU repL*; ori; *bgaR* and P_{bgaL} upstream of *mazF*; Th^r and *fdh* flanked by *sigF* homology regions	This study
pKOD_MazF	Th^r MLS^r; *ccdB repL*; ori; *bgaR* and P*bgaL* upstream of *mazF*; DEST cassette	(Al-Hinai, Fast et al. 2012)

pKO_MazF	Th^r-FRT/MCS; *repL*; *bgaR* and P*bgaL* upstream of *mazF*	This study
pKISigE::FeS/MTR/Gly_MazF	Th^r-FRT and 3 gene operon (c37530, c37540, c37610) under the thiolase promoter flanked by *sigE* homology; *repL*; *bgaR* and P_{bgaL} upstream of *mazF*;	This study

Table 5.2 List of primers used for plasmid construction and sq-RT-PCR

Primer	**Sequence (5'- 3')**	**Description**
MCS_F	GATCCCAATCTAGAATCCGCGGTAGCATGCATCC ATGGTTGAGCTCATGGACGCGTAAAG	Multicloning site
MCS_R	GCGCCTTTACGCGTCCATGAGCTCAACCATGGAT GCATGCTACCGCGGATTCTAGATTGG	Multicloning site
C37590_XbaI_F	TAGAGCTCTAGATATAAGGAGGTTGTACTATGGG ATATA	Amplify *acsA*
C37590_SacII_R	ATACCGCGGTTACTTAAATAATTTTTACTTAGCA GT	Amplify *acsA*
C37560_NcoI_F	ACTCCCATGGATAGGAGGTCATCTGAACATGGAT AAATT	Amplify *acsB*
C37560_MluI_R	TAGCACGCGTCTACATTATTGGATCCATCTTTAAT GCA	Amplify *acsB*
C08930_ncoi_r	TATACCCCATGGTTGATAAAAGTTAATTTGCAGT TAC	Amplify *fdh*
C08930_sacii_f	TTTACTCCGCGGGTTATTATGGAGAATAAAGTAT TAA	Amplify *fdh*
C37660 SacII F	ATAAAGCCGCGGAGGAGGGACTACATATGAAAA TGAAAATG	Amplify *cooC2*
C37660 NcoI R	GACTACCCATGGTTAAAAAACCCCCATTTCTAAT TTTTG	Amplify *cooC2*

P94_sphi_f	TTAATAGCATGCTCGACTGTGGATGGAGTTAA	Amplify *fdh* operon
P94_sphi_r	TTAATCGCATGCTGACCATGATTACGAATTCTATGA	Amplify *fdh* operon
RT c37570 F	GCTTATGCCCTAGTCTGTGAAG	Sq-RT PCR
RT c37570 R	CTGCAACCTTTCCTGGGATTA	Sq-RT PCR
RT c37580 F	GTGCTGATCCAAACGGTACA	Sq-RT PCR
RT c37580 R	CTGTTATGTCTTCCTGGCTTC	Sq-RT PCR
RT c37590 F	TGTAGCAGGTAAGGGTGGTA	Sq-RT PCR
RT c37590 R	CATCGGCACAACTCCTACTAAA	Sq-RT PCR
RT FeS Protein F	GCCTGTCAGTGTGAGGTTAAA	Sq-RT PCR
RT FeS Protein R	TCCACATTCCCGAAGACAATAC	Sq-RT PCR
RT c37610 F	CTGAAATGGCACCTCCAAAG	Sq-RT PCR
RT c37610 R	CTCCATCGCAAAGTCCTGAT	Sq-RT PCR

5.2.2 Plasmid and strain construction

All restriction endonucleases, ligase, and NEBuilder HiFi DNA Assembly Master Mix were purchased from New England Biolabs (NEB), Ipswitch, MA.

5.2.2.1 Replicating plasmids for the expression of WLP genes

The cloning vectors p94_MCS and p95_MCS were constructed by digesting the existing vectors pSOS94 and pSOS95, respectively, with BamHI and KasI (NEB), and the digested plasmid backbones were ligated with a pair of annealed primers to form multiple cloning sites for use in future cloning steps.

The ACS/CODH expression vector (p95ACS) was constructed as follows. First, the ACS/CODH beta subunit (c37660) from *C. ljungdahlii* was PCR amplified from genomic DNA (gDNA) using primers incorporating the BamHI and SacII (NEB) digestion sites and then ligated into BamHI/SacII (NEB) digested p95MCS, yielding p95ACSbeta. Next, the methyl transferase (c37650) and the ACS/CODH alpha subunit (c37550) were amplified from *C. ljungdahlii* gDNA using primers that added NcoI and MluI (NEB) sites, and the resulting fragment was cloned into NcoI/MluI (NEB) digested p95ACSbeta to form p95ACSalphabeta. Next, the cooC2 (c37660) was amplified with SacII and NcoI (NEB) overhangs and cloned into SacII/NcoI (NEB) digested p95ACSalphabeta to form p95ACS, which contained the four genes from *C. ljungdahlii*. Finally, the *metF* gene from *Escherichia coli* was codon optimized for *C. acetobutylicum* and synthesized into a gBlock (Integrated DNA Technologies, Coralville, Iowa). The synthesized *metF* was PCR amplified to generate compatible ends for Gibson assembly into NcoI-digested p95ACS to generate p95ACS_MetF.

The corrinoid iron-sulfur protein expression vector (pJIR_CFeSP) was constructed by digesting pJIR750 with EcoRI and BamHI (NEB), and inserting the *pta* promoter (P_{pta}), a 270 bp region immediately upstream of the *pta* gene PCR amplified with compatible EcoRI/BamHI ends from *C. acetobutylicum* gDNA, to form pJIR_pta. A three-gene operon containing c37590, c37580, and c37570 was PCR amplified from

C. ljungdahlii gDNA with BamHI and SacII overhangs, was digested, and ligated into BamHI/SacII (NEB) digested pJIR_pta to form pJIR750_CFeSP.

5.2.2.2 Generation of FDH and FeS/MTR/Gly integration strains

5.2.2.2.1 Integration of the *fdh* gene in the *sigK*-gene site in strain M5

As previously described (Al-Hinai, Fast et al. 2012), the *C. ljungdahlii* formate dehydrogenase (c08930) was integrated into the *sigK* region of *C. acetobutylicum* mutant M5. Briefly, the formate dehydrogenase (*fdh*) gene was amplified from *C. ljungdahlii* gDNA using primers containing flanking NcoI and SacII digestion sites. The resulting PCR product was digested and cloned into the NcoI/SacII (NEB) digested p94MCS plasmid to create p94FDH, which contained the *fdh* gene flanked upstream and downstream by a clostridial promoter and terminator, respectively. The full operon was PCR amplified from p94FDH, phosphorylated, and cloned into pKOSIGK_mazF that had been NotI (NEB) digested and blunt-ended with Klenow fragment to yield pKOSIGK::FDH_mazF. The pKOSIGK::FDH_mazF vector was methylated and transformed into *C. acetobutylicum* mutant M5. After isolation, the transformed M5 strain on thiamphenicol plates, colonies were picked and serially transferred in 2xYTG to allow time for recombination to occur. After ten serial transfers, the MazF counter-selection marker was induced with 40 mM lactose in the liquid medium such that all colonies containing the complete plasmid were killed. After plating on thiamphenicol/lactose plates, the only colonies remaining were those that had undergone a double-crossover event, thereby losing the plasmid containing the toxic *mazF* but retaining the antibiotic resistance marker at the *sigK* integration site. The confirmed integration strain M5 *sigK::fdh* was transformed with the flippase

plasmid p94FLP_asRepL, and selection was performed on dual antibiotic plates with both thiamphenicol and erythromycin. This strain was grown overnight in 10 mL of CGM supplemented with erythromycin, and a 10% inoculum was transferred to a fresh 10 mL tube of CGM which was incubated at 30 ºC for 6 hrs to ensure proper flippase activity. Dilutions were plated onto solid 2xYTG supplemented with erythromycin, and after observing colony formation, replica plates were made on 2xYTG plates supplemented with thiamphenicol. Colonies that showed growth on erythromycin but not thiamphenicol were screened by PCR to confirm the excision of the antibiotic resistance and the creation of the strain M5 *sigK::fdh_um*. Following confirmation, the flippase plasmid was removed by the lactose-induced expression of an asRNA fragment targeting the replicon *repL*.

5.2.2.2.2 Integration of the *fdh* gene in the *sigF*-gene site in strain 824

The *fdh* integration vector for the *sigF* locus was constructed in the same manner as the *sigK* integration vector. The *fdh* operon was PCR amplified from p94FDH, was phosphorylated, and ligated into NotI (NEB) digested, blunt-end, pKOSIGF_mazF to yield pKOSIGF::FDH_mazF. This vector was methylated and transformed into *C. acetobutylicum* 824 cells. After transformation, the strain *C. acetobutylicum* 824 (pKOSIGF::FDH_mazF) was serially transferred through 10 passages, induced with 40 mM lactose, and plated under lactose and thiamphenicol selection. Positive colonies for the double crossover integration strain, 824 *sigF::fdh*, were screened by PCR. The integrated thiamphenicol selection marker was excised using the flippase method described above to create the strain 824 *sigF::fdh_um*

5.2.2.2.3 Integration of the gene coding for the methylene-THF reductase and Fe-S protein in the *sigE* chromosomal locus site

The *mthfr/orf7/gly* integration vector was constructed by PCR amplifying the operon including both *orf7* (c37530) and *gly* (c37540) and cloning the digested PCR fragment into BamHI/SacII digested p95MCS to create p95ORF7. The annotated methylene tetrahydrofolate reductase (c37610) was PCR amplified and cloned into SacII/SphI digested p95ORF7 to create p95MRORF7. Due to the large size of the genes to be integrated, we modified the integration vector pKOD_MazF by removing the destination cassette and MLS^R and adding multi-cloning sites adjacent to both sides of the thiamphenicol resistance marker through PCR to create pKO_MazF. The integration vector was constructed by PCR amplifying a 535-bp fragment from the *sigE* region of C. *acetobutylicum* gDNA with AgeI/SphI overhangs and ligating this fragment into AgeI/SphI-digested pKO_MazF to create pKO_E1. A second 523-bp region of homology was PCR amplified from gDNA with MluI/NcoI overhangs and was ligated into MluI/NcoI-digested pKO_E1 to create pKOSIGE. The three-gene operon from p95ORF7 was amplified with flanking AscI sites and was ligated into MluI-digested pKOSIGE to form pKISigE::FeS/MTR/Gly_MazF.

5.2.3 Semi-quantitative RT-PCR (SQ-RT-PCR)

RNA was extracted using the RNEasy Kit (Qiagen, Hilden, Germany) with a modified protocol as follows: Cells were thawed on ice and washed and resuspended in 220 µl RNase-free SET Buffer + 20 µl Proteinase K. Samples were sonicated for 10 minutes using 15 second pulses on/off at 40% amplitude using a Sonic Dismembrator ultrasonic processor FB-505 (Thermo Fisher Scientific, Waltham, MA) with a 3” cup horn attachment (Qsonica, Newtown, CT). 1 ml of Trizol was added to each sample, split in two and another 400 µl Trizol was added to a final volume of 1 ml. 200 µl of

ice-cold chloroform was added and vigorously mixed for 15 seconds, then incubated at room temperature for 3 minutes. Samples were spun at <12000 rpm for 15 minutes at 4°C. The upper aqueous phase was mixed with 500 µl of 70% ethanol and RNEasy protocol was followed per manual. Sample concentration was determined using a Nanodrop ND-3300 spectrophotometer (Thermo Fisher Scientific, Waltham, MA). Concentrations ranged from ~50 ng/µl to 500 ng/µl depending on sample. cDNA was synthesized using a high-capacity cDNA reverse transcription kit (Applied Biosystems), and resultant cDNA was used for qRT-PCR.

5.2.4 Carbon monoxide dehydrogenase (CODH) enzyme assay

For the assay, cell pellet was re-suspended under anoxic conditions in appropriate volume of P buffer (0.5 mM KPO_4, 10 mM Sodium pyruvate, 10 mM dithiothreitol, 0.2 mM phenylmethylsulfonyl) pH 7.0 for an A_{600} ~10-20 in a minimum of 500 µl. Cell lysates were prepared under anoxic conditions by vortexing the re-suspended cells in 40 mg of glass beads for 1 min and then incubating on ice for 1 min, repeating the vortexing/cooling 5 times. Cell debris were removed by centrifugation at 16,000xg for 30 min at 4^{o}C. Carbon monoxide dehydrogenase (CODH) activity was determined by enzymatic activity assay under anoxic conditions. The assay was performed in 50 mM KPO_4 (pH 7.00) with 5mM methyl viologen used as an electron acceptor and 1 atm of CO as substrate. The reaction was initiated by adding 10 µl of the cell extract. The increase in A_{578} was recorded to determine enzyme activity. Reaction conditions without addition of the CO were used as baseline readings for all reactions.

5.3 Results

5.3.1 Identification of genes for functional WLP expression

In determining which genes are necessary for WLP expression in *C. acetobutylicum*, comparative genetic analysis of *C. ljungdahlii, C. carboxidivorans,* and *C. difficile* showed that the WL pathway genes of all three organisms are concentrated in a highly conserved, 18 kilobase region in their respective genomes (Fig. 5.1). While a subset of these genes was found to have homologues in *C. acetobutylicum*, the majority of the WLP genes are not found in *C. acetobutylicum* and need to be expressed heterologously through the use of replicating plasmids or genome integrations. The subset of genes required for expression includes both subunits of the acetyl-CoA synthase/carbon monoxide dehydrogenase complex (ACS/CODH) (Doukov, Iverson et al. 2002), both subunits of the corrinoid iron-sulfur protein (CFeSP) that carries the methyl group from tetrahydrofolate to acetyl-CoA (Ragsdale, Lindahl et al. 1987), the methyltransferase that transfers the methyl group from 5-methyltetrahydrofolate onto the CFeSP, two annotated nickel insertases that are involved in the creation and activation of the catalytic sites in the CODH/ACS complex (Jeon, Cheng et al. 2001), a ferredoxin-containing protein referred to as *orf7* that has been shown to regenerate the CFeSP active site (Hennig, Jeoung et al. 2012), and a formate dehydrogenase that directly reduces CO_2 to formate allowing for its assimilation into the 1-C pool by the formate-tetrahydrofolate ligase (Li 1966). This analysis identified more than 13 kb of heterologous DNA that needed to be actively expressed in *C. acetobutylicum*, which would be the largest set of heterologous genes ever overexpressed in *C. acetobutylicum*. Two strategies were developed to facilitate the transfer of such a large amount of genetic material. First, two compatible vectors

were identified that could be co-expressed in *C. acetobutylicum*, one of which contained the previously used RepL origin of replication and the other contained the pIP404 replicon from *C. perfringens* (Sloan, Warner et al. 1992). Additionally, it was proposed that the *mazF* counter-selection system could be used to integrate the remainder of the genetic material that would not fit on the replicating plasmids (Al-Hinai, Fast et al. 2012). An expression strategy was developed as shown in Figure 5.2. Genes were organized in synthetic operons such that all subunits of a given enzyme would be expressed from the same plasmid. Additionally, the most important non-native genetic elements, namely the CODH/ACS complex and the CFeSP, were chosen to be expressed from multi-copy plasmids rather than from chromosomal integrations to increase overall protein expression.

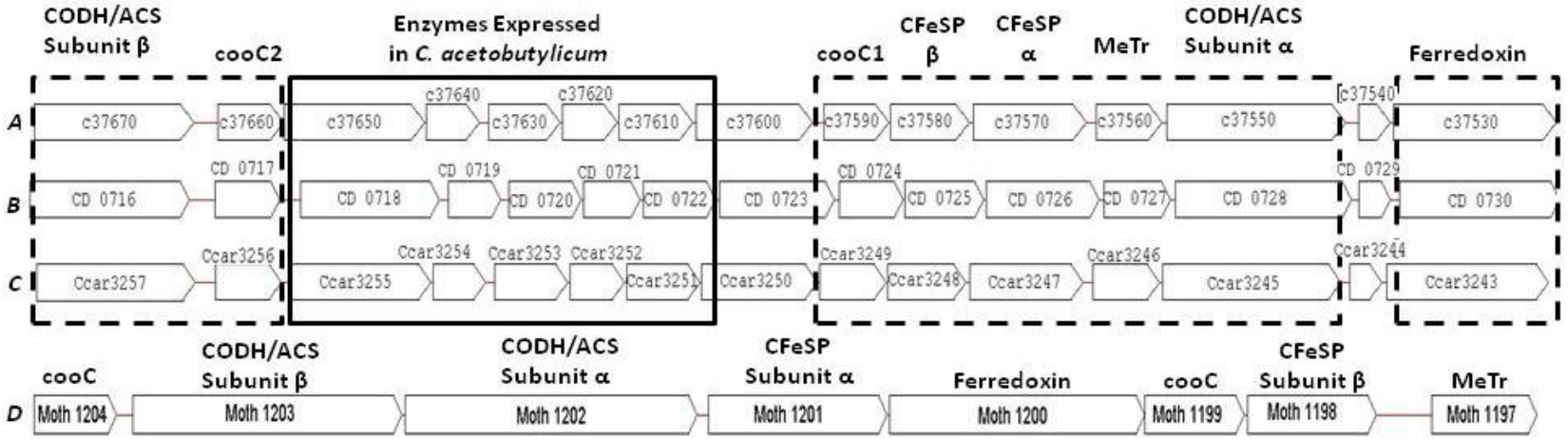

Figure 5.1. The WL region in the *C. ljungdahlii* (A), *C. difficile* (B), *C. carboxidivorans* (C), and *M. thermoacetica* (D) genomes. The region in the *Clostridium* acetogens is highly conserved in both order and homology. The genes involved in the *CO dehydrogenase/acetyl-CoA synthase* are also consolidated into one region of the thermophilic *M. thermoacetica* genome that has different organization than the other examined clostridia; however, the other *M. thermoacetica* WL genes are distributed throughout its chromosome. The dashed boxes contain the enzymes important to pathway functionality that are not present in *C. acetobutylicum*. The solid box indicates genes already present in *C. acetobutylicum*. The following genes are labeled with their gene product in the: CODH/ACS Subunits (α and β), which comprise the major parts of the CO dehydrogenase/CoA synthase; cooC1 and cooC2, nickel insertion proteins that are required to form the CODH/ACS active sites.

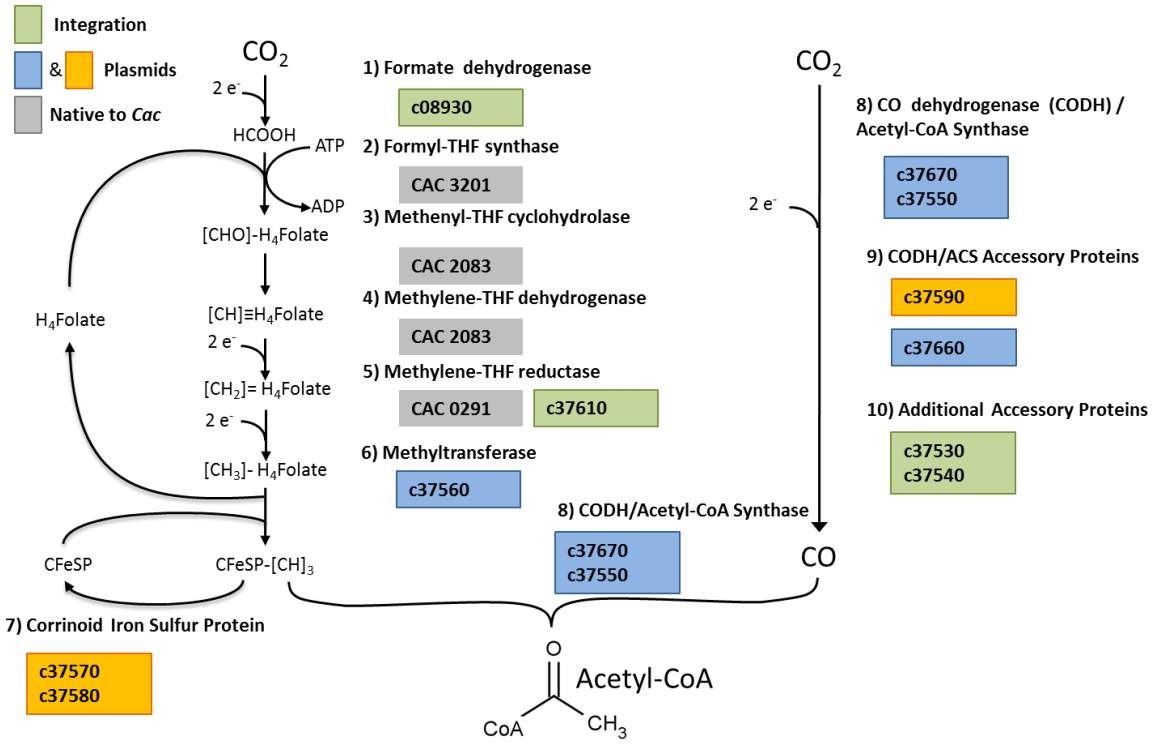

Figure 5.2. The Wood-Ljungdahl pathway with enzyme annotation adapted from (Ragsdale, Pierce et al. 2008). 2 e^- represents a reducing equivalent such as NADH, NADPH, or reduced ferredoxin. Grey boxed gene IDs indicate the WL pathway genes natively expressed in C. acetobutylicum. Blue and yellow boxes indicate genes expressed on p95ACS and pJIR_CFeSP, respectively. Green boxes indicate genes that have been integrated on the *C. acetobutylicum* chromosome.

Table 5.3. List of genes for expression/integration into *C. acetobutylicum*

p95_ACS		**pJIR_CFeSP**		**Integration**		
Function	Gene	Function	Gene	Function	Gene	Locus
ACS/CODH (β)	c37670	cooC1	c37590	FDH	c08930	Sig F
cooC2	c37660	CFeSP (β)	c37580	M-THF Reductase	c37610	Sig E
MeTr	c37560	CFeSP (α)	c37570	Ferredoxin	c37540	Sig E
ACS/CODH (α)	c37550			Glycine Cleavage H	c37530	Sig E

5.3.2 Integration of *fdh* in the *sigK*-gene locus of strain M5

Due to the number and size of the genetic elements that were originally considered necessary to convey WLP functionality in *C. acetobutylicum*, two integrations into the *C. acetobutylicum* chromosome were performed because not all of these genes could be expressed on our two-plasmid system. Integrations were performed using the mazF counter-selection marker that was previously developed in our lab (Al-Hinai, Fast et al. 2012).

The *C. ljungdahlii fdh* gene (c08930) was the first gene integrated into the *C. acetobutylicum* chromosome. While *C. ljungdahlii* contains three annotated *fdh* genes (c07020, c06990, and c08930), the c08930 gene was selected for integration in *C. acetobutylicum* because it does not contain a selenocysteine residue. The presence of a selenocysteine in the formate dehydrogenase enzymes of *C. ljungdahlii* complicates their expression in *C. acetobutylicum*. Because *C. acetobutylicum* does not natively express any selenoproteins, it does not have the translational tools required to insert the selenocysteine into a polypeptide (Kryukov and Gladyshev 2004). While there were some concerns that selenocysteine might play an important role in *fdh* functionality (Zinoni, Birkmann et al. 1987), another study had shown that reductive formate dehydrogenase activity could be observed in non-selenocysteine containing formate dehydrogenase (Alissandratos, Kim et al. 2013).

The integration of the *fdh* operon into the *sigK* locus of *C. acetobutylicum* mutant M5 served as a proof-of-concept that the MazF counter-selection marker could be used to integrate large fragments of heterologous DNA, and the p94FLP_asRepL plasmid could be used to excise the antibiotic resistance marker, allowing for successive integrations (Al-Hinai, Fast et al. 2012). Mutant M5 was chosen as a host

due to the relative ease of transformation as compared to *C. acetobutylicum* 824. The integration scheme, PCR confirmation of successful integration, and expression confirmation are shown in Figure 5.3.

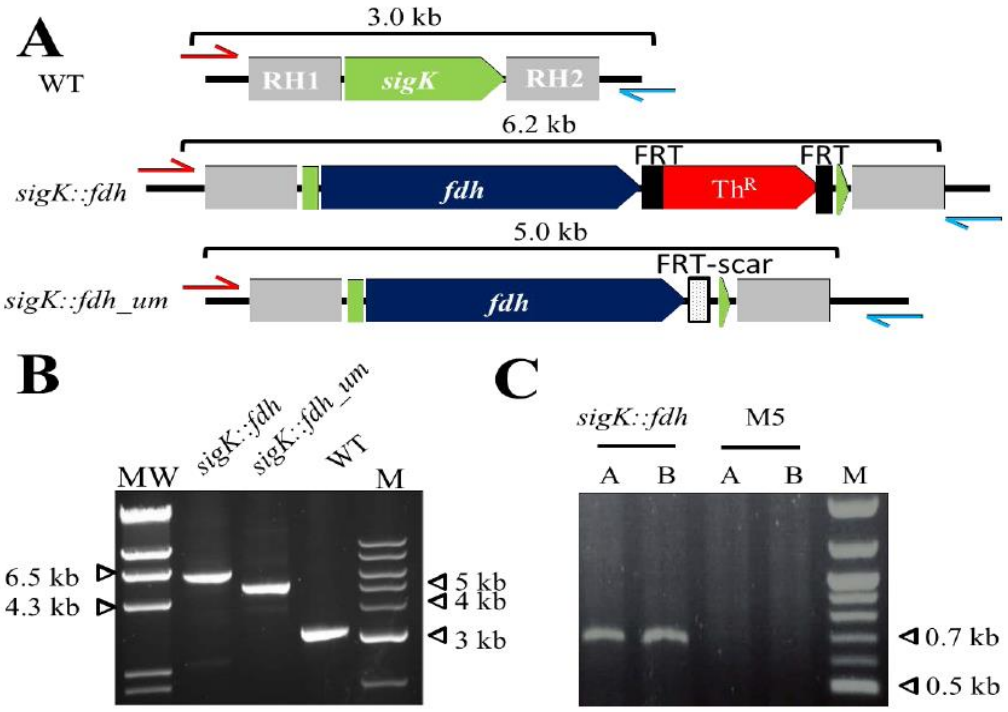

Figure 5.3. Isolation of the unmarked *fdh* integration into the *sigK* region on the *C. acetobutylicum* M5 chromosome (A) Schematic showing the *sigK* region of the M5 chromosome under WT, marked and unmarked *fdh* integration in the M5 *sigK* locus as well as the expected amplicon sizes with the indicated primers. (B) PCR confirmation of *fdh* integration strains with primers indicated in (A). The corresponding bands for the unmarked strain (*sigK::fdh_um*) and WT M5 strain are also shown. MW, λ *Hind*III digest ladder (NEB); M, 2-log ladder (NEB). (C) sq-RT-PCR confirming the expression of the integrated *fdh* gene in the M5 *sigK* locus. Primers were designed to amplify 700 bp in the middle of the *fdh* transcript. Two biological replicates are shown for both the integration strain as well as the control M5 strain. M, 2-log ladder (NEB).

5.3.2 Construction of 824 *fdh::sigF*

Originally, *C. acetobutylicum* mutant M5 was chosen for cloning because it does not produce solvents and is relatively easier to genetically modify than the wild type *C. acetobutylicum* 824. One consideration that we failed to consider is that 824

has two hydrogenase enzymes, both NiFe hydrogenase and Fe-Fe hydrogenase. Mutant M5 has only the Fe-Fe hydrogenase, which is now understood to be a production hydrogenase (i.e., produces H_2 from reducing equivalents). For the cells to uptake hydrogen to fix CO_2 using reducing equivalents from H_2, it is necessary to transfer the WL pathway genes into an organism with a NiFe hydrogenase. Therefore, the *fdh* integration was repeated in *C. acetobutylicum* 824. Additionally, because the NiFe hydrogenase is only expressed during solventogenesis (Jones, Paredes et al. 2008), *sigF* was chosen as an integration site over *sigK*, so that solventogenesis would not be disrupted through the *fdh* integration. The integration vector was constructed as described above with regions of homology targeting the *sigF* locus. The integration scheme and PCR confirmation are shown in Figure 5.4. Following integration, the thiamphenicol antibiotic resistance was removed to allow for successive integrations.

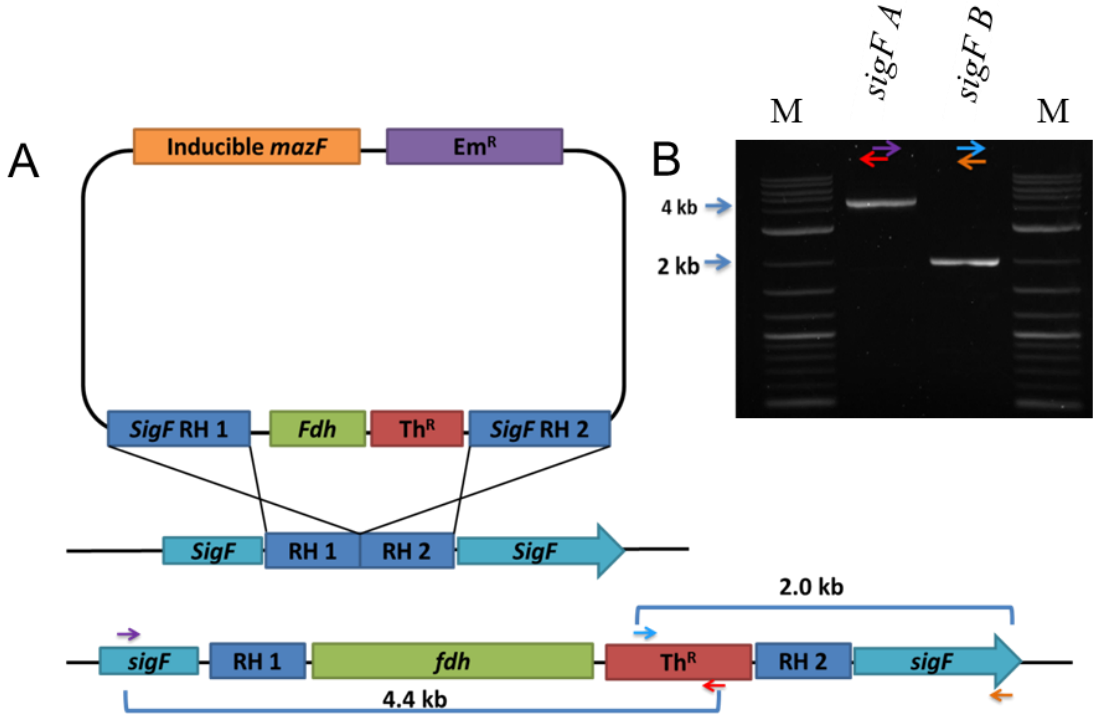

Figure 5.4. A) Scheme for integration of *fdh* into the 824 chromosome using the *mazF* counterselection marker. B) Integration was confirmed by PCR bands shown at right in the gel picture as well as from DNA sequencing.

5.3.3 Construction of 824 *sigF::fdh sigG::feS/mthfr/gcvH2*

The second operon for integration contained the *orf7* gene (c37540) involved in CFeSP regeneration and the glycine cleavage protein (*gcvH2*, c37530), which are natively expressed from a polycistronic operon in *C. ljungdahlii*, as well as an annotated methylene tetrahydrofolate reductase gene (c37610). In order to carry out this integration, pKISigE::FeS/MTR/Gly_MazF wast transformed into 824 *fdh::sigF_um*, and integration mutants were obtained as discussed above. The integration scheme and PCR confirmation are shown in Figure 5.5. Following PCR and sequencing confirmation, the antibiotic resistance marker was removed using p94FLP to allow for the expression of replicating plasmids using the thiamphenicol

resistance marker. This is the first example of two successive integrations of heterologous genes into the *C. acetobutylicum* chromosome, and fully demonstrates that the *mazF* counterselection marker can be a powerful tool for clostridial strain engineering.

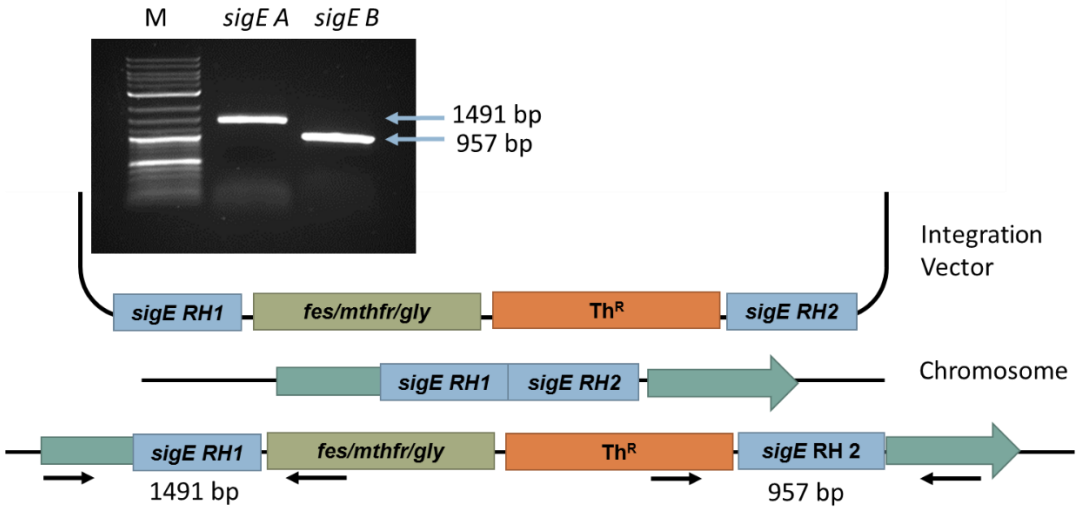

Figure 5.5. Integration of the *fes/mthfr/gly* operon into the into 824 *sigF::fdh* chromosome using *mazF* counterselection marker has been confirmed from the PCR bands shown in the gel image as well as DNA sequencing.

5.3.4 Characterizing the WLP Strain *C. acetobutylicum* 824 *sigF::fdh sigG::feS/mthfr/gcvH2* (p95ACS, pJIRCFeSP)

After the construction of the 824 strain containing both unmarked integrations, the two replicating plasmids were transformed into the mutant strain to create 824 *sigF::fdh sigG::feS/mthfr/gcvH2* (p95ACS, pJIR_CFeSP), which contained the full set of WLP genes that we believed were necessary for functional expression in *C. acetobutylicum*.

5.3.4.1 mRNA expression confirmed by sq-RT-PCR

To determine whether the synthetic operons on both plasmids were successfully expressed, we performed semi-quantitative reverse-transcription PCR (sq-RT-PCR) on mRNA from both expression vectors, p95ACS and pJIR_CFeSP. RNA was extracted from samples at the mid-exponential phase (6 hr), early stationary phase (12 hr), and stationary phase (24 hr). The total RNA was reverse transcribed and PCR was performed on 50 ng of cDNA. The p95ACS plasmid contains both subunits of the CODH/ACS complex as well as the methyltransferase required to transfer the methyl-group from 5-methyltetrahydrofolate onto the CFeSP. Expression of all three genes was confirmed using sq-RT-PCR on RNA collected from 824 (p95ACS).

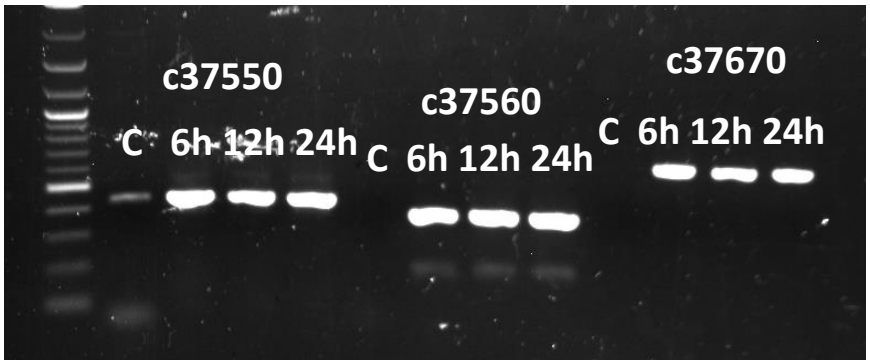

Figure 5.6. Semi-quantitative RT-PCR on mRNA from p95ACS strain to show expression of *C. ljungdahlii* genes c37550, c37560, and c37670 at 6, 12, and 24-hour timepoints as well as negative controls with the RNA template.

Similarly, mRNA expression from pJIR750_CFeSP was confirmed using primers for the corrinoid protein subunits (CFeSP α & β) and cooC1 (nickel inserting

protein) that are under the control of PTA promoter was confirmed as shown in Figure 5.7. As a negative control, equal quantities of RNA were used as the template for PCR to test for DNA contamination.

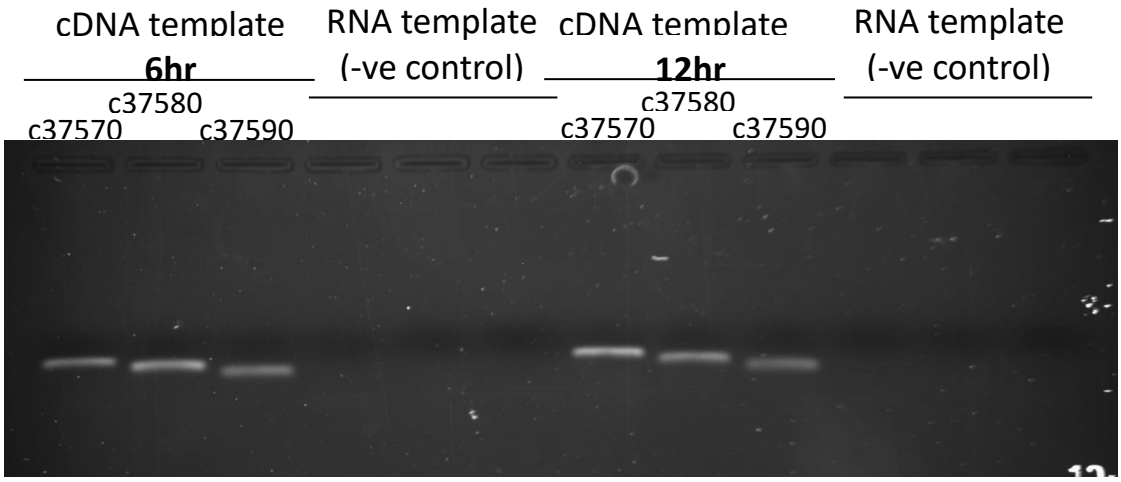

Figure 5.7. Semi quantitative RT-PCR on pJIR750_CFeSP strain showing the mRNA expression of corrinoid protein subunits CFeSP α (c37570), CFeSP β (c37580) and Ni inserting protein (c37590). Mid-exponential (6 hr) and early stationary phase (12 hr) cultures are shown.

5.3.4.2 *In vitro* CODH assay shows that the CODH is actively expressed from p95ACS

In addition to semi-quantitative RT-PCR, we interrogated the enzyme activity of the recombinant *C. ljungdahlii* CODH in *C. acetobutylicum*. Carbon monoxide dehydrogenase (CODH) is a part of carbon monoxide dehydrogenase/acetyl-CoA synthase (CODH/ACS) enzyme complex and performs a crucial step in reducing CO_2 to form CO, which can then be combined with a methyl-group to form acetyl-CoA. CODH activity is measured through the oxidation of CO to CO_2, which uses methyl viologen as an in vitro electron acceptor. One can observe the reaction at A_{578} due to

the increase in absorbance of methyl viologen Figure 5.8. The specific activity of the heterologous CODH in *C. acetobutylicum* was observed to be 0.51 ± 0.03 U/mg ($mMmin^{-1}mg^{-1}$) for two biological replicates, in comparison to an activity of 0.00 U/mg in wild-type. As positive control, the CODH assay was performed with *C. ljungdahlii* extracts from cells grown on CO_2+H_2, and CODH activity was observed to be 3.55 U/mg. While the CODH activity in *C. acetobutylicum* is not as high as that of *C. ljungdahlii*, the specific activity is of the same order of magnitude, and could potentially be increased through expression and media optimization.

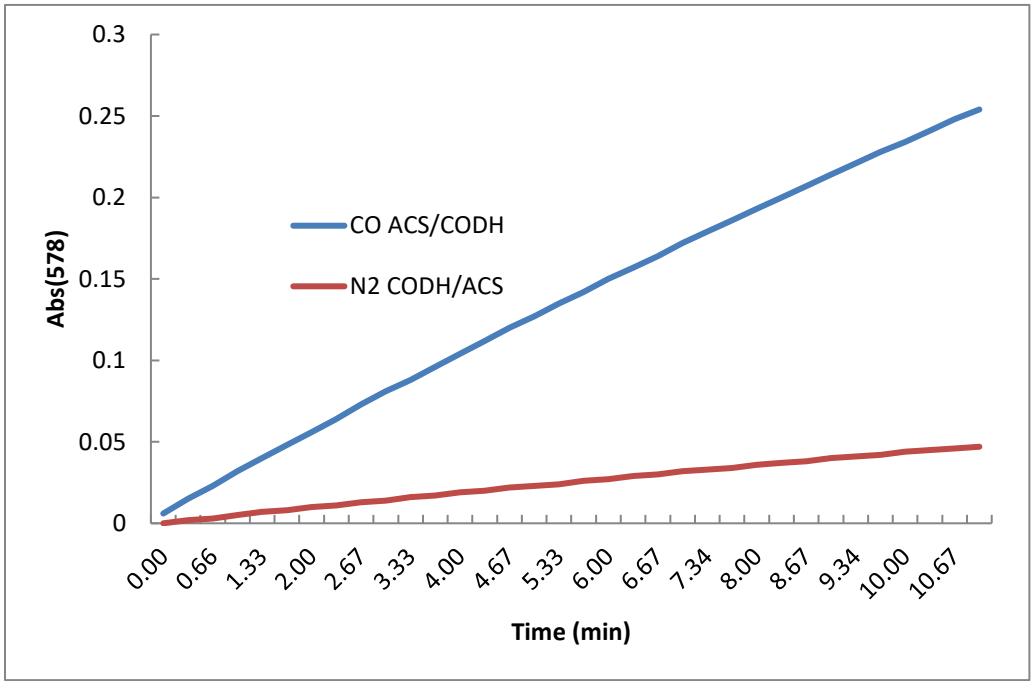

Figure 5.8. *In vitro* CODH Assay. A representative replicate for the *in vitro* enzyme assay of heterologous CODH expressed in *C. acetobutylicum*. CODH activity is determined by the reduction of methyl viologen (A_{578}) in the presence of CO as compared to the N_2 control. Two biological replicates showed an average activity of 0.51 ± 0.03 U/mg.

5.3.4.3 Labeling from ^{13}C bicarbonate and ^{13}C formate

After construction of the final *C. acetobutylicum* strain containing two sets of integrated genes and the two plasmids that contain the remainder of the WL pathway genes, we began testing the resulting strain for evidence of CO_2 flux into metabolites and biomass using ^{13}C labeling. We chose to use ^{13}C sodium bicarbonate for one set of cultures, which would label metabolites from both the Eastern and Western branches of the WL pathway if all the incorporated genes were functioning *in vivo*. Another set of cultures was performed using ^{13}C-labeled sodium formate in addition to the ^{13}C labeled bicarbonate. The formate was added to provide a carbon source for the Eastern branch of the WL pathway if the formate dehydrogenase enzyme from *C. ljungdahlii* was not functional in *C. acetobutylicum.* GC-MS analysis was performed by Maciek Antoniewicz and Jennifer Au. Results from this analysis are shown in Figures 5.9 and 5.10.

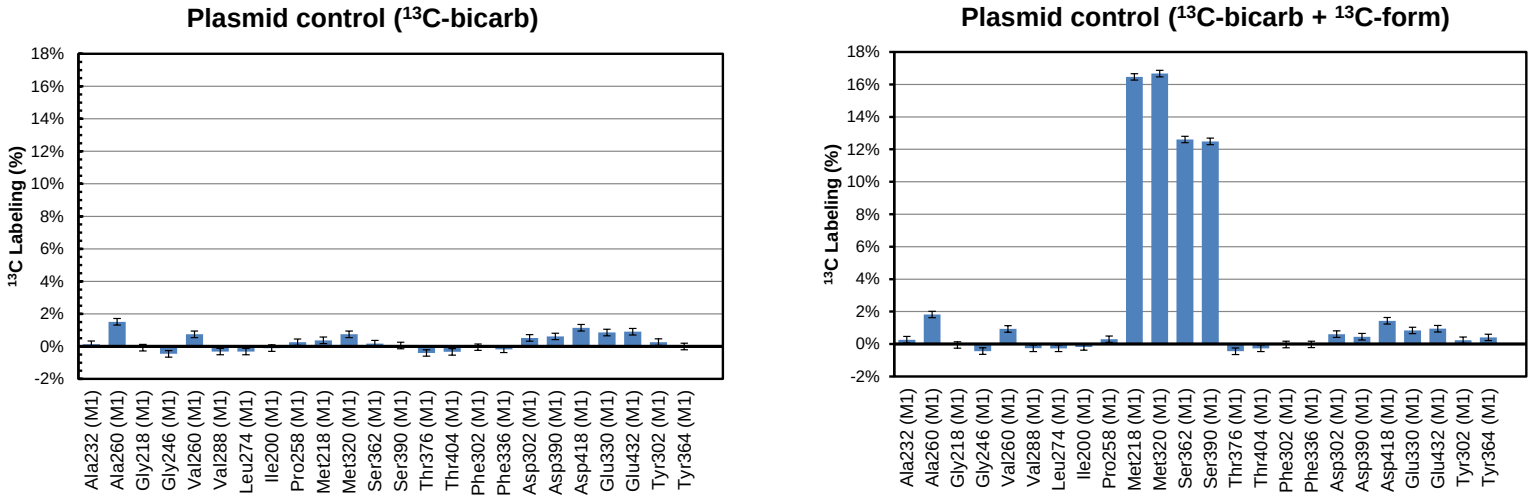

Figure 5.9. Labeling profiles obtained from the WL pathway final strain grown with ^{13}C-bicarbonate (left) and ^{13}C-bicarbonate/^{13}C-formate (right). Labeling is observed at alanine, aspartate, and glutamate for the bicarbonate label and at methionine and serine for the formate label. The apparent label at valine is likely due to noise.

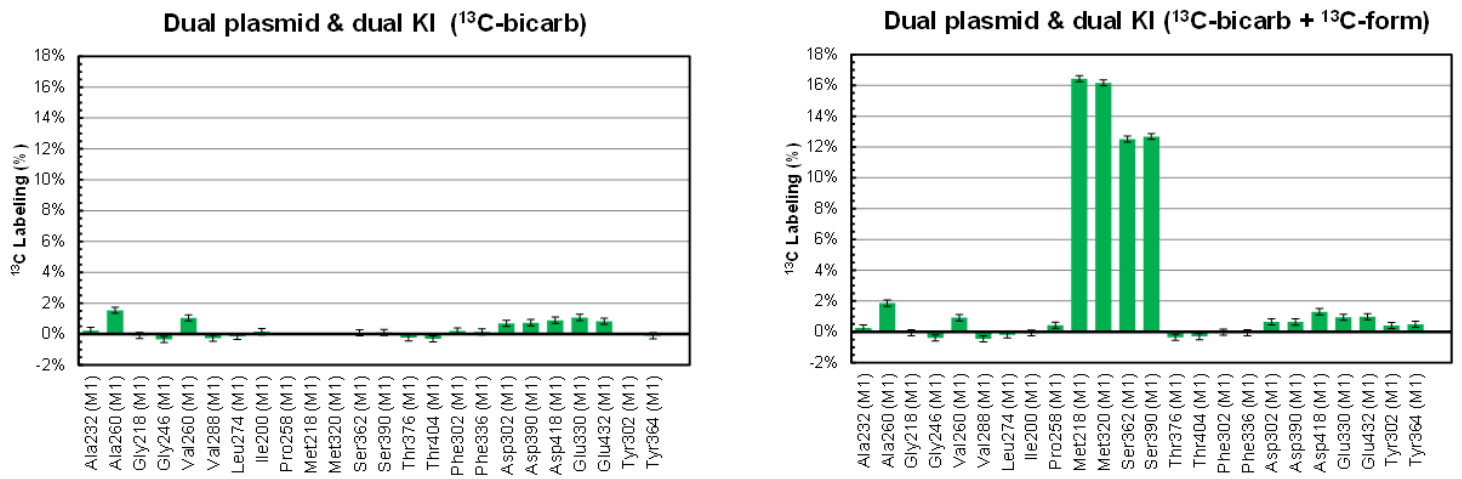

Figure 5.10. Labeling profiles obtained from the plasmid control grown with 13C-bicarbonate (left) and 13C-bicarbonate/13C-formate (right). As with the WL pathway strain, labeling is observed at alanine, aspartate, and glutamate for the bicarbonate label and at methionine and serine for the formate label

From the bicarbonate sample (left panel of Figure 5.9 and 5.10), we can observe labeling in alanine, asparagine, and glutamate, which are labeled by the pyruvate carboxylation reactions that occur natively in *C. acetobutylicum* shown in Figure 5.11.

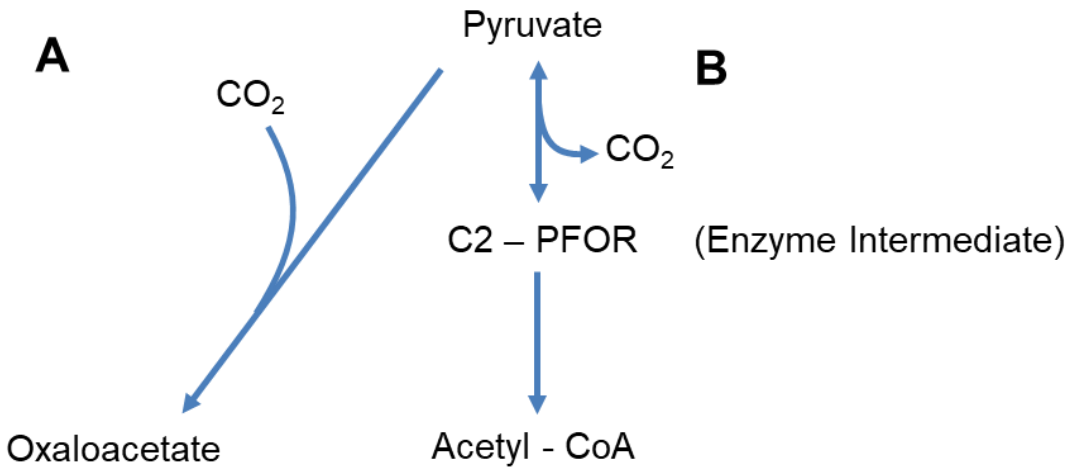

Figure 5.11. Carboxylation reactions in native *C. acetobutylicum*. *C. acetobutylicum* can incorporate gaseous CO_2 through two reactions involving pyruvate. A) Pyruvate carboxylase catalyzes the irreversible carboxylation of pyruvate to form oxaloacetate, which requires the hydrolysis of ATP (not shown). B) The decarboxylation of pyruvate to form acetyl-CoA proceeds in two steps. In the first step, pyruvate is reversibly decarboxylated, and the remaining two carbons form an intermediate with the pyruvate ferredoxin oxidoreductase (PFOR). The two-carbon intermediate can be carboxylated to form pyruvate transferred irreversibly onto CoA to form acetyl-CoA

When formate is included in the labeling pool (right panel of Figure 5.9 and 5.10), we observe labeling of methionine and serine, which is consistent with labeling of the C_1-pool, shown in Eqs. 4-6.

$$\text{Formate} + \text{THF} \rightarrow \text{Formyltetrahydrofolate (C1 Pool)} \quad \text{(Eq. 4)}$$

$$\text{Glycine} + \text{C1} \rightarrow \text{Serine} \quad \text{(Eq. 5)}$$

$$\text{Aspartate} + \text{C1} \rightarrow \text{Methionine} \quad \text{(Eq. 6)}$$

This indicates that the *C. acetobutylicum* is successfully assimilating formate into 10-formyltetrahydrofolate, which is a necessary step for WLP functionality. However, because we do not observe C_1-pool labeling in the strain grown in ^{13}C-bicarbonate, we know that the formate dehydrogenase is not functioning to convert the $^{13}CO_2$ into ^{13}C-formate. Furthermore, despite observing C_1 labeling, labeling is not observed for the amino acids derived from acetyl-CoA, including leucine, isoleucine, and proline. This indicates that there is no flux from the C_1 pool to the acetyl-CoA synthase.

From the labeling pattern, we can determine a subset of enzymes that should be targeted to achieve WLP functionality. First, the formate dehydrogenase (c08930) is clearly not functioning in the reductive direction. Perhaps this is due to the lack of selenocysteine in this enzyme, as discussed above. Ultimately it may be necessary to identify other non-seleno formate dehydrogenase proteins for expression; however, for the purposes of this proof of concept, we can simply feed the organism formate to circumvent this enzyme. A greater concern is the absence of labeling observed for the acetyl-CoA derived amino acids as well as acetate and butyrate which will be discussed below.

5.4 Discussion

The construction of the heterologous WLP in *C. acetobutylicum* required the expression of more heterologous genes than had previously been demonstrated in a clostridial host. To accomplish the expression of more than 13 kbp of additional genetic material, a dual-plasmid system was constructed using two compatible replication origins. Additionally, two successive integrations were performed to integrate a non-selenocysteine containing formate dehydrogenase on the chromosome at the *sigF* locus and a synthetic operon containing a methylene tetrahydrofolate reductase, the Fe-S protein, and glycine cleavage protein at the *sigE* locus. This is the first genetic engineering effort in clostridia to utilize two successive integration steps and two replicating plasmids.

The resulting strain, 824 *sigF::fdh sigG::feS/mthfr/gcvH2* (p95ACS, pJIR_CFeSP), was characterized for mRNA expression using SQ-RT-PCR and activity of the heterologously expressed CODH was confirmed by *in vitro* enzyme assay. However, labeling analysis did not show any ^{13}C labeling incorporation into acetyl-CoA or formate. The implications of the labeling pattern are two-fold. First, because the strain grown in the presence of labeled CO_2 did not show a different labeling pattern than the plasmid control, and neither the plasmid control nor the recombinant strain showed the same labeling pattern as the ^{13}C formate labeled strain, we can conclude that the integrated formate dehydrogenase is non-functional. The lack of FDH functionality may be because we had selected a non-selenocysteine containing formate dehydrogenase gene (c08930) for expression. Most of the well-characterized formate dehydrogenase genes from acetogenic host uses the alternative amino acid, selenocysteine, in their active sites (Yamamoto, Liu et al. 1982, Zinoni, Birkmann et al. 1987, Gollin, Li et al. 1998, Alissandratos, Kim et al. 2013). However, *C.*

acetobutylicum does not have the prerequisite genes for the synthesis of selenocystine or for its incorporation into proteins, which had motivated the choice of a non-selenocysteine FDH. One potential alternative would be to use the formate dehydrogenase from *C. pasteurianum*, a close relative of *C. acetobutylicum*. While *C. pasteurianum* is not a native acetogen and is not able to fix CO_2 for autotrophic growth, extracts of *C. pasteurianum* have been shown to catalyze the reduction of CO_2 to formate (Jungermann, Kirchniawy et al. 1970), and its annotated formate dehydrogenase gene does not contain a selenocysteine residue. Alternatively, formate can also be produced from CO_2 through the reductive carboxylation of acetyl-CoA to pyruvate by a fully reversible pyruvate ferredoxin oxidoreductase, and the resulting pyruvate can be cleaved to form pyruvate and acetyl-CoA by a pyruvate formate lyase (Jungermann, Thauer et al. 1968).

Secondly, the lack of labeling in acetate and butyrate even when the cells are supplied with ^{13}C labeled formate shows that the link between the 1-C folate pool (i.e., methylene-THF) and the ACS is broken. This reaction is catalyzed by four separate enzymes: the methylene-THF reductase, 5-methyltetrahydrofolate methyltransferase, the CFeSP, and the CODH/ACS complex. The most significant of these is the CODH/ACS complex. In this chapter, we showed *in vitro* activity of the CODH in the oxidative direction. However, it is unclear whether the heterologously expressed CODH can act in the reductive direction to produce CO *in vivo*, which will be discussed further in Chapter 6. Additionally, the ACS subunit, which is responsible for catalyzing the condensation of the methyl-group with CO to form acetyl-CoA, is difficult to assay *in vitro*, and has thus only been demonstrated on purified proteins (Raybuck, Bastian et al. 1988). Chapter 6 will focus on detecting the expression of this

protein via protein blotting and also developing an *in vivo* enzyme assay to determine its activity.

While confirming the expression and characterizing the activity of the CODH/ACS complex is the most urgent goal for achieving WLP activity, it was discovered that the heterologous methylene-THF reductase that we express is likely just one-subunit of a multimeric complex (Bertsch, Öppinger et al. 2015). Furthermore, the native methylenetetrahydrofolate reductase from *C. acetobutylicum* is a bifunctional enzyme that catalyzes not only the reduction of 5,10-methylenetetrahydrofolate to 5-methyltetrahydrofolate but also the transfer of the methyl-group from 5-methyltetrahydrofolate to homocysteine to form methionine. Therefore, there may not be any available 5-methyltetrahydrofolate available for condensation into acetyl-CoA, requiring the expression of a second methylene-THF reductase.

Chapter 6

CHARACTERIZING THE ENGINEERED WOOD-LJUNGDAHL PATHWAY IN CLOSTRIDIUM ACETOBUTYLICUM

6.1 Introduction

The previous chapter (Chapter 5) focused on the incorporation of a broad set of Wood-Ljungdahl pathway genes in the solvent-producing *C. acetobutylicum*, and discussed some of the advances in clostridial genetics including the expression of multiple co-existing plasmids and multiple sequential integrations that were required to incorporate the Wood-Ljungdahl pathway genes into *C. acetobutylicum*. Still, ^{13}C-labeling experiments showed that the expression of the selected Wood-Ljungdahl pathway genes in *C. acetobutylicum* was not sufficient to allow for the carbon fixation into acetyl-CoA, but ^{13}C formate did lead to label incorporation in the amino acids methionine and serine. These two amino acids are directly labeled from 5,10-methylenetetrahydrofolate (Figure 6.1) (Amador-Noguez, Feng et al. 2010), a key metabolite of the Eastern branch of the Wood-Ljungdahl pathway. The labeling of these amino acids indicates that the native *C. acetobutylicum* 1-C pool genes that are necessary for synthetic Wood-Ljungdahl pathway functionality are operating as expected to convert formate into 5,10-methylenetetrahydrofolate. In the original strategy to engineer the synthetic Wood-Ljungdahl pathway in *C. acetobutylicum*, we had planned on using the native 5,10-methylenetetrahydrofolate reductase (CAC_0291) to catalyze the conversion of 5,10-methylenetetrahydrofolate to 5-methyltetrahydrofolate, which is a necessary intermediate in the generation of the

methyl-group in acetyl-CoA. However, the native methylenetetrahydrofolate reductase is a bifunctional enzyme that catalyzes not only the reduction of 5,10-methylenetetrahydrofolate to 5-methyltetrahydrofolate but also the transfer of the methyl-group from 5-methyltetrahydrofolate to homocysteine to form methionine. If both the reduction reaction and the methyl transferase reaction happened simultaneously, there would be no available 5-methyltetrahydrofolate available to provide a methyl-group to the corrinoid iron-sulfur protein and ultimately the acetyl-CoA synthase, thereby placing a bottleneck in the synthetic Wood-Ljungdahl pathway. To overcome this, we propose the addition of a heterologous methylenetetrahydrofolate reductase. The methylenetetrahydrofolate reductase from *E. coli* was chosen as a source rather than the *C. ljungdahlii* methylenetetrahydrofolate reductase because the protein in *E. coli* has been shown to be monomeric and interact primarily with NADH as an electron carrier (Sheppard, Trimmer et al. 1999). The methylene tetrahydrofolate reductase from *C. ljungdahlii* has not been purified or characterized; however, other acetogenic methylenetetrahydrofolate reductase proteins are multi-component enzyme complexes (Bertsch, Öppinger et al. 2015), and gene homology suggests that the methylenetetrahydrofolate reductase from *C. ljungdahlii* is part of an enzyme complex, though the components are not fully annotated or experimentally verified.

This chapter will focus on the efforts to modify the synthetic Wood-Ljungdahl pathway expression system in *C. acetobutylicum* through the inclusion of a codon-optimized methylenetetrahydrofolate reductase, to characterize the modified WLP expression system through examination of the mRNA and protein level, and to

measure the *in vitro* activity of the CODH/ACS complex in its ability to convert CO_2 into CO.

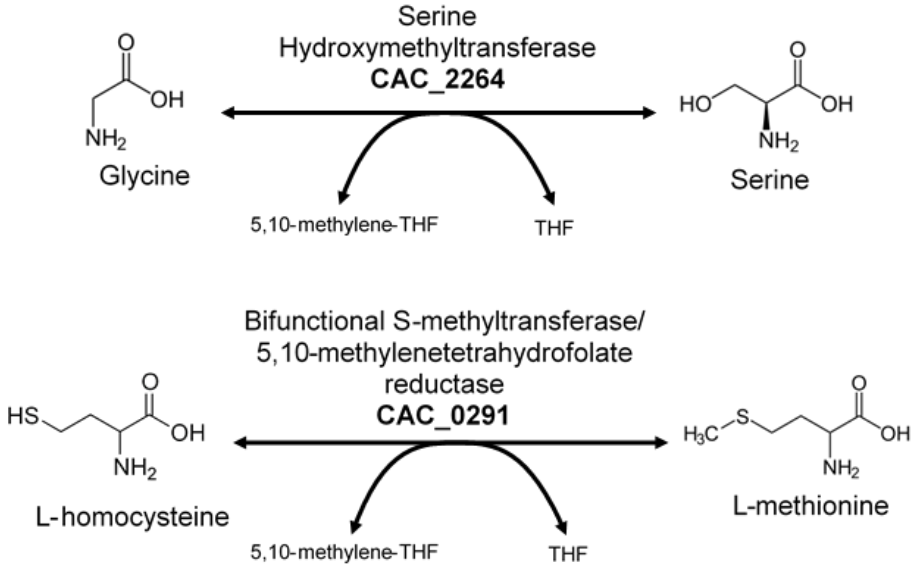

Figure 6.1. One-carbon metabolism of *C. acetobutylicum* leads to labeling of methionine and serine in the presence of ^{13}C formate. Formate attached to the tetrahydrofolate coenzyme through the formyltetrahydrofolate synthase. The resulting 10-formyltetrahydofolate is dehydrated and reduced to form 5,10-methylenetetrahydrofolate, which is incorporated into amino acids via the reactions shown above.

6.2 Materials and Methods

6.2.1 Bacterial strains, media, and growth conditions

The bacterial strains and plasmids used in this work are listed in Table 5.1. *Escherichia coli* strains were grown aerobically at 37º C and 250 rpm in liquid LB media or solid LB with agar (1.5%) media supplemented with the appropriate antibiotics (ampicillin at 100 µg/mL, chloramphenicol at 35 µg/mL, or kanamycin 25 µg/mL). *E. coli* strains were stored at -85 ºC in 15% glycerol. *C. acetobutylicum* ATCC 824 was grown anaerobically in liquid clostridial growth media (CGM), liquid 2x yeast-tryptone-glucose (pH 5.2) (2xYTG), and solid 2xYTG media at 37º C. Plasmid-containing and knockout/integration strains were grown with appropriate antibiotics (erythromycin at 100 µg/mL and thiamphenicol at 10 µg/mL). For spore forming strains, colonies were grown on 2xYTG for at least 5 days and heat shocked for 10 minutes at 80º C prior to growth, which serves to kill vegetative cells and ensure the presence of the megaplasmid pSOL1. *C. ljungdahlii* was grown in American Type Culture Collection (ATCC) medium 1754. Growth was monitored by measuring the optical density at 600 nm (OD_{600nm}). For CO-formation studies, a 5% inoculum of mid-exponential phase (OD_{600nm} of 0.8-1.5) was used to inoculate 27 ml serum bottles (Wheaton), with 5 ml of culture media and 22 ml of gas headspace.

Table 6.1 Strains and plasmids

Bacterial strain or plasmid	**Relevant Characteristics**	**Source or Reference**
E. coli strains		
ER2275	*hsdR mcrA recA1 endA1*	NEB
Turbo	F' *proA*$^{+}$*B*$^{+}$ *lacI*^{q} Δ*lacZM15 / fhuA2* Δ*(lac-proAB) glnV galK16 galE15 R(zgb-210::Tn10)*Tet^{S} *endA1 thi-1* Δ*(hsdS-mcrB)5*	NEB
Clostridium strains		
ATCC 824	Wild-type strain	ATCC
Plasmids		
pAN1	Cm^{r}; Φ3T I gene; p15A origin	(Mermelstein and Papoutsakis 1993)
pAN2	Amp^{r}; Φ3T I gene; p15A origin	(Mermelstein and Papoutsakis 1993)
pAN3	Km^{r}; Φ3T I gene; p15A origin	(Al-Hinai, Fast et al. 2012)
p95ACS	Amp^{r} MLS^{r}; RepL; *thl* promoter; *acsA, acsB, cooC2, meTr*	This study
p95ACS_MetF	Amp^{r} MLS^{r}; RepL; *thl* promoter; *acsA, acsB, cooC2, meTr, metF*	This study
p95MetF	Amp^{r} MLS^{r}; RepL; *thl* promoter; *metF*	This study
pJIR750	Cm/Th^{r}; pIP404; *lac* promoter	(Bannam and Rood 1993)
pJIR750_pta	Cm/Th^{r}; pIP404; *pta* promoter	This study
pJIR750_CFeSP	Cm/Th^{r}; pIP404; *pta* promoter; *acsC, acsD, cooC1*	This study
C. ljungdahlii DSM-13528	Wild-type Strain	DSMZ

Table 6.2 List of primers used for plasmid construction, sq-RT-PCR, and Northern probe generation

Primer	**Sequence (5'- 3')**	**Description**
MetF_F	TAGAGCTCTAGATATAAGGAGGTTGTACTATGGGATATA	Amplify *metF*
MetF_R	ATACCGCGGTTACTTAAATAATTTTTACTTAGCAGT	Amplify *metF*
MetF_BamHI	ACTCCCATGGATAGGAGGTCATCTGAACATGGATAAATT	Amplify *metF*
MetF_KasI	TAGCACGCGTCTACATTATTGGATCCATCTTTAATGCA	Amplify *metF*
p94_AcsI_F	TTAATAGCATGCTCGACTGTGGATGGAGTTAA	Amplify *metF* operon
p94_AcsI_R	TTAATCGCATGCTGACCATGATTACGAATTCTATGA	Amplify *metF* operon
MetF_Gibson_F	GATCCCAATCTAGAATCCGCGGTAGCATGCATCCATGGTTGAGCTCATGGACGCGTAAAG	Gibson Assembly into p95ACS
MetF_Gibson_R	GCGCCTTTACGCGTCCATGAGCTCAACCATGGATGCATGCTACCGCGGATTCTAGATTGG	Gibson Assembly into p95ACS
RT MetF F	CTGAAATGGCACCTCCAAAG	Sq-RT PCR
RT MetF R	CTCCATCGCAAAGTCCTGAT	Sq-RT PCR
RT c37550 F	GCTTATGCCCTAGTCTGTGAAG	Sq-RT PCR
RT c37550 R	CTGCAACCTTTCCTGGGATTA	Sq-RT PCR
RT c37560 F	GTGCTGATCCAAACGGTACA	Sq-RT PCR
RT c37560 R	CTGTTATGTCTTCCTGGCTTC	Sq-RT PCR
RT c37660 F	TGTAGCAGGTAAGGGTGGTA	Sq-RT PCR
RT c37660 R	CATCGGCACAACTCCTACTAAA	Sq-RT PCR
RT c37670 F	GCCTGTCAGTGTGAGGTTAAA	Sq-RT PCR
RT c37670 R	TCCACATTCCCGAAGACAATAC	Sq-RT PCR

6.2.2 Plasmid and Strain Construction

All restriction endonucleases, ligase, and NEBuilder HiFi DNA Assembly Master Mix were purchased from New England Biolabs (NEB), Ipswitch, MA. Codon optimization was performed using the Integrated DNA Technologies Codon Optimization Tool (Integrated DNA Technologies, Coralville, IA).

6.2.2.1 Construction of p95_ACS_metF

The methylenetetrahydrofolate reductase (*metF*) from *E. coli* was codon optimized and synthesized as a gBlock. The gBlock was PCR amplified with BamHI and KasI overhangs and ligated into BamHI/KasI digested p95_MCS to create p95MetF. To insert the *metF* gene into the synthetic WLP operon from p95ACS, the *metF* gene was PCR amplified with overhangs to allow for Gibson assembly. The p95ACS vector was digested with NcoI and column purified. The two fragments were then assembled using Gibson assembly to form p95ACS_MetF.

6.2.3 RNA Extraction and Northern Blots

RNA was extracted using the RNEasy Kit (Qiagen, Hilden, Germany) with a modified protocol as follows: Cells were thawed on ice and washed and resuspended in 220 µl RNase-free SET Buffer + 20 µl Proteinase K. Samples were sonicated for 10 minutes using 15 second pulses on/off at 30% amplitude using a Sonic Dismembrator ultrasonic processor FB-505 (Thermo Fisher Scientific, Waltham, MA) with a 3” cup horn attachment (Qsonica, Newtown, CT). 1 ml of Trizol was added to each sample, split in two and another 400 µl Trizol was added to a final volume of 1 ml. 200 µl of ice-cold chloroform was added and vigorously mixed for 15 seconds, then incubated at room temperature for 3 minutes. Samples were spun at >12,000 rpm for 15 minutes at 4°C. The upper aqueous phase was mixed with 500 µL of 70% ethanol and RNEasy

protocol was followed per manual. Sample concentration was determined using a Nanodrop ND-3300 spectrophotometer (Thermo Fisher Scientific, Waltham, MA). Concentrations ranged from ~1.2 µg/µl – 3.6 µg/µl depending on sample. For semi-quantitative RT-PCR (SQ-RT-PCR), cDNA was synthesized from 2 µg or total RNA using a high-capacity cDNA reverse transcription kit (Applied Biosystems). For Northern blots, 10 µg RNA was added to an appropriate volume of loading dye (NEB, Ipswitch, MA) and heated at 65 ºC for 10 minutes. The RNA was loaded and separated on a denaturing 1% agarose gel in MOPS buffer with formaldehyde at 90V for 2 hr. The gel was rinsed twice for 15 minutes in DEPC-treated water, followed by incubation for 10 minutes in 20x SSC buffer. The gel was blotted overnight onto nitrocellulose through the capillary method using a reservoir of 20x SSC. RNA was immobilized on the membrane by UV crosslinking using a Stratalinker 2400 (Stratagene, La Jolla, CA). DNA probes were synthesized by PCR. Radiolabeling was performed using the Affymetrix Sequenase Random Primer Labeling Kit (Affymetrix, Santa Clara, CA) according to the manufacturer recommendations. Briefly, 25ng of the template DNA was mixed with random primers and denatured by heating to 98 ºC for 5 minutes. The mixture was chilled on ice for 2 minutes to allow primers to anneal to the DNA. After chilling the DNA mixture, nucleotides (-dCTP), [α-^{32}P]-dCTP, and polymerase were added. The labeling reaction was incubated at 37 ºC for 10 minutes. The unincorporated nucleotides and primers were column purified using the QIAquick PCR purification kit (Qiagen, Hilden, Germany). Prehybridization of the RNA membrane was performed at 42 ºC for 4hr with ULTRAhyb Ultrasensitive Hybridization Buffer (Fisher Scientific, Waltham, MA). The radiolabeled probes were added to the prehybridization buffer and incubated overnight in the hybridization oven

at 42 ºC. Following hybridization, the membranes were washed twice in 0.1X SSC, 0.1% SDS for 10 minutes, and then exposed to a phosphor screen for 24 hrs.

6.2.4 Western Blots and Dot Blots

Cell lysates of *C. ljungdahlii* and *C. acetobutylicum* were prepared by pelleting 30-50 mL of *C. ljungdahlii* or 3-10 mL of *C. acetobutylicum*. The cell pellets were resuspended in 500 µL of 1x SDS buffer and sonicated for 10 minutes using 15 seconds pulse on/off at 40% amplitude using a Sonic Dismembrator ultrasonic processor FB-505 (Thermo Fisher Scientific, Waltham, MA) with a 3" cup horn attachment (Qsonica, Newtown, CT). Protein was quantified by the Bio-Rad RC DC Protein Assay kit (Hercules, CA). 50 µg of total protein was resolved on 4-20% PAGE gels along with 5 µL of the Bio-Rad Precision Plus Kaleidoscope Standard. For dot blots, 10 µg of protein was spotted onto nitrocellulose membrane and allowed to dry. Affinity purified, polyclonal antibodies against ACS α, ACS β, and Adhe1 were custom made in rabbits by ProteinTech (Chicago, IL). Biorad Goat Anti-Rabbit IgG (H+L)-HRP Conjugate was used for visualization. Blocking was performed for 2 hrs in 5% w/v milk in TBST. The primary and secondary antibodies were diluted at 1:3000 and 1:10,000, respectively, in 2.5% w/v milk in TBST.

6.2.5 CO_2 Reduction Assay

The *in vivo* CO_2 reduction assay was performed in 5 mL defined CGM, supplemented with 100 µM $NiCl_2$ and Wolfe's vitamin solution (Atlas 2010). The culture media was inoculated with a 5% inoculum of overnight culture OD ~ 0.8 and was supplemented with erythromycin at 100 µg/mL and thiamphenicol at 10 µg/mL. The cultures were transferred to sealed serum bottles, and the headspace was flushed

and pressurized with 10 psi H_2/CO_2 (80:20, H_2:CO_2). The headspace gas composition was monitored using a Carboxen 1006 Plot capillary column (30 m x 0.32 mm, 15µm phase thickness, Sigma, St. Louis, Missouri) in a Shimadzu GC-2010 Plus with a GCMS-QP2010 Ultra (Shimadzu, Kyoto, Japan). Helium flow was maintained at 5 ml/min. The source temperature was maintained at 200 ºC, interface temperature at 180 ºC, and the injection port at 160 ºC. The oven temperature was held at 30 ºC for 2.5 minutes and ramped at 40 ºC/min to 120 ºC. Gas samples of 50 µl were collected using an airtight syringe and injected at a 1:10 split ratio.

6.2.6 Acetyl-CoA Exchange Assay

The *in vivo* acetyl-CoA assay was performed in 5 mL defined CGM, supplemented with 100 µM $NiCl_2$, Wolfe's vitamin solution, and either 40 g/L or 5 g/L glucose. The media was supplemented with 30 mM sodium acetate-1-^{13}C. Preculture of the recombinant WLP strain and the plasmid control were grown to an OD of 1.0, and concentrated 3x before inoculation in the dCGM medium. Headspace samples taken and measured by GC as described above. Endpoint metabolites were quantified on an Agilent 1200 HPLC equipped with a Bio-Rad Aminex HPX 87H column using a 5 mM H_2SO_4 mobile phase (Buday, Linden et al. 1990).

6.3 Results

6.3.1 Confirmation of Expression from p95ACS_MetF

6.3.1.1 SQ-RT PCR and Northern blots confirm expression of the synthetic WLP operon from p95ACS_MetF.

Transcript expression of the complete Wood-Ljungdahl pathway operon from the plasmid p95ACS_MetF (Figure 6.2), which expresses the five-gene synthetic operon containing c37550, c37560, c37660, c37670 and the *E. coli metF*, was confirmed with SQ-RT-PCR and Northern blotting. For the SQ-RT-PCR, RNA was collected from the recombinant *C. acetobutylicum* strain containing p95ACS_MetF and wild-type *C. ljungdahlii*. RNA from the recombinant *C. acetobutylicum* strain without reverse-transcriptase was used as a negative control against DNA contamination. As shown in Figure 6.3, expression of the four genes from *C. ljungdahlii* (i.e., c37550, c37560, c37660, and c37670) is observed in both *C. acetobutylicum* p95ACS_MetF and wild-type *C. ljungdahlii*. As expected, the expression of the codon-optimized *metF* from *E. coli* is only observed in the *C. acetobutylicum* p95ACS_MetF RNA.

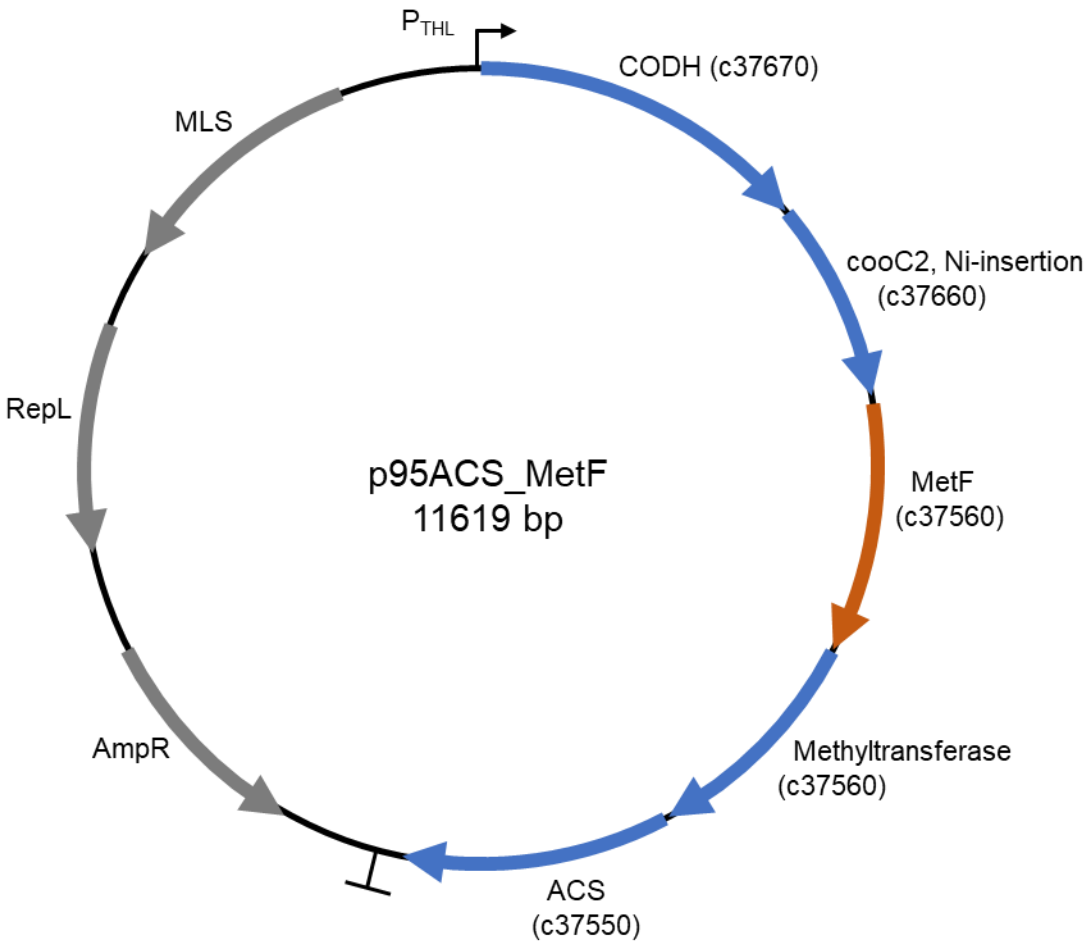

Figure 6.2. Schematic of the expression plasmid p95ACS_MetF. The WLP genes are expressed as part of a synthetic operon under control of the thiolase promoter from C. acetobutylicum, and the ⊤ following the ACS gene indicates the location of a rho-independent terminator. This plasmid differs from p95ACS from Chapter 5 due to its inclusion of the codon optimized metF gene from E. coli (highlighted in orange).

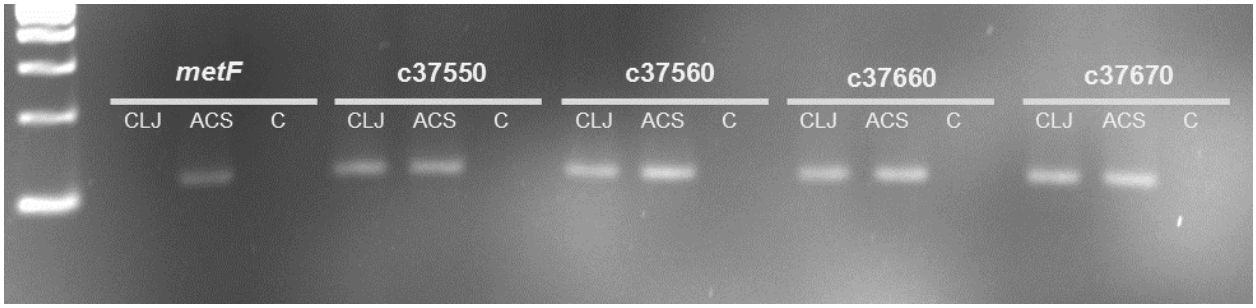

Figure 6.3. SQ-RT-PCR of *metF*, c37550, c37560, c37660, and c37670 for *C. ljungdahlii (*CLJ), *C. acetobutylicum* p95ACS_MetF (ACS), and a no reverse transcriptase control (C). The expected 120 bp band is observed in both the *C. ljungdahlii* sample *C. acetobutylicum* p95ACS_MetF for all four genes sourced from *C. ljungdahlii*. *metF* expression is only observed in the recombinant *C. acetobutylicum* strain, as the *metF* is not natively found in *C. ljungdahlii*.

Northern blotting was conducted on the recombinant *C. acetobutylicum* with WT *C. acetobutylicum* and *C. ljungdahlii* as negative and positive controls, respectively. A 300-bp DNA probe targeting ACS-encoding RNA was generated by PCR and subsequently labeled with α-^{32}P dCTP. RNA was extracted from actively growing cultures at OD = 1 and was separated using a denaturing 1% agarose gel in MOPS buffer. The expected 6700 bp band is found in all recombinant *C. acetobutylicum* strains (Figure 6.4), although there is RNA degradation in all samples. For the *C. ljungdahlii*, a band is observed at ~9900 bp when probed with the c37550 and c37560 probes that corresponds to the predicted operon. In the *C. ljungdahlii* RNA probed against c37660 and c37670, a faint band can be observed at ~7800 bp, which is the approximate size of their putative operon. For all probes, the RNA from the *C. acetobutylicum* plasmid control (p95MCS) shows no probe binding.

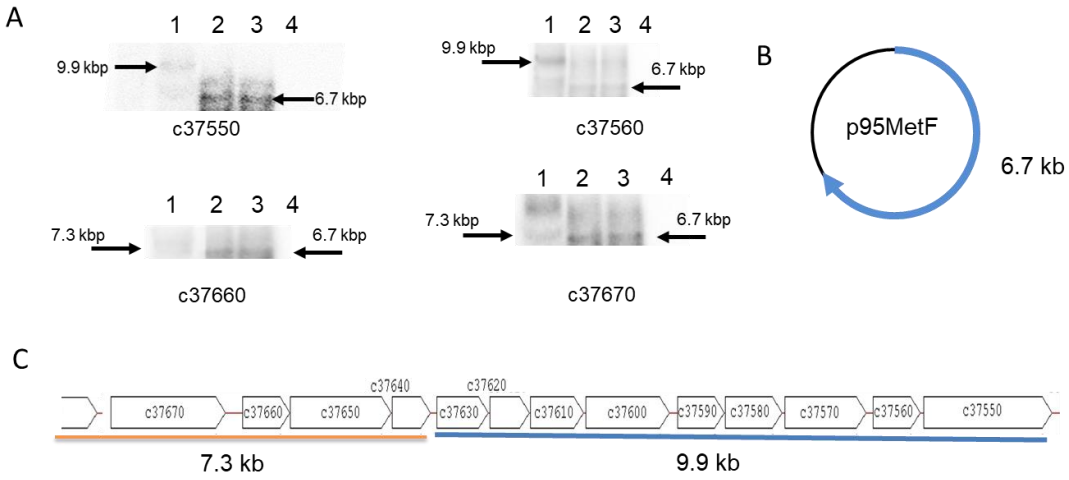

Figure 6.4**.** Northern blot of *acs* (c37550), *meTR* (c37560), *cooC* (c37660), and *codh* (c37670). Lane 1 is WT *C. ljungdahlii*, lanes 2 & 3 are replicates of the recombinant *C. acetobutylicum* WLP strain, and WT *C. acetobutylicum* RNA was run as a negative control in lane 4. The expected 6700 bp band is found in all recombinant *C. acetobutylicum* strains. For the *C. ljungdahlii*, a band is observed at ~9900 bp when probed with the c37550 and c37560 probes that corresponds to the predicted operon. In the *C. ljungdahlii* RNA probed against c37660 and c37670, a faint band can be observed at ~7800 bp.

6.3.1.2 Western blot analysis to confirm protein expression of CODH and ACS

The presence of CODH and ACS protein was determined by Western blot on protein samples collected from wild-type *C. ljungdahlii*, the recombinant strain *C. acetobutylicum* (p95ACS_MetF, pJIR_CFeSP), the recombinant strain *C. acetobutylicum* (p95ACS, pJIR_CFeSP) – described in Chapter 5 – and WT *C. acetobutylicum* (Figure 6.5).

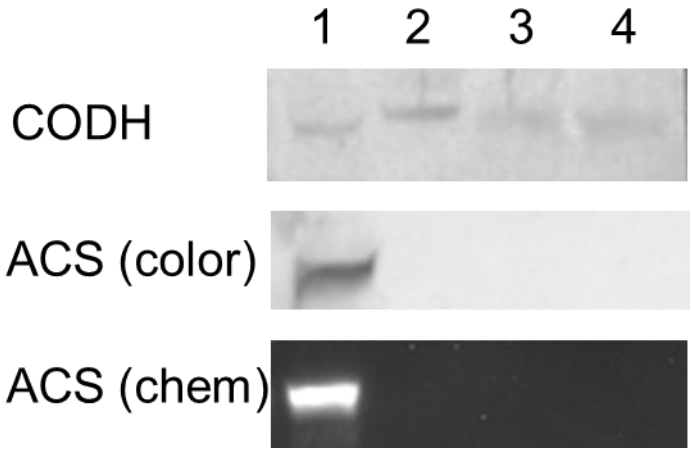

Figure 6.5. Western Blot of the CODH and ACS in cell extracts of *C. ljungdahlii* (lane 1), *C. acetobutylicum* (p95ACS, pJIR_CFeSP) (lane 2), and *C. acetobutylicum* (p95ACS_MetF, pJIR_CFeSP) (lanes 3 and 4). The CODH band is observed at ~67.5 kDa, and the ACS band is observed at 72 kDa. The ACS protein was assayed with both colorimetric detection and chemiluminescent detection; however, neither detection method showed ACS expression in the recombinant strains.

The colorimetric Western blot of CODH confirms expression in the recombinant CODH in all samples tested as well as in the *C. ljungdahlii* positive control. The initial colorimetric Western blot of ACS, however, only showed expression for the *C. ljungdahlii* positive control. Because colorimetric detection is known to have limited sensitivity, the Western blot of the ACS was repeated using a luminol-based chemiluminescent detection with higher sensitivity. The chemiluminescent detection also showed a lack of ACS expression in the recombinant

C. acetobutylicum extracts. The nature and cause of this lack of expression will be discussed further below.

Dot blotting was used as a second method to assess the presence of the CODH and ACS enzymes in the recombinant *C. acetobutylicum* strains (Figure 6.6). For the CODH, protein expression can be observed in both replicates of the *C. ljungdahlii* positive control (lanes A and B) as well as the recombinant *C. acetobutylicum* (WLP). No CODH expression is observed in the plasmid control strain (PC). The blot for ACS does not show expression in the first replicate of the *C. ljungdahlii* (A) or for the *C. acetobutylicum* plasmid control strain. Faint ACS expression is observed in both the recombinant *C. acetobutylicum* strain and in the second replicate of *C. ljungdahlii* as evidenced by the faint black circles on the perimeter of both protein dots. The absence of any binding in one of the *C. ljungdahlii* replicates and only faint binding in both the second *C. ljungdahlii* replicate may indicate that less stringent blocking conditions are necessary. The absence of ACS antibody binding in the plasmid control blot confirms that there is no non-specific binding to WT *C. acetobutylicum* protein. A dot blot for the bifunctional aldehyde/alcohol dehydrogenase (CAP_0162, AdhE1) was used as a positive control for the *C. acetobutylicum* strains. The blot confirmed the presence in AdhE1 in both the recombinant *C. acetobutylicum* and the plasmid control. Interestingly, the AdhE1 antibody also showed affinity for the *C. ljungdahlii* sample, which is likely because the *C. ljungdahlii* aldehyde/alcohol dehydrogenase shows 68% identity and 83% similarity to that of *C. acetobutylicum*.

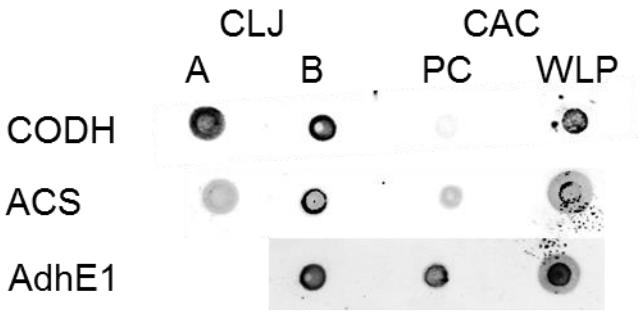

Figure 6.6. Dot blot of CODH, ACS, and AdhE1 in cell extracts of *C. ljungdahlii*, *C. acetobutylicum* (p95ACS_MetF, pJIR_CFeSP) and the plasmid control *C. acetobutylicum* (p95MCS, pJIR750). The presence of CODH is observed in both *C. ljungdahlii* replicates and also the recombinant *C. acetobutylicum*. Faint expression of ACS is observed in replicate B of the *C. ljungdahlii* control as well as the recombinant *C. acetobutylicum*; however, no ACS is observed in the first replicate of the *C. ljungdahlii* positive control. AdhE1 expression is observed in all samples tested.

6.3.2 Construction of complete WLP in *C. acetobutylicum* catalyzes the reduction of CO_2 to CO; however, CO_2 fixation into products is not observed

To test whether the recombinant strain showed WLP functionality, cultures were growth under 30 psi CO_2/H_2, with 20 mM ^{13}C formate (to feed into the methyl-branch), and 5 g/L glucose to allow for energy generation and cell maintenance, but not so much glucose as to dilute the potential ^{13}C labeling in acetate. Additionally, sodium acetate, which is typically used as a pH buffer in clostridial growth media, was omitted to avoid diluting the ^{13}C label. Under these conditions, if the recombinant WLP were functional, the ^{13}C-formate would be assimilated through the 1-C pool and condensed at the ACS with CO to form acetyl-CoA. The resulting ^{13}C-labeled acetyl-CoA would appear in products. The endpoint metabolite concentrations show that between 5 and 6 mM ^{13}C formate have been consumed; however, the acetate produced by these cultures showed an average labeling of only 2.9% ^{13}C-labeling, the same as

the plasmid control, indicating that the full pathway is not functioning (Figure 6.7 and Figure 6.8).

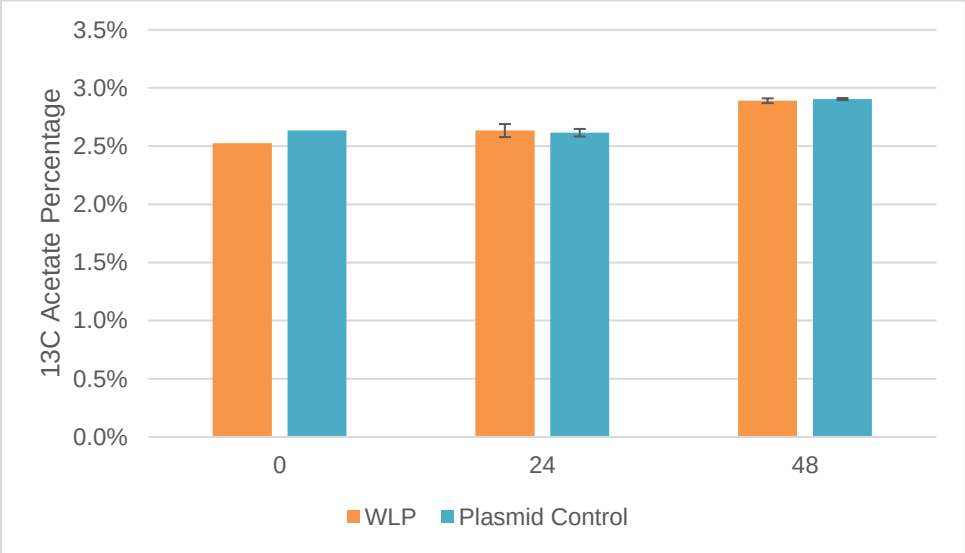

Figure 6.7. ^{13}C-acetate labeling profile. The recombinant strain and a plasmid control were cultured with 5 g/L glucose and 20 mM ^{13}C-formate under 30 psig H_2/CO_2 (80:20). The ^{13}C-formate was not incorporated into the acetate metabolite as shown by the similar labeling patterns for both the plasmid control and the recombinant strain. (n=3)

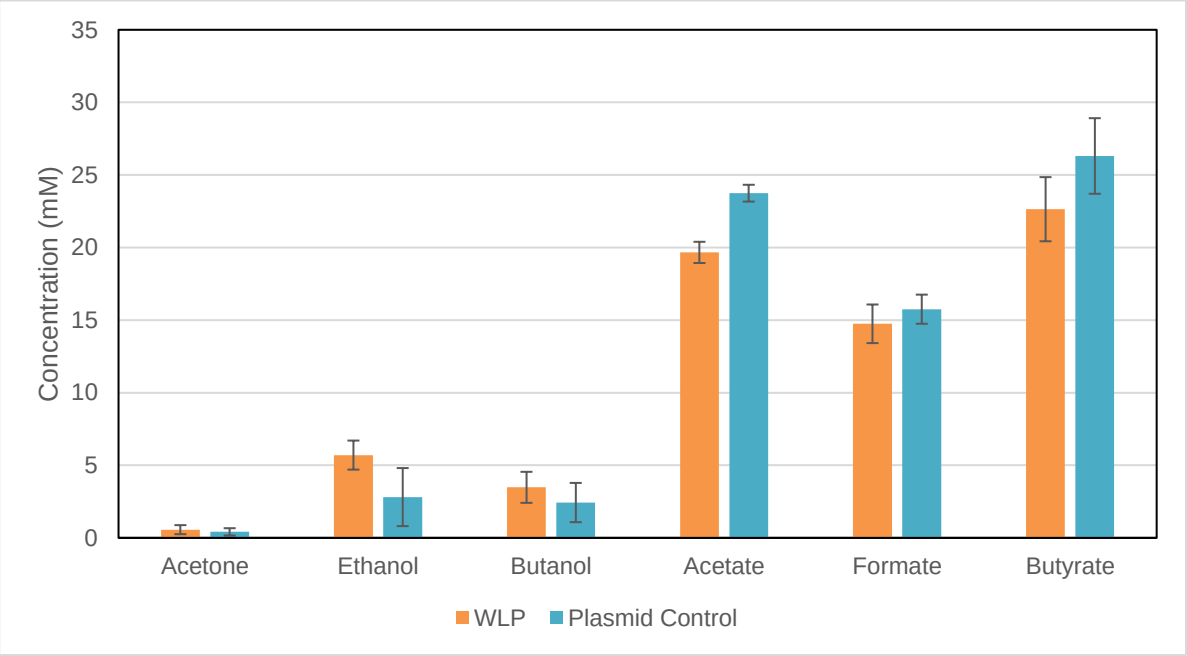

Figure 6.8. Endpoint metabolite concentrations for the ^{13}C-formate incorporation cultures for both the recombinant WLP strain and the plasmid control.

Given the lack of ^{13}C incorporation into products, we sought to understand whether the CODH and ACS, the most essential elements of carbon fixation in acetogens, were functioning as expected. The first component tested was the CODH enzyme. While we had previously shown the activity of this enzyme *in vitro* (Chapter 5), we had not observed an *in vivo* activity for this enzyme. Additionally, the previous *in vitro* assay of the recombinant *C. ljungdahlii* CODH discussed in Chapter 5 had only been used to show the oxidation of CO to CO_2, which is more thermodynamically favorable under most conditions. To determine whether *in vivo* CO_2 reduction could be observed, the recombinant *C. acetobutylicum* strain was grown in defined clostridial growth media (CGM) with 40 g/L sugar. The headspace was pressurized with 10 psig H_2/CO_2 (80:20, H_2:CO_2) to provide a reduced

environment with available CO_2 that would enrich the reduced ferredoxin pool, thereby favoring the production of CO. Under these conditions, the recombinant *C. acetobutylicum* strain produced approximately 4 µmol CO (Figure 6.9). No CO production was observed for the plasmid control. Like H_2 production in native *C. acetobutylicum*, the production of CO is growth associated and is dependent on the availability of reduced ferredoxin produced during glycolysis.

In general, net CO production is not observed in native acetogens because all the CO produced is immediately consumed to form acetyl-CoA by the ACS. Likewise, if the recombinant WLP were functioning as expected in *C. acetobutylicum*, one would expect the concentration of CO to be very low.

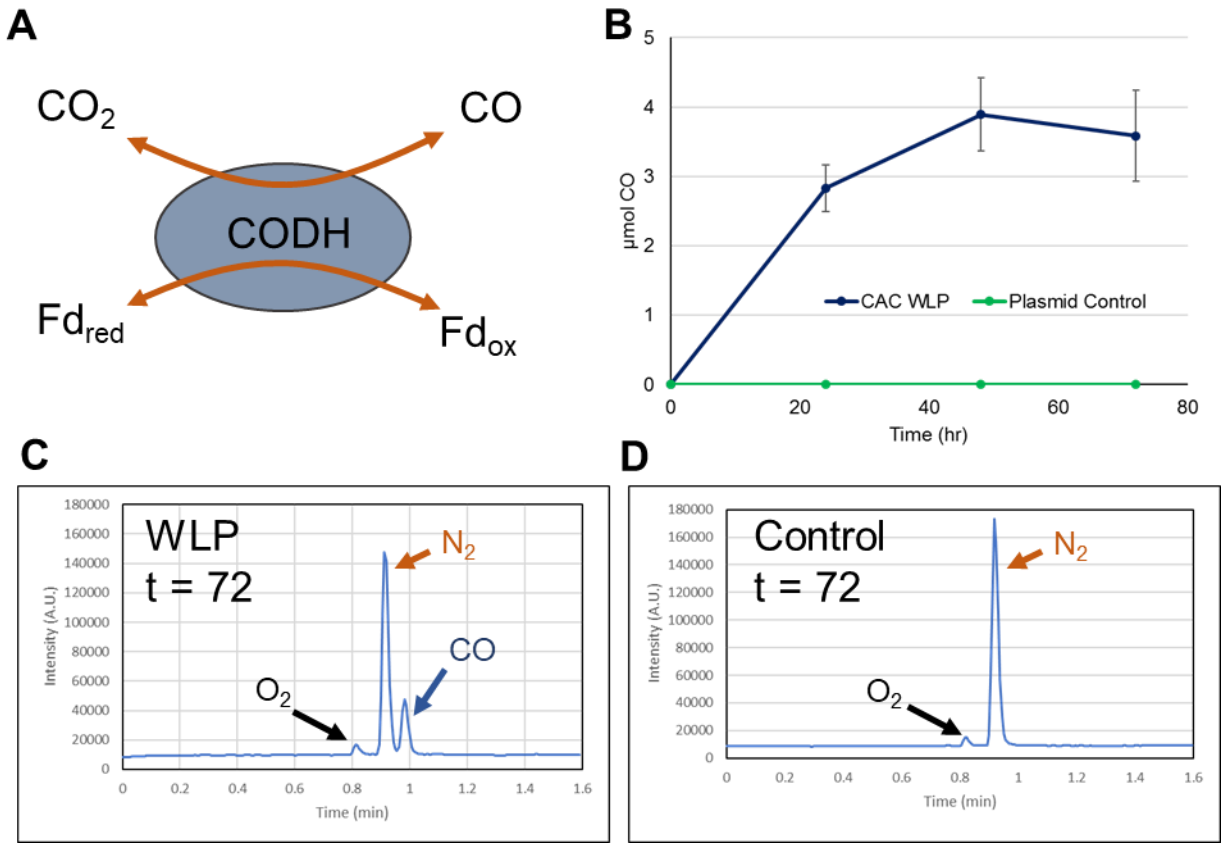

Figure 6.9. In vivo reduction of CO_2 by C. acetobutylicum overexpressing the C. ljungdahlii CODH. Cells were grown in defined media with 40 g/L glucose and 10 psi CO_2/H_2. No CO reduction observed in the plasmid control.

6.3.3 ACS activity can be measured through the exchange of ^{13}C between intracellular acetyl-CoA and headspace CO

In troubleshooting the lack of acetate labeling from the combined WLP strain, we sought to measure the activity of the heterologous ACS (Figure 6.10). When researchers initially elucidated the enzymology of the WLP in the 1980s, it was shown

that purified ACS could catalyze the exchange of the carbonyl-moiety of acetyl-CoA *in vitro* (Figure 6.10) (Raybuck, Bastian et al. 1988). In the original *in vitro* assay of purified ACS, acetyl-CoA was radiolabeled with ^{14}C at the carbonyl carbon. In the presence of unlabeled CO, ACS activity was measured by observing a decrease in radioactivity in the liquid sample. Here we propose using an *in vivo* assay where the acetyl-CoA pool is labeled with the addition of ^{13}C-acetate, and the exchange reaction occurs between the labeled acetyl-CoA and unlabeled CO in the headspace, which is generated during the course of the fermentation from unlabeled CO_2 by the CODH as described above.

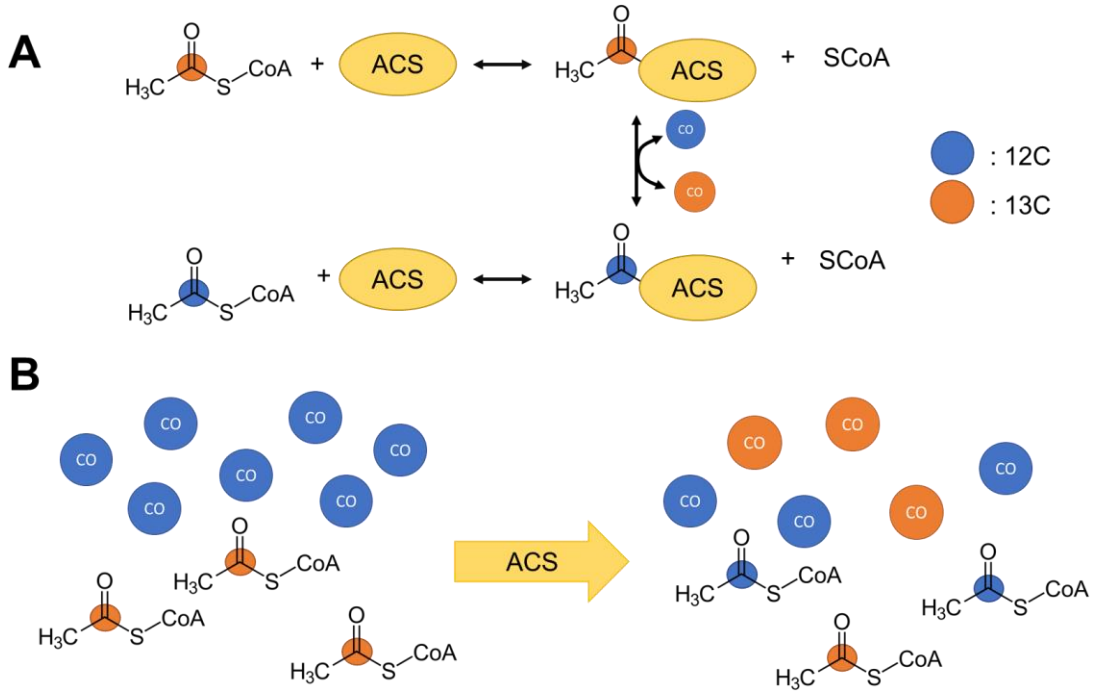

Figure 6.10. Schematic of ACS activity assay via carbon exchange. A) ACS catalyzes the exchange of the labeled carbonyl moiety of acetyl-CoA using the nickel active site to bind both CO and the CoA coenzyme, allowing for CO exchange with headspace CO. B) Proposed *in vivo* assay of CO exchange. In the presence of acetyl-CoA labeled with ^{13}C at the carbonyl-carbon, unlabeled headspace CO is exchanged with the acetyl-CoA resulting in labeled headspace CO.

To test the feasibility of the proposed ACS assay, cells were grown in dCGM with 40 g/L glucose buffered with 30 mM sodium acetate-1-^{13}C and a headspace pressurized with 10 psig CO_2/H_2. As a control, the recombinant strain was grown under the same conditions with unlabeled sodium acetate. The assumption was that cell will take up acetate and convert part of it to acetyl-CoA by the action of the CoA transferase (Sillers, Chow et al. 2008) or the reversal of the acetate formation pathway in *C. acetobutylicum* involving the acetate kinase and phosphotransacetylase (Amador-Noguez, Brasg et al. 2011) (Figure 6.11).

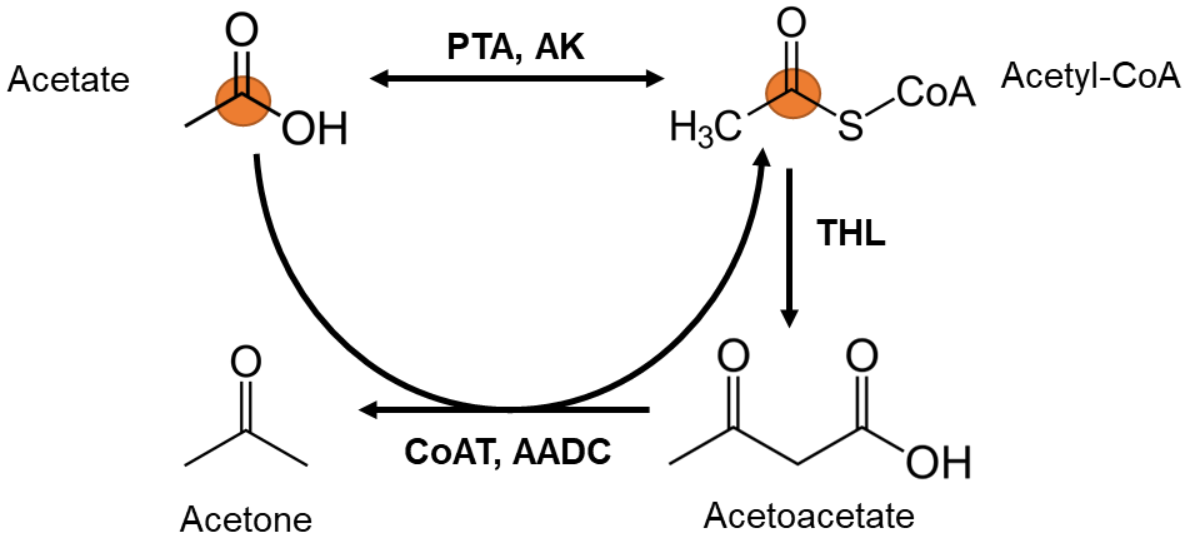

Figure 6.11 Acetate uptake into *C. acetobutylicum* metabolism. Labeled acetate can label the acetyl-CoA pool through two pathways. A) The phosphotransacetylase and acetate kinase act reversibly to uptake ^{13}C sodium acetate into acetyl-CoA. B) The CoA transferase, which acts to uptake free acids by transferring the CoA moiety from acetoacetyl-CoA

We had predicted that the activity of ACS would increase the level of labeling in the headspace CO (Figure 6.10 B) by exchanging unlabeled CO for the ^{13}C labeled carbonyl. Indeed, we observed CO labeling as high as 2% for the ^{13}C-acetate condition as compared to ~1% – the natural ^{13}C abundance – for the ^{12}C-acetate condition (Figure 6.12). However, when we considered the labeling profile of headspace CO_2, we also observed increased levels of ^{13}C labeling (Figure 6.12**)**, which led to two hypotheses: 1) the CO-exchange from acetyl-CoA was leading to greater labeling in headspace CO, which was then being oxidized to CO_2 or 2) the carbonyl carbon from acetyl-CoA was being decarboxylated, leading to increased CO_2 labeling, which in turn led to an increase in the ^{13}CO pool. The reaction in *C. acetobutylicum* that could result in the decarboxylation of the carbonyl-carbon from acetyl-CoA is the acetoacetate decarboxylase, which occurs during solventogenesis to produce acetone (Figure 6.13). Solventogenesis and acetone production are inhibited under low concentrations of sugars. Therefore, we repeated the exchange assay using only 5 g/L glucose to inhibit the formation of solvents and the decarboxylation of acetoacetate (Figure 6.14). Acetone production was not detected by HPLC, and differential ^{13}C labeling was not observed in the headspace CO_2, which showed labeling of 1.5% for both the ^{13}C acetate and ^{12}C acetate cultures. The lower glucose concentration also led to delayed CO production, which was not observed until 48 hrs for the ^{13}C acetate conditions and 72 hrs for the ^{12}C acetate conditions. The CO produced at this time point had average labeling of 5.9% for the ^{13}C acetate cultures as compared to 2.5% labeling in the ^{12}C acetate control. The labeling in the ^{12}C control above the natural ^{13}C abundance of 1.08% is due to the very low concentration of CO (~1.3 µM), which causes noise in the measurement of isotope fractions. Because the labeling in CO is

not coming from the headspace CO_2, as is evident from the lack of acetone production and absence of measured ^{13}C label in the headspace CO_2, we can conclude that the labeled CO is due to carbonyl-exchange from the acetyl-CoA catalyzed by the ACS.

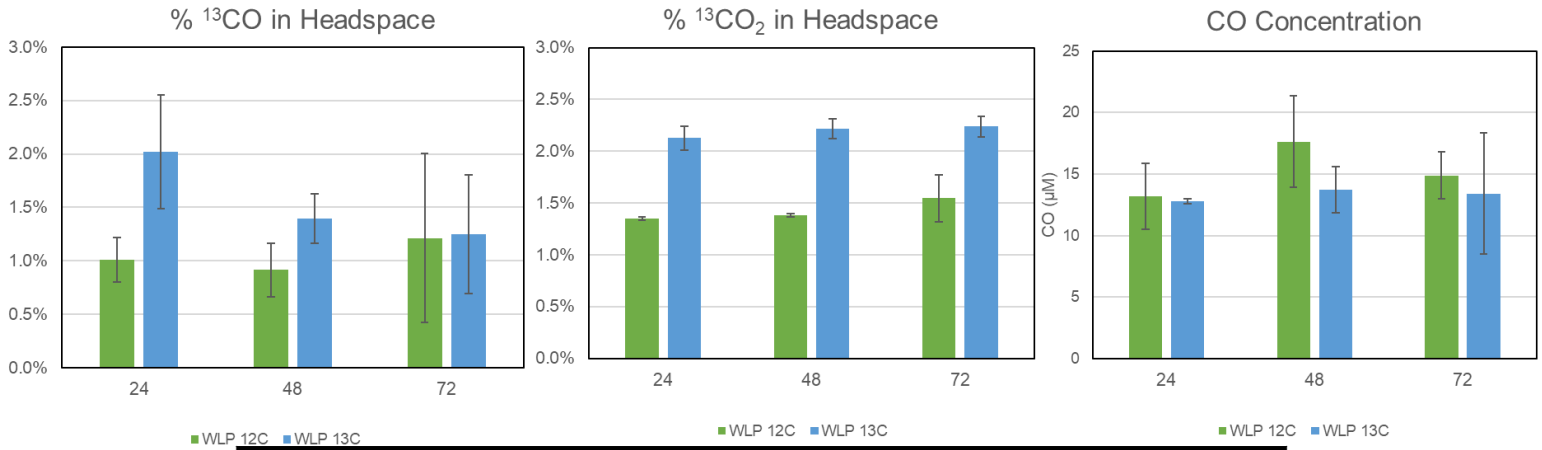

Glucose (Consumed)	Acetate	Ethanol	Butyrate	Acetone	Butanol	Acetoin
79	27	38	7	41	70	34

Figure 6.12. Recombinant WLP strain grown on dCGM with 40 g/L glucose, 30 mM sodium acetate (labeled at the carbonyl carbon and unlabeled control), and 10 psig CO_2/H_2. The ^{12}C sodium acetate samples show labeling of ~1%, which is due to the natural abundance of ^{13}C of 1.08%. Headspace CO shows higher labeling at 24h and 48h when grown in the presence of the ^{13}C sodium acetate as compared to the unlabeled acetate control. However, this labeling is potentially due to the decarboxylation of acetoacetate to form acetone resulting in labeled ^{13}C CO_2. (n=3)

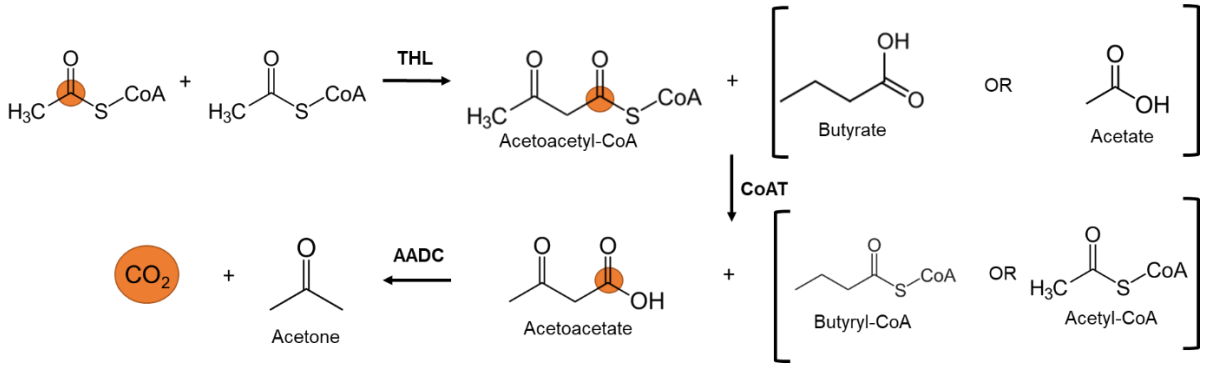

Figure 6.13. Labeled acetyl-CoA leads to the generation of labeled CO_2. The labeled carbonyl carbon of acetyl-CoA can be decarboxylated to form CO_2 through the formation of acetate. The acetyl-CoA is condensed by the thiolase (THL) with a second acetyl-CoA, which can create acetoacetyl-CoA that is labeled at the first carbon. During solvent formation, the CoA from acetoacetyl-CoA is transferred by the CoA transferase (CoAT) onto the accumulated butyrate and acetate to form butyryl-CoA and acetyl-CoA, respectively, in addition to acetoacetate. The acetoacetate decarboxylase (AADC) decarboxylates the first carbon of acetoacetate to form acetone and CO_2. Thus, if the first carbon of acetoacetate is derived from labeled acetyl-CoA, the resulting decarboxylation reaction creates ^{13}C labeled CO_2

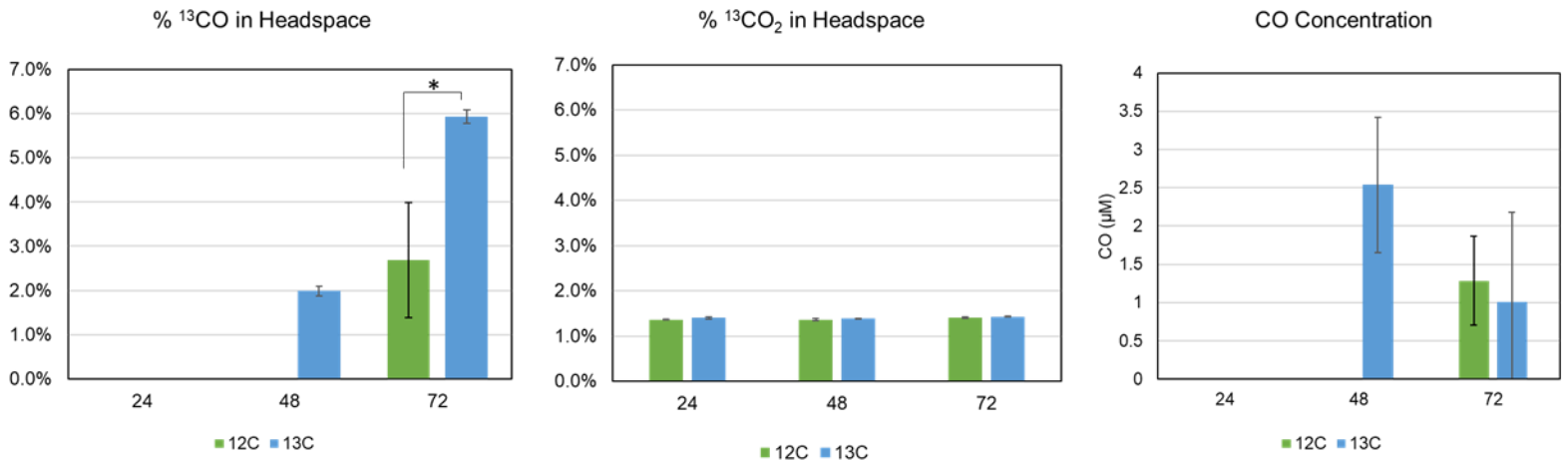

Glucose (Consumed)	Acetate	Ethanol	Butyrate	Acetone	Butanol	Acetoin
24	10	1	18.2	0	0	0

Figure 6.14. Recombinant WLP strain grown on dCGM with 5 g/L glucose, 30 mM sodium acetate (labeled at the carbonyl carbon and unlabeled control), and 10 psig CO_2/H_2. Only 2 replicates of the ^{13}C acetate cultures had headspace CO at 72 hrs. Lower sugar concentration results in abated acetone and CO production. (n=3, * $p < 0.05$)

To provide further evidence of ACS activity, we repeated the experiment under low sugar conditions with a larger inoculum and a decreased headspace volume to increase the partial pressure of CO in the headspace, thereby increasing the sensitivity of the assay (Figure 6.15). Under these conditions, we measured CO in the headspace starting at 24 hours, whereas the previous set of experiments did not show headspace CO production until 72 hours. Additionally, the CO concentrations were ~ 5x higher in the second round of experiments. The ^{13}C labeling observed in the headspace CO was significantly higher than the negative control at 72 hours ($p < 0.05$), and the labeling in CO was higher with significance at $p < 0.1$ at the other timepoints. These results provide a second confirmation of ACS exchange activity in the recombinant strain.

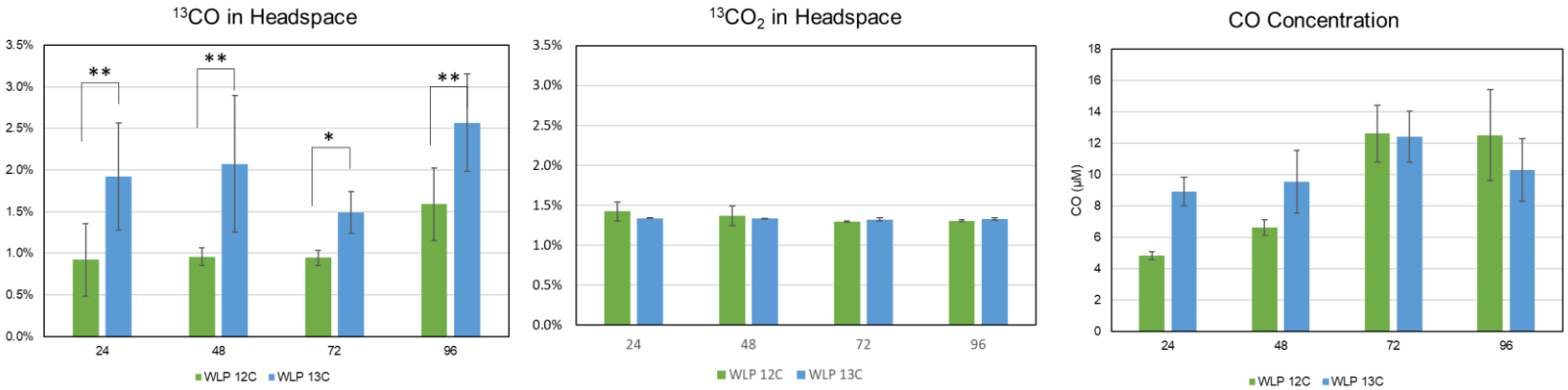

Glucose (Consumed)	Acetate	Ethanol	Butyrate	Acetone	Butanol	Acetoin
28.4	12.5	5.1	21.2	0	0	0

Figure 6.15. Recombinant strain growth from a high-density inoculum, low sugar concentration, and reduced headspace volume. (n=3, ** $p < 0.1$, * $p<0.05$)

6.4 Discussion and Conclusions

The bi-functional methylenetetrahydrofolate reductase/homocysteine S-methyltransferase (CAC_0291), which acts to reduce 5,10-methylene-tetrahydrofolate to 5-methyltetrahydrofolate, was identified as a potential cause for the incomplete Eastern branch in the engineered *C. acetobutylicum* strain due to the second function of CAC_01291 (i.e., the transfer the methyl-group from 5-methyltetrahydrofolate onto L-homocysteine). The bifunctional enzyme completes both the reduction reaction and the methyltransferase reaction at one time, leaving no 5-methyltetrahydrofolate intermediate, which is necessary for the acetogenic methyltransferase to transfer to the corrinoid iron-sulfur protein and the acetyl-CoA synthase.

Expression of the complete synthetic operon from p95ACS_MetF was confirmed through SQ-RT-PCR and Northern blotting. Protein expression of the CODH subunit was confirmed through Western and dot blotting. The expression of ACS was confirmed through dot blotting, but not through Western blotting, which may be due to low or truncated translation of the ACS RNA. Protein samples from the recombinant strain have been sent for analysis by a commercial Western service to determine whether the protein samples can be concentrated to improve detection. When testing for CO_2 and formate fixation with the use of ^{13}C tracers, no labeling was observed in either the acetate and butyrate pools, which led to further interrogation of the specific WLP enzymes.

The lack of carbon flux from the Wood-Ljungdahl pathway into acetyl-CoA shows that one or more of the Wood-Ljungdahl pathway enzymes responsible for connecting the Eastern branch of the pathway from 5,10-methyltetrahydrofolate to the Western branch of the pathway at carbon monoxide is not functioning as intended.

The enzymes responsible for connecting these two branches are the 5,10-methylenetetrahydrofolate reductase, the methyl transferase, the corrinoid iron-sulfur protein, and the CODH/ACS complex. The CODH/ACS is of particular interest given its vital importance to WLP carbon fixation.

Activity of the CODH enzyme was shown through the production of CO under growth conditions. When cells were grown with 40 g/L glucose under a H_2/CO_2 headspace, they produced ~ 4 µmol of CO over 48 hours. The dependence of the CODH on reduced ferredoxin requires actively growing cells to regenerate the reduced ferredoxin pool through the decarboxylation of pyruvate by the pyruvate ferredoxin oxidoreductase. Additionally, the addition of exogenous hydrogen also acts to reduce intracellular ferredoxin and increase the amount of CO produced.

Activity of the ACS was measured through an *in vivo* ACS exchange assay in which the carbonyl-carbon from acetyl-CoA is exchanged with headspace CO. The production of acetone at high sugar concentrations resulted in labeling from acetyl-CoA to appear in the headspace CO_2, which complicated the measurement of ^{13}CO. To address this, sugar concentrations were decreased to 5 g/L to prevent the formation of acetone and $^{13}CO_2$. While the decreased sugar concentration also resulted in decreased CO production, we could still observe the formation of labeled CO in the headspace by increasing the culture volume and decreasing headspace volume.

One possible cause for the low expression of the ACS subunit may be due to the gene organization of p95ACS_MetF. The *acs* gene (c37550) sits at the end of the 6.7 kb synthetic operon of p95ACS_MetF. It has previously been shown that protein translation is partially determined by the position of within an operon, with genes closer to the promoter showing higher protein expression levels than genes at the end

of an operon even when equal levels of mRNA are present (Lim, Lee et al. 2011). Given the opportunity to engineer this construct from scratch, it would be prudent to create shorter operons or even place each gene on a separate transcript. While in some cases codon optimization can be used to improve gene expression levels (Gouy and Gautier 1982), *C. ljungdahlii* and *C. acetobutylicum* are both low-GC-content bacteria and as such have similar codon usage. Only 1.9% of the codons used in the *C. ljungdahlii* ACS are low-frequency codons, which better than some highly expressed *C. acetobutylicum* genes such as the butyrate kinase which is encoded by 4.5% low-usage codons. Given their similarity, codon optimization should not be necessary.

Once the expression levels of the ACS are corrected, the next step in engineering carbon fixation in *C. acetobutylicum* will be to individually interrogate the activities of the 5,10-methylenetetrahydrofolate reductase, the methyl transferase, and the corrinoid iron-sulfur protein. While *in vitro* assays exist for these enzymes (Clark and Ljungdahl 1984, Lu, Harder et al. 1990), the activities are not observable in cell extracts, and instead require the use of purified proteins. Additionally, the extreme oxygen sensitivity of these proteins necessitates that all purification and assay steps be conducted anaerobically. As such, these enzymes could be marked with a His-tag, expressed individually, purified with affinity chromatography under anaerobic conditions, and then assayed.

Chapter 7

CONCLUSIONS AND FUTURE WORK

The aim of this work was to analyze and implement carbon fixation as a part of industrial fermentation to increase product yield. This was accomplished by the identification of carbon fixation pathways best suited for high-yield anaerobic non-photosynthetic fermentation (Chapter 2), the consideration of mixotrophic fermentation conditions that would allow for improved yields in standard sugar fermentations (Chapter 3), the characterization of mixotrophic growth in native acetogens which shows improved yields and a lack of carbon catabolite repression (Chapter 4), the development and application of genetic techniques in the industrial organism C. acetobutylicum that would enable the introduction of the heterologous Wood-Ljungdahl pathway (Chapter 5), and the characterization of a heterologously-expressed Wood-Ljungdahl pathway in C. acetobutylicum (Chapter 6). This chapter summarizes the conclusions from this work and proposes applications, extensions, and future work.

7.1 Overall Conclusions

Carbon fixation provides a promising way to generate biofuels and chemicals by using inexpensive feedstocks, including waste streams, rather than through the fermentation of agricultural products that could otherwise be used for food. Chapter 2 focused on the analysis of non-photosynthetic prokaryotic systems/programs from the point of view of the efficiency with which they fix CO_2. There are six natural carbon

fixation pathways that are known to support autotrophic growth (Bar-Even, Noor et al. 2010). The 3-hydroxypropionate pathway and the dicarboxylate-4-hydroxybutyrate pathway were excluded from analysis because require a photosynthetic host or elemental sulfur (S^0) as an electron acceptor, respectively. For the remaining four pathways – the reductive pentose phosphate cycle (Calvin cycle), the reductive TCA cycle, the Wood-Ljungdahl pathway, and the 3-hydroxypropionate-4-hydroxybutyrate (3HP4HB) pathway --stoichiometric analysis was used to assess the ATP and reducing energy (H_2 or equivalent electrons) requirements of these pathways, and subsequently their expected capabilities to produce model biofuel molecules (acetate, ethanol, butanol, 2,3-butanediol).

The results of this analysis showed that for small molecules that could support cellular metabolism through substrate-level-phosphorylation (i.e., acetate), the Wood-Ljungdahl pathway was the most efficient due to its low ATP requirement. High ATP requirements for the reductive pentose phosphate pathway, the reductive TCA cycle, and the 3HB4HP pathways necessitate the use of the electron transport chain to convert reducing energy (e.g., NADH, NADPH, Fd_{red}, etc.) to chemical energy (i.e., ATP) through oxidative phosphorylation, which decreases the fermentation efficiency with respect to the limiting substrate (i.e., the reducing energy from H_2 or CO). Because the Wood-Ljungdahl pathway contains several highly oxygen-sensitive enzymes that preclude the use of oxidative phosphorylation, CO_2 is the sole terminal electron acceptor in acetogens. The reactions of the WLP do not produce the net ATP required for biosynthesis through substrate level phosphorylation. Instead, autotrophically grown acetogens couple the most exergonic reduction reactions of the WLP to the translocation of protons or Na^+ ions across the cell membrane, as has been

reviewed (Müller 2003). However, the stoichiometric model shown in Chapter 2 shows that the absence of oxidative phosphorylation places constraints on the metabolic capabilities of native acetogens grown chemoautotrophically. Specifically, it shows that acetogens are not well-suited to the production of butyrate, butanol, or 2,3-butanediol from gaseous substrates because these molecules do not provide sufficient ATP through substrate level phosphorylation. Thus, the model predicts that these chemicals can be produced autotrophically only if significant levels of acetate are produced as a byproduct, which has been observed in recent studies that produced four-carbon compounds under autotrophic conditions either through natural (Bruant, Lévesque et al. 2010, Köpke, Mihalcea et al. 2011) or engineered pathways (Köpke, Held et al. 2010, Ueki, Nevin et al. 2014).

Additionally, the model predicts that ethanol can only be produced autotrophically by the Wood-Ljungdahl pathway through the aldehyde oxidoreductase (AOR) reaction, which directly reduces acetate to form acetaldehyde. It had been proposed, but not experimentally confirmed, that acetogens produce ethanol through two different metabolic pathways: a direct route in which acetyl-CoA is reduced to acetaldehyde by a CoA-dependent aldehyde dehydrogenase and then to ethanol by an alcohol dehydrogenase and an indirect route in which acetate is reduced to acetaldehyde by the AOR and then reduced to alcohol by the alcohol dehydrogenase. The AOR pathway allows the cells to produce ATP through the production of acetate, and then directly reduce this acetate to ethanol without requiring an ATP-activation step, allowing the cells to detoxify acetate while also gaining ATP from substrate level phosphorylation. Since the publication of these calculations, the necessity of the aldehyde oxidoreductase reaction for autotrophic ethanol production has been

demonstrated experimentally in *C. autoethanogenum*. In their study, Liew *et al* show that autotrophic ethanol production in *C. autoethanogenum* is abolished when both annotated AOR genes are removed (Liew, Henstra et al. 2016). Moreover, they show that autotrophic ethanol production from CO can be improved by redirecting carbon flux to the AOR pathway through the knockout of the bifunctional aldehyde-alcohol dehydrogenase. Given its importance in improving the energetic efficiency of alcohol production, the AOR will be a promising engineering target for improving the alcohol titers in ATP-limited acetogenic systems.

The ability to achieve high mass yields from carbohydrate fermentations is impeded by CO_2 loss during classical Embden-Meyerhof-Parnas (EMP) glycolysis. Due to the decarboxylation of pyruvate when forming acetyl-CoA, one third of hexose carbons cannot be recovered as useful products. In practice, this means that the theoretical maximum mass yields for gasoline replacements range from 33% for 3-methyl-1-butanol to 51% for ethanol (Rude and Schirmer 2009). In response, there have been efforts based on biological approaches to minimize or ideally eliminate CO_2 loses, as this could theoretically result in complete conversion of carbohydrate sources to acetyl-CoA (Fast and Papoutsakis 2012, Tracy, Jones et al. 2012, Bogorad, Lin et al. 2013), a central building block of metabolism. The focus of Chapter 3 is on how glycolytic yields could be improved using mixotrophic fermentation in acetogenic bacteria. Stoichiometric models for heterotrophic, autotrophic, mixotrophic, and supplemented mixotrophic fermentation were presented to determine which strategy would result with the best fermentation yields for a wide array of chemicals. The results showed that limited mixotrophic fermentation can improve yields for less reduced targets. For instance, the mass yields of acetate and butyrate can be improved

in limited mixotrophic fermentation by 51% and 22% over heterotrophic fermentation, respectively. The secondary alcohols, isopropanol and 2-pentanol, also show improved yields under limited mixotrophic conditions of 35% and 22%, respectively, as they are produced through a decarboxylation reaction, rather than a stepwise reduction of the carboxyl-group using NAD(P)H. Limited mixotrophic fermentation does not improve yields for fully reduced alcohols such as ethanol or butanol because all the electrons from glucose are incorporated into the target fuel molecule, leaving no available electrons for the reassimilation of CO_2 by the Wood-Ljungdahl pathway. However, the primary alcohols can achieve higher yields via mixotrophic fermentation if an exogenous electron source is supplied in the form of gaseous H_2 or CO, a scenario described as supplemented mixotrophic fermentation. The determination of which molecules can be improved by limited mixotrophic fermentation and which will require electron supplementation can be deduced from the ratio of NAD(P)H per acetyl-CoA required to produce a given target chemical. This ratio was shown to be inversely proportional to the percent yield increase that could be found in the limited mixotrophic case as compared to the heterotrophic case, with lower NAD(P)H:Acetyl-CoA ratios resulting in higher yield increases observed in mixotrophic case over heterotrophic. As such, this work highlights target molecules that should be pursued in future acetogenic engineering strategies. Unreduced carboxylic acids such as butyrate could be produced at high glycolytic yields through mixotrophic fermentation in both engineered (Ueki, Nevin et al. 2014) and native (Bruant, Lévesque et al. 2010) organisms. For solvent production, acetone, isopropanol and 2-pentanol are also strong targets for consideration due to the lower electron requirements allowing for carbon

fixation. Already, efforts have been made to engineer both acetone and isopropanol production in acetogens (Schiel-Bengelsdorf and Dürre 2012, Jones, Fast et al. 2016).

Although calculations showed that mixotrophy could result in very high glycolytic efficiencies when producing less-reduced target molecules, it had remained unclear whether mixotrophy was a generalized phenomenon in acetogens and moreover, whether the relative rates of sugar and gas consumption were comparable, a necessity if mixotrophy were to be used to recapture CO_2 from industrial fermentation processes. Mixotrophy has been previously demonstrated in the type acetogen *M. thermoacetica* when producing stoichiometric amounts acetate from glucose as well as in *Acetobacterium woodii* when grown on mixtures of sugars and H_2/CO_2 (Fontaine, Peterson et al. 1942, Braun and Gottschalk 1981). In some cases, however, catabolite repression of the Wood-Ljungdahl pathway genes is clearly observed in the presence of carbohydrate sources, which would hinder the implementation of mixotrophic fermentation in these organisms. While *C. aceticum* readily consumes H_2/CO_2 in the absence of fructose, only small amounts of H_2/CO_2 consumption were observed in the presence of fructose, and much lower hydrogenase activity was observed in fructose-grown cells as compared to that of cells grown on H_2/CO_2 (Braun and Gottschalk 1981). Similarly, both *M. thermoacetica* and *Eubacterium limosum* have previously been shown to exhibit CCR (Loubière, Gros et al. 1992, Huang, Wang et al. 2012).

In Chapter 4, we show through ^{13}C labeling that, in the case of CLJ, gas incorporation occurs concurrently with fructose consumption and that the relative rates of gas and sugar consumption allow for more than 40% of acetate to be derived from the Wood-Ljungdahl pathway rather than glycolysis. The mRNA expression data from *C. ljungdahlii* confirmed that the WLP is not downregulated at an mRNA level even

when sugars are present, and the relative expression of several Wood-Ljungdahl pathway genes that have multiple paralogs in *C. ljungdahlii* such as the hydrogenase genes, the accessory CODH genes, and the three formate dehydrogenase genes indicates that some are expressed at low levels, even during autotrophic growth, indicating that these paralogs are not in fact important for WLP functionality. While previous RNA expression studies showed conflicting results regarding the WLP gene expression in the presence of sugars (Nagarajan, Sahin et al. 2013, Tan, Liu et al. 2013), both the growth and mRNA expression data in this chapter clearly show that the Wood-Ljungdahl pathway is active in the presence of sugars, which makes it an attractive organism for engineering a process development.

Additionally, Chapter 4 shows that mixotrophy is a wide-spread phenomenon across all acetogens tested. *C. ljungdahlii*, *C. autoethanogenum*, *E. limosum*, and *M. thermoacetica* all demonstrated the capability to simultaneously consume sugars and gases by producing metabolites at yields higher than that which could be achieved through heterotrophic fermentation alone. The fermentation of all four strains resulted in endpoint carbon yields between 0.72 – 0.83 $C_{product}/C_{fructose}$, which is greater than then theoretical maximum carbon yield for heterotrophic fermentation of 0.66 $C_{product}/C_{fructose}$. However, the amount of CO_2 from glucose or fructose that could be reassimilated into metabolites differed between the four organisms depending on the product profile. The strains that produced more reduced metabolites – *C. autoethanogenum* produced ethanol and *E. limosum* produced butyrate – showed lower overall carbon yields because fewer electrons were available for CO_2 fixation.

In the publication based partly on this work in Chapter 4, researchers at White Dog Labs applied the principles of mixotrophic fermentation to a strain of *C.*

ljungdahlii that contained an engineered acetone production pathway, consisting of the thiolase gene from *C. kluyveri*, the CoA-transferase gene from *C. acetobutylicum*, and the acetoacetate decarboxylase gene from *C. acetobutylicum*. Additionally, the *C. ljungdahlii* secondary alcohol dehydrogenase (SADH) responsible for the native production of 2,3-butanediol was knocked out, due to its activity towards acetone, which results in the production of isopropanol. Under batch fermentation, the engineered *C. ljungdahlii* strain showed a total molar yield of 82%, with acetone as the primary metabolite. With the addition of exogenous H_2, the overall molar yield for metabolites was increased to >90%. Acetone and 3-hydroxybutyrate, which were deemed the acetone pathway products, accounted for 37 wt.% of the fructose consumed, which is more than the theoretical maximum yield of 32 wt.% under standard heterotrophic conditions.

In Chapter 5, we considered the construction of a non-native carbon fixation pathway in the solvent-producing *C. acetobutylicum*. As most of the essential carbon fixing genes (i.e., the carbon monoxide dehydrogenase/acetyl-CoA synthase, the formate dehydrogenase, and the corrinoid iron-sulfur protein) for the Wood-Ljungdahl pathway are not natively expressed in *C. acetobutylicum*, expressing this heterologous pathway required the use of new genetic techniques expression techniques in *C. acetobutylicum*. While mRNA analysis showed that the full set of the Wood-Ljungdahl pathway genes was expressed, ^{13}C-labeling in this strain did not show any incorporation into acetyl-CoA, though it did confirm activity in the Eastern branch of the Wood-Ljungdahl pathway in *C. acetobutylicum*. This led us to conclude that the link between methylene-THF and the acetyl-CoA synthase is broken between the 5,10-methyltetrahydrofolate and the acetyl-CoA synthase.

The bi-functional methylenetetrahydrofolate reductase/homocysteine S-methyltransferase (CAC_0291), which acts to reduce 5,10-methylene-tetrahydrofolate to 5-methyltetrahydrofolate, was identified as a potential cause for the incomplete Eastern branch in the engineered *C. acetobutylicum* strain due to the second function of CAC_01291 (i.e., the transfer the methyl-group from 5-methyltetrahydrofolate onto L-homocysteine). The bifunctional enzyme completes both the reduction reaction and the methyltransferase reaction at one time, leaving no 5-methyltetrahydrofolate intermediate, which is necessary for the acetogenic methyltransferase to transfer to the corrinoid iron-sulfur protein and the acetyl-CoA synthase. Chapter 6 discusses the efforts to correct this through the expression of a methylene-tetrahydrofolate reductase (*metF*) from *E. coli*, which was codon-optimized and cloned alongside the other Wood-Ljungdahl pathway genes, as well as further characterization of this strain was conducted at the mRNA level through Northern blotting and the protein level through Western blotting and *in vivo* enzyme assays.

7.2 Recommendations for Future Work

7.2.1 Acetogen Physiology and Genetics

The enzymology of the Wood-Ljungdahl pathway has been an object of study since the early 1970s (Drake, Gößner et al. 2008), which has resulted in a complete elucidation of the Wood-Ljungdahl pathway. Unlike industrial organisms such as *C. acetobutylicum*, for which there is a preponderance of fermentation data, many acetogens – especially recently isolated strains – lack foundational studies concerning the regulatory mechanisms that govern Wood-Ljungdahl pathway expression and determine the product profiles observed under various growth conditions

(heterotrophic vs. autotrophic conditions, high vs low pH and temperature, continuous fermentation vs batch culture, etc.). Several recent publications have highlighted the impact that adjusting fermentation conditions can have on final products (Guo, Xu et al. 2010, Richter, Martin et al. 2013, Abubackar, Bengelsdorf et al. 2016, Abubackar, Fernández-Naveira et al. 2016, Martin, Richter et al. 2016). In the case of *C. carboxidivorans*, for instance, a recent study showed that by reducing fermentation temperatures from 37 ºC to 25 ºC solvent titers could be increased by an order of magnitude, and the low temperatures also stimulated the production of the C6 compounds hexanol and caproate, which are not observed when cells are grown at higher temperatures (Ramió-Pujol, Ganigué et al. 2015). The increasing availability of "-omics" technologies will allow for a more thorough understanding of acetogens and acetogenesis, as a more detailed understanding of acetogenic metabolism and gene regulation becomes available (Marcellin, Behrendorff et al. 2016). Likewise, the development of *in silico* models for acetogens such as *C. ljungdahlii* has led to the identification of several predicted genetic targets that could be inserted or deleted to improve strain productivity (Chen and Henson 2016).

Despite recent advances in the availability of genetic tools in acetogenic hosts, the application of genetic tools in acetogens is limited relative to other clostridia and type organisms such as *E. coli* and *S. cerevisiae*. Like in *C. acetobutylicum*, the restriction endonucleases of acetogens serve as a protection against the transformation of foreign DNA, such as that carried by bacteriophages; however, the restriction systems also prevent the transformation of plasmids for engineering purposes (Pyne, Bruder et al. 2014). PacBio sequencing of these organisms may provide insight into the DNA methylation patterns that protect native DNA from restriction endonucleases,

leading to new ways to protect heterologous DNA during transformation (Flusberg, Webster et al. 2010). Alternatively, conjugation has been a successful method for genetically engineering intractable organisms in the past, and recent work has highlighted its continued utility (Purdy, O'Keeffe et al. 2002, Yu, Du et al. 2012).

Group II intron based chromosomal modifications have been applied to clostridial acetogens in several instances (Mock, Zheng et al. 2015, Liew, Henstra et al. 2016, Marcellin, Behrendorff et al. 2016). CRISPR/Cas9-based editing techniques in acetogens could allow for the selective genome editing without the need for a counter-selection marker or an inducible promoter. Briefly, the CRISPR nuclease Cas9 can be targeted to a specific region on a chromosome using a synthetic single guide RNA (sgRNA). Once targeted, the Cas9 nuclease generates a double-stranded break in DNA, which leads to cell death. Thus, one can generate a chromosomal mutation through homologous recombination, and then one can screen for the deletion by selectively targeting the wild-type chromosome with the sgRNA. CRISPR/Cas9-based editing has recently been demonstrated in clostridial systems (Wang, Zhang et al. 2015, Nagaraju, Davies et al. 2016, Pyne, Bruder et al. 2016), and recently CRISPR/Cas9-based genome editing was also demonstrated in acetogenic clostridia, whereby Huang *et al* constructed knockout mutants of *pta, adhE1, ctf,* and *pyrE* in *C. ljungdahlii* (Huang, Chai et al. 2016).

7.2.2 Heterologous Expression of the WLP

One of the primary questions in the heterologous expression of the Wood-Ljungdahl pathway in *C. acetobutylicum* is which subset of genes need to be expressed for full pathway functionality. While at the start of this research, many of the individual proteins had been isolated and tested *in vitro,* the lack of genetic tools in

acetogens has meant that no direct genetic studies had been performed to test which accessory genes might be required for pathway functionality that had not previously been identified. For instance, Liew *et al*. used group-II introns to knockout the CODH component of the CODH/ACS complex (*acsA*) as well as two other CODH genes (*cooS1* and *cooS2*) that are located on the chromosome outside of the Wood-Ljungdahl pathway locus (Liew, Henstra et al. 2016). They found that the CODH from the CODH/ACS complex was required for autotrophic growth, as expected. However, they also found that the disruption of the *cooS1* led to a growth deficiency on CO, with the KO strain reaching lower ODs and producing less acetate. Similar knockout studies should be performed on other genes that are part of the conserved Wood-Ljungdahl pathway genetic locus in clostridial acetogens but have no known function in relation to the Wood-Ljungdahl pathway, such as the glycine cleavage proteins (Poehlein, Cebulla et al. 2015) or *orf7* (Ragsdale and Pierce 2008). Similarly, genes outside of the Wood-Ljungdahl pathway cluster also have an impact on carbon fixation and should be investigated. For instance, there are three annotated formate dehydrogenase genes in *C. ljungdahlii* (Köpke, Held et al. 2010), two of which contain the selenocysteine residue, and it remains unclear which of these formate dehydrogenase genes is important for Wood-Ljungdahl pathway functionality and which, if any, are superfluous.

Another study in *A. woodii* tested the overexpression of the Eastern branch enzymes responsible for the 1-C tetrahydrofolate pathway that is present in a diverse array of bacteria, but is essential for autotrophic CO_2 metabolism in acetogens. Overexpression of the Eastern branch genes led to higher growth ODs and higher acetate titers (Straub, Demler et al. 2014). This suggests that the Eastern branch genes,

which were originally left out of the engineered pathway in *C. acetobutylicum* due to their presence on the *C. acetobutylicum* chromosome, could be overexpressed as well to provide higher flux through the Eastern branch pathway and increase the availability of 5-methyltetrahydrofolate.

Ultimately, the engineered Wood-Ljungdahl pathway in *C. acetobutylicum* showed functionality of the Eastern branch of the pathway due to the formation of labeled 5,10-methylenetetrahydrofolate from labeled formate and a functional Western branch of the Wood-Ljungdahl pathway in the formation of CO from CO_2. However, the connection of these two branches was not observed in any labeling of acetyl-CoA observed in the acetate and butyrate pools. The enzymes responsible for connecting these two branches are the 5,10-methylenetetrahydrofolate reductase, the methyl transferase, the corrinoid iron-sulfur protein, and the acetyl-CoA synthase. While *in vitro* assays exist for these enzymes (Clark and Ljungdahl 1984, Lu, Harder et al. 1990), the activities are not observable in cell extracts, and instead require the use of purified proteins. The extreme oxygen sensitivity of these proteins necessitates that all purification and assay steps be conducted anaerobically. To test for successful expression in *C. acetobutylicum* these enzymes could be tagged, purified, and measured *in vitro*.

The original goal of engineering the Wood-Ljungdahl pathway in *C. acetobutylicum* was to create a means of carbon-fixation in a developed industrial organism. As discussed above, much research is already being conducted on acetogens to develop genetic and fermentation tools to expand their industrial application. However, another alternative approach would be to combine the solvent-producing utility of *C. acetobutylicum* with the carbon fixing utility of an acetogenic strain such

as *C. ljungdahlii*, *C. carboxidivorans*, or *B. methylotrophicum* through co-culture. Previously, it was shown that the cellulolytic bacterium *C. cellulolyticum* showed an improved rate of cellulose utilization when co-cultured with *C. acetobutylicum* due to an exchange of metabolites (Salimi and Mahadevan 2013). *C. acetobutylicum*, which produces large quantities of H_2 and CO_2 when growing on glucose, could be grown in co-culture with an acetogenic bacterium that could utilize the H_2/CO_2 byproduct thereby increasing the total carbon yield in a pseudo-mixotrophic fermentation. Similar co-culture experiments have been demonstrated with *C. autoethanogenum* and *C. kluyveri* (Diender, Stams et al. 2016). The acetogen *C. autoethanogenum* can grow on syngas as a sole carbon source but is unable to make 4C or 6C metabolites, and *C. kluyveri* does not have a functional native Wood-Ljungdahl pathway but uses a reversed β-oxidation pathway to generate C4, C6, and C8 compounds. In co-culture, these organisms were shown to convert CO into butyrate, caproate, butanol, and hexanol.

REFERENCES

Abdou, L., C. Boileau, P. de Philip, S. Pagès, H.-P. Fiérobe and C. Tardif (2008). "Transcriptional Regulation of the *Clostridium cellulolyticum* cip-cel Operon: a Complex Mechanism Involving a Catabolite-Responsive Element." Journal of Bacteriology **190**(5): 1499-1506.

Abubackar, H. N., F. R. Bengelsdorf, P. Dürre, M. C. Veiga and C. Kennes (2016). "Improved operating strategy for continuous fermentation of carbon monoxide to fuel-ethanol by clostridia." Applied Energy **169**: 210-217.

Abubackar, H. N., Á. Fernández-Naveira, M. C. Veiga and C. Kennes (2016). "Impact of cyclic pH shifts on carbon monoxide fermentation to ethanol by *Clostridium autoethanogenum*." Fuel **178**: 56-62.

Al-Hinai, M. A., A. G. Fast and E. T. Papoutsakis (2012). "Novel System for Efficient Isolation of *Clostridium* Double-Crossover Allelic Exchange Mutants Enabling Markerless Chromosomal Gene Deletions and DNA Integration." Applied and Environmental Microbiology **78**(22): 8112-8121.

Al-Hinai, M. A., S. W. Jones and E. T. Papoutsakis (2015). "The *Clostridium* Sporulation Programs: Diversity and Preservation of Endospore Differentiation." Microbiology and Molecular Biology Reviews **79**(1): 19-37.

Alber, B., M. Olinger, A. Rieder, D. Kockelkorn, B. Jobst, M. Hügler and G. Fuchs (2006). "Malonyl-Coenzyme A Reductase in the Modified 3-Hydroxypropionate Cycle for Autotrophic Carbon Fixation in Archaeal *Metallosphaera* and *Sulfolobus* spp." J Bacteriol **188**(24): 8551-8559.

Alissandratos, A., H.-K. Kim, H. Matthews, J. E. Hennessy, A. Philbrook and C. J. Easton (2013). "*Clostridium carboxidivorans* Strain P7T Recombinant Formate

Dehydrogenase Catalyzes Reduction of CO_2 to Formate." Applied and Environmental Microbiology **79**(2): 741-744.

Amador-Noguez, D., I. A. Brasg, X.-J. Feng, N. Roquet and J. D. Rabinowitz (2011). "Metabolome Remodeling during the Acidogenic-Solventogenic Transition in *Clostridium acetobutylicum*." Applied and Environmental Microbiology **77**(22): 7984-7997.

Amador-Noguez, D., X.-J. Feng, J. Fan, N. Roquet, H. Rabitz and J. D. Rabinowitz (2010). "Systems-Level Metabolic Flux Profiling Elucidates a Complete, Bifurcated Tricarboxylic Acid Cycle in *Clostridium acetobutylicum*." Journal of Bacteriology **192**(17): 4452-4461.

Annous, B. A., J. S. Shieh, G. J. Shen, M. K. Jain and J. G. Zeikus (1996). "Regulation of hydrogen metabolism in *Butyribacterium methylotrophicum* by substrate and pH." Applied Microbiology and Biotechnology **45**(6): 804-810.

Arai, H., H. Kanbe, M. Ishii and Y. Igarashi (2010). "Complete genome sequence of the thermophilic, obligately chemolithoautotrophic hydrogen-oxidizing bacterium *Hydrogenobacter thermophilus* TK-6." J Bacteriol **192**(10): 2651-2652.

Atlas, R. M. (2010). Handbook of microbiological media. Washington, D.C., ASM Press, CRC Press/Taylor & Francis.

Au, J., J. Choi, S. W. Jones, K. P. Venkataramanan and M. R. Antoniewicz (2014). "Parallel labeling experiments validate *Clostridium acetobutylicum* metabolic network model for ^{13}C metabolic flux analysis." Metabolic Engineering **26**: 23-33.

Auernik, K. S. and R. M. Kelly (2008). "Identification of components of electron transport chains in the extremely thermoacidophilic crenarchaeon *Metallosphaera sedula* through iron and sulfur compound oxidation transcriptomes." Appl Environ Microbiol **74**(24): 7723-7732.

Banerjee, A., C. Leang, T. Ueki, K. P. Nevin and D. R. Lovley (2014). "Lactose-Inducible System for Metabolic Engineering of *Clostridium ljungdahlii*." Applied and Environmental Microbiology **80**(8): 2410-2416.

Bannam, T. L. and J. I. Rood (1993). "*Clostridium perfringens-Escherichia coli* Shuttle Vectors That Carry Single Antibiotic Resistance Determinants." Plasmid **29**(3): 233-235.

Bar-Even, A., E. Noor, N. E. Lewis and R. Milo (2010). "Design and analysis of synthetic carbon fixation pathways." Proceedings of the National Academy of Sciences of the United States of America **107**(19): 8889-8894.

Berg, I. A., D. Kockelkorn, W. Buckel and G. Fuchs (2007). "A 3-Hydroxypropionate/4-Hydroxybutyrate Autotrophic Carbon Dioxide Assimilation Pathway in Archaea." Science **318**(5857): 1782-1786.

Berg, I. A., D. Kockelkorn, W. H. Ramos-Vera, R. F. Say, J. Zarzycki, M. Hugler, B. E. Alber and G. Fuchs (2010). "Autotrophic carbon fixation in Archaea." Nat Rev Microbiol **8**(6): 447-460.

Bertsch, J., C. Öppinger, V. Hess, J. D. Langer and V. Müller (2015). "Heterotrimeric NADH-Oxidizing Methylenetetrahydrofolate Reductase from the Acetogenic Bacterium Acetobacterium woodii." Journal of Bacteriology **197**(9): 1681-1689.

Boeke, J. D., J. Trueheart, G. Natsoulis and G. R. Fink (1987). "5-Fluoroorotic Acid as a Selective Agent in Yeast Molecular-Genetics." Methods in Enzymology **154**: 164-175.

Bogorad, I. W., T.-S. Lin and J. C. Liao (2013). "Synthetic non-oxidative glycolysis enables complete carbon conservation." Nature **502**(7473): 693-697.

Borden, J. R., S. W. Jones, D. Indurthi, Y. L. Chen and E. T. Papoutsakis (2010). "A genomic-library based discovery of a novel, possibly synthetic, acid-tolerance mechanism in Clostridium acetobutylicum involving non-coding RNAs and ribosomal RNA processing." Metabolic Engineering **12**(3): 268-281.

Borden, J. R. and E. T. Papoutsakis (2007). "Dynamics of genomic-library enrichment and identification of solvent tolerance genes for *Clostridium acetobutylicum*." Applied and Environmental Microbiology **73**(9): 3061-3068.

Boyle, N. R. and R. T. Gill "Tools for genome-wide strain design and construction." Current Opinion in Biotechnology. doi: 10.1016/j.copbio.2012.01.012.

Boyle, N. R. and J. A. Morgan (2011). "Computation of metabolic fluxes and efficiencies for biological carbon dioxide fixation." Metabolic Engineering **13**(2): 150-158.

Braun, K. and G. Gottschalk (1981). "Effect of molecular hydrogen and carbon dioxide on chemo-organotrophic growth of Acetobacterium woodii and Clostridium aceticum." Archives of Microbiology **128**(3): 294-298.

Brennan, L. and P. Owende (2010). "Biofuels from microalgae—A review of technologies for production, processing, and extractions of biofuels and co-products." Renewable and Sustainable Energy Reviews **14**(2): 557-577.

Bruant, G., M.-J. Lévesque, C. Peter, S. R. Guiot and L. Masson (2010). "Genomic Analysis of Carbon Monoxide Utilization and Butanol Production by Clostridium carboxidivorans Strain P7T." PLOS ONE **5**(9): e13033.

Buday, Z., J. C. Linden and M. N. Karim (1990). "Improved acetone-butanol fermentation analysis using subambient HPLC column temperature." Enzyme and Microbial Technology **12**(1): 24-27.

Calvin, M. and A. A. Benson (1948). "The path of carbon in photosynthesis." Science **107**(2784): 476-480.

Campbell, B. J., A. S. Engel, M. L. Porter and K. Takai (2006). "The versatile epsilon-proteobacteria: key players in sulphidic habitats." Nat Rev Microbiol **4**(6): 458-468.

Chen, J. and M. A. Henson (2016). "In silico metabolic engineering of Clostridium ljungdahlii for synthesis gas fermentation." Metabolic Engineering **38**: 389-400.

Clark, J. E. and L. G. Ljungdahl (1984). "Purification and properties of 5,10-methylenetetrahydrofolate reductase, an iron-sulfur flavoprotein from Clostridium formicoaceticum." Journal of Biological Chemistry **259**(17): 10845-10849.

Daniel, S. L., T. Hsu, S. I. Dean and H. L. Drake (1990). "Characterization of the H_2- and CO-dependent chemolithotrophic potentials of the acetogens *Clostridium thermoaceticum* and *Acetogenium kivui*." J Bacteriol **172**(8): 4464-4471.

Das, A., J. Hugenholtz, H. Vanhalbeek and L. G. Ljungdahl (1989). "Structure and Function of a Menaquinone Involved in Electron-Transport in Membranes of Clostridium-Thermoautotrophicum and Clostridium-Thermoaceticum." Journal of Bacteriology **171**(11): 5823-5829.

de Marco, A. (2007). "Protocol for preparing proteins with improved solubility by co-expressing with molecular chaperones in *Escherichia coli*." Nature Protocols **2**(10): 2632-2639.

de Marco, A., E. Deuerling, A. Mogk, T. Tomoyasu and B. Bukau (2007). "Chaperone-based procedure to increase yields of soluble recombinant proteins produced in *E. coli*." BMC Biotechnol **7**.

Desai, R. P. and E. T. Papoutsakis (1999). "Antisense RNA strategies for metabolic engineering of Clostridium acetobutylicum." Appl Environ Microbiol **65**.

Diender, M., A. J. M. Stams and D. Z. Sousa (2016). "Production of medium-chain fatty acids and higher alcohols by a synthetic co-culture grown on carbon monoxide or syngas." Biotechnology for Biofuels **9**(1): 82.

Dong, H., W. Tao, F. Gong, Y. Li and Y. Zhang (2014). "A functional recT gene for recombineering of Clostridium." Journal of Biotechnology **173**(0): 65-67.

Doukov, T. I., T. M. Iverson, J. Seravalli, S. W. Ragsdale and C. L. Drennan (2002). "A Ni-Fe-Cu Center in a Bifunctional Carbon Monoxide Dehydrogenase/ Acetyl-CoA Synthase." Science **298**(5593): 567-572.

Drake, H. L. (1994). Acetogenesis. New York, Chapman & Hall.

Drake, H. L. and S. L. Daniel (2004). "Physiology of the thermophilic acetogen Moorella thermoacetica." Research in Microbiology **155**(6): 422-436.

Drake, H. L., A. S. Gößner and S. L. Daniel (2008). "Old Acetogens, New Light." Annals of the New York Academy of Sciences **1125**(1): 100-128.

Edwards, J. S., Ramakrishna, R., Schilling, C. H. , and Palsson, B. O. (1999). Metabolic Flux Balance Analysis. Metabolic Engineering. New York, Marcel Dekker**:** 13 - 58.

Evans, M. C., B. B. Buchanan and D. I. Arnon (1966). "A new ferredoxin-dependent carbon reduction cycle in a photosynthetic bacterium." Proc Natl Acad Sci U S A **55**(4): 928-934.

Fairley, P. (2011). "Next generation biofuels." Nature **474**(7352): S2-S5.

Farmer, W. R. and J. C. Liao (2000). "Improving lycopene production in *Escherichia coli* by engineering metabolic control." Nat Biotechnol **18**(5): 533-537.

Fast, A. G. and E. T. Papoutsakis (2012). "Stoichiometric and energetic analyses of non-photosynthetic CO2-fixation pathways to support synthetic biology strategies for production of fuels and chemicals." Current Opinion in Chemical Engineering **1**(4): 380-395.

Fast, A. G., E. D. Schmidt, S. W. Jones and B. P. Tracy (2015). "Acetogenic mixotrophy: novel options for yield improvement in biofuels and biochemicals production." Curr Opin Biotechnol **33**: 60-72.

Fischbach, M. and C. A. Voigt (2010). "Prokaryotic gene clusters: a rich toolbox for synthetic biology." Biotechnol J **5**(12): 1277-1296.

Flusberg, B. A., D. R. Webster, J. H. Lee, K. J. Travers, E. C. Olivares, T. A. Clark, J. Korlach and S. W. Turner (2010). "Direct detection of DNA methylation during single-molecule, real-time sequencing." Nature methods **7**(6): 461-465.

Fontaine, F. E., W. H. Peterson, E. McCoy, M. J. Johnson and G. J. Ritter (1942). "A new type of glucose fermentation by Clostridium thermoaceticum n sp." Journal of Bacteriology **43**(6): 701-715.

Fuchs, G. (1986). "CO_2 Fixation in Acetogenic Bacteria - Variations on a Theme." FEMS Microbiology Reviews **39**(3): 181-213.

Genthner, B. R. S. and M. P. Bryant (1982). "Growth of Eubacterium limosum with Carbon Monoxide as the Energy Source." Applied and Environmental Microbiology **43**(1): 70-74.

Gibson, D. G., L. Young, R.-Y. Chuang, J. C. Venter, C. A. Hutchison and H. O. Smith (2009). "Enzymatic assembly of DNA molecules up to several hundred kilobases." Nat Meth **6**(5): 343-345.

Girbal, L., I. Mortier-Barriere, F. Raynaud, C. Rouanet, C. Croux and P. Soucaille (2003). "Development of a sensitive gene expression reporter system and an inducible promoter-repressor system for Clostridium acetobutylicum." Applied and Environmental Microbiology **69**(8): 4985-4988.

Gnansounou, E. and A. Dauriat (2010). "Techno-economic analysis of lignocellulosic ethanol: A review." Bioresource Technology **101**(13): 4980-4991.

Gollin, D., X. L. Li, S. M. Liu, E. T. Davies and L. G. Ljungdahl (1998). "Acetogenesis and the primary structure of the NADP-dependent formate dehydrogenase of Clostridium thermoaceticum, a tungsten-selenium-iron protein." Advances in Chemical Conversions for Mitigating Carbon Dioxide **114**: 303-308.

Gorke, B. and J. Stulke (2008). "Carbon catabolite repression in bacteria: many ways to make the most out of nutrients." Nat Rev Micro **6**(8): 613-624.

Gottesman, S. (2004). "The small RNA regulators of *Escherichia coli*: roles and mechanisms." Annual review of microbiology **58**: 303-328.

Gouy, M. and C. Gautier (1982). "Codon usage in bacteria: correlation with gene expressivity." Nucleic acids research **10**(22): 7055-7074.

Grethlein, A. J., R. M. Worden, M. K. Jain and R. Datta (1991). "Evidence for production of n-butanol from carbon monoxide by *Butyribacterium methylotrophicum*." Journal of Fermentation and Bioengineering **72**(1): 58-60.

Guo, Y., J. Xu, Y. Zhang, H. Xu, Z. Yuan and D. Li (2010). "Medium optimization for ethanol production with Clostridium autoethanogenum with carbon monoxide as sole carbon source." Bioresource Technology **101**(22): 8784-8789.

Hartman, A. H., H. Liu and S. B. Melville (2011). "Construction and Characterization of a Lactose-Inducible Promoter System for Controlled Gene Expression in Clostridium perfringens." Applied and Environmental Microbiology **77**(2): 471-478.

Hawkins, A. S., Y. Han, H. Lian, A. J. Loder, A. L. Menon, I. J. Iwuchukwu, M. Keller, T. T. Leuko, M. W. W. Adams and R. M. Kelly (2011). "Extremely Thermophilic Routes to Microbial Electrofuels." ACS Catalysis **1**(9): 1043-1050.

Heap, J. T., M. Ehsaan, C. M. Cooksley, Y. K. Ng, S. T. Cartman, K. Winzer and N. P. Minton (2012). "Integration of DNA into bacterial chromosomes from plasmids without a counter-selection marker." Nucleic Acids Research **40**(8).

Heap, J. T., O. J. Pennington, S. T. Cartman, G. P. Carter and N. P. Minton (2007). "The ClosTron: a universal gene knock-out system for the genus Clostridium." J Microbiol Methods **70**.

Hennig, S. E., J.-H. Jeoung, S. Goetzl and H. Dobbek (2012). "Redox-dependent complex formation by an ATP-dependent activator of the corrinoid/iron-sulfur protein." Proceedings of the National Academy of Sciences **109**(14): 5235-5240.

Herter, S., G. Fuchs, A. Bacher and W. Eisenreich (2002). "A bicyclic autotrophic CO2 fixation pathway in Chloroflexus aurantiacus." Journal of Biological Chemistry **277**(23): 20277-20283.

Hess, V., K. Schuchmann and V. Müller (2013). "The Ferredoxin: NAD(+) Oxidoreductase (Rnf) from the Acetogen Acetobacterium woodii Requires Na+ and Is Reversibly Coupled to the Membrane Potential." Journal of Biological Chemistry **288**(44): 31496-31502.

Hoffmeister, S., M. Gerdom, F. R. Bengelsdorf, S. Linder, S. Flüchter, H. Öztürk, W. Blümke, A. May, R.-J. Fischer, H. Bahl and P. Dürre (2016). "Acetone production with metabolically engineered strains of Acetobacterium woodii." Metabolic Engineering **36**: 37-47.

Huang, H., C. Chai, N. Li, P. Rowe, N. P. Minton, S. Yang, W. Jiang and Y. Gu (2016). "CRISPR/Cas9-Based Efficient Genome Editing in Clostridium ljungdahlii, an Autotrophic Gas-Fermenting Bacterium." ACS Synthetic Biology.

Huang, H. Y., S. N. Wang, J. Moll and R. K. Thauer (2012). "Electron Bifurcation Involved in the Energy Metabolism of the Acetogenic Bacterium Moorella thermoacetica Growing on Glucose or H-2 plus CO2." Journal of Bacteriology **194**(14): 3689-3699.

Huber, C., J. Caldeira, J. A. Jongejan and H. Simon (1994). "Further characterization of two different, reversible aldehyde oxidoreductases from *Clostridium formicoaceticum* , one containing tungsten and the other molybdenum." Archives of Microbiology **162**(5): 303-309.

Huber, H., M. Gallenberger, U. Jahn, E. Eylert, I. A. Berg, D. Kockelkorn, W. Eisenreich and G. Fuchs (2008). "A dicarboxylate/4-hydroxybutyrate autotrophic carbon assimilation cycle in the hyperthermophilic Archaeum *Ignicoccus hospitalis*." Proc Natl Acad Sci U S A **105**(22): 7851-7856.

Hugler, M., H. Huber, S. J. Molyneaux, C. Vetriani and S. M. Sievert (2007). "Autotrophic CO*2* fixation via the reductive tricarboxylic acid cycle in different lineages within the phylum Aquificae: evidence for two ways of citrate cleavage." Environ Microbiol **9**(1): 81-92.

Jang, Y. S., J. Y. Lee, J. Lee, J. H. Park, J. A. Im, M. H. Eom, J. Lee, S. H. Lee, H. Song, J. H. Cho, D. Y. Seung and S. Y. Lee (2012). "Enhanced Butanol Production Obtained by Reinforcing the Direct Butanol-Forming Route in Clostridium acetobutylicum." Mbio **3**(5).

Jensen, P. R. and K. Hammer (1998). "The sequence of spacers between the consensus sequences modulates the strength of prokaryotic promoters." Applied and Environmental Microbiology **64**(1): 82-87.

Jeon, W. B., J. Cheng and P. W. Ludden (2001). "Purification and Characterization of Membrane-associated CooC Protein and Its Functional Role in the Insertion of Nickel into Carbon Monoxide Dehydrogenase from Rhodospirillum rubrum." Journal of Biological Chemistry **276**(42): 38602-38609.

Ji, X. J., H. Huang and P. K. Ouyang (2011). "Microbial 2,3-butanediol production: a state-of-the-art review." Biotechnol Adv **29**(3): 351-364.

Jones, D. T. and D. R. Woods (1986). "Acetone-butanol fermentation revisited." Microbiol Rev **50**.

Jones, S. W., A. G. Fast, E. D. Carlson, C. A. Wiedel, J. Au, M. R. Antoniewicz, E. T. Papoutsakis and B. P. Tracy (2016). "CO2 fixation by anaerobic non-photosynthetic mixotrophy for improved carbon conversion." Nature Communications **7**: 12800.

Jones, S. W., C. J. Paredes, B. Tracy, N. Cheng, R. Sillers, R. S. Senger and E. T. Papoutsakis (2008). "The transcriptional program underlying the physiology of clostridial sporulation." Genome Biology **9**(7): R114.

Jungermann, K., H. Kirchniawy and R. K. Thauer (1970). "Ferredoxin dependent CO2 reduction to formate in clostridium pasteurianum." Biochemical and Biophysical Research Communications **41**(3): 682-689.

Jungermann, K., R. K. Thauer and K. Decker (1968). "The Synthesis of One-Carbon Units from CO2 in Clostridium kluyveri." European Journal of Biochemistry **3**(3): 351-359.

Kerby, R., W. Niemczura and J. G. Zeikus (1983). "Single-carbon catabolism in acetogens: analysis of carbon flow in Acetobacterium woodii and Butyribacterium methylotrophicum by fermentation and 13C nuclear magnetic resonance measurement." Journal of Bacteriology **155**(3): 1208-1218.

Kerby, R. and J. G. Zeikus (1983). "Growth ofClostridium thermoaceticum on H2/CO2 or CO as energy source." Current Microbiology **8**(1): 27-30.

Kim, J., S. G. Shin, G. Han, V. O'Flaherty, C. Lee and S. Hwang (2011). "Common key acidogen populations in anaerobic reactors treating different wastewaters: Molecular identification and quantitative monitoring." Water Research **45**(8): 2539-2549.

Kita, A., Y. Iwasaki, S. Sakai, S. Okuto, K. Takaoka, T. Suzuki, S. Yano, S. Sawayama, T. Tajima, J. Kato, N. Nishio, K. Murakami and Y. Nakashimada (2013). "Development of genetic transformation and heterologous expression system in carboxydotrophic thermophilic acetogen Moorella thermoacetica." Journal of Bioscience and Bioengineering **115**(4): 347-352.

Klein-Marcuschamer, D. and H. W. Blanch (2015). "Renewable fuels from biomass: Technical hurdles and economic assessment of biological routes." Aiche Journal **61**(9): 2689-2701.

Klein-Marcuschamer, D., P. Oleskowicz-Popiel, B. A. Simmons and H. W. Blanch (2012). "The challenge of enzyme cost in the production of lignocellulosic biofuels." Biotechnology and bioengineering **109**(4): 1083-1087.

Köpke, M., M. L. Gerth, D. J. Maddock, A. P. Mueller, F. Liew, S. D. Simpson and W. M. Patrick (2014). "Reconstruction of an Acetogenic 2,3-Butanediol Pathway Involving a Novel NADPH-Dependent Primary-Secondary Alcohol Dehydrogenase." Applied and Environmental Microbiology **80**(11): 3394-3403.

Köpke, M., C. Held, S. Hujer, H. Liesegang, A. Wiezer, A. Wollherr, A. Ehrenreich, W. Liebl, G. Gottschalk and P. Durre (2010). "Clostridium ljungdahlii represents a microbial production platform based on syngas." Proceedings of the National Academy of Sciences of the United States of America **107**(29): 13087-13092.

Köpke, M., C. Mihalcea, F. Liew, J. H. Tizard, M. S. Ali, J. J. Conolly, B. Al-Sinawi and S. D. Simpson (2011). "2,3-Butanediol Production by Acetogenic Bacteria, an Alternative Route to Chemical Synthesis, Using Industrial Waste Gas." Applied and Environmental Microbiology **77**(15): 5467-5475.

Köpke, M., S. Simpson, F. Liew and W. Chen (2012). Fermentation process for producing isopropanol using a recombinant microorganism. USPTO.

Kozak, M. (2005). "Regulation of translation via mRNA structure in prokaryotes and eukaryotes." Gene **361**: 13-37.

Kryukov, G. V. and V. N. Gladyshev (2004). "The prokaryotic selenoproteome." EMBO reports **5**(5): 538-543.

Kuehne, S., J. Heap, C. Cooksley, S. Cartman and N. Minton (2011). ClosTron-Mediated Engineering of Clostridium. Strain Engineering. J. A. Williams, Humana Press. **765:** 389-407.

Kusian, B. and B. Bowien (1997). "Organization and regulation of cbb CO_2 assimilation genes in autotrophic bacteria." Fems Microbiology Reviews **21**(2): 135-155.

Leang, C., T. Ueki, K. P. Nevin and D. R. Lovley (2013). "A Genetic System for Clostridium ljungdahlii: a Chassis for Autotrophic Production of Biocommodities and a Model Homoacetogen." Applied and Environmental Microbiology **79**(4): 1102-1109.

Lederle, S. M. (2010). Heterofermentative Acetonproduktion, s.n.].

Lee, K. H., J. H. Park, T. Y. Kim, H. U. Kim and S. Y. Lee (2007). "Systems metabolic engineering of *Escherichia coli* for L-threonine production." Mol Syst Biol **3**: 149.

Leonard, E., P. K. Ajikumar, K. Thayer, W. H. Xiao, J. D. Mo, B. Tidor, G. Stephanopoulos and K. L. Prather (2010). "Combining metabolic and protein engineering of a terpenoid biosynthetic pathway for overproduction and selectivity control." Proc Natl Acad Sci U S A **107**(31): 13654-13659.

Li, F., J. Hinderberger, H. Seedorf, J. Zhang, W. Buckel and R. K. Thauer (2008). "Coupled Ferredoxin and Crotonyl Coenzyme A (CoA) Reduction with NADH Catalyzed by the Butyryl-CoA Dehydrogenase/Etf Complex from Clostridium kluyveri." Journal of Bacteriology **190**(3): 843-850.

Li, H., P. H. Opgenorth, D. G. Wernick, S. Rogers, T. Y. Wu, W. Higashide, P. Malati, Y. X. Huo, K. M. Cho and J. C. Liao (2012). "Integrated Electromicrobial Conversion of CO_2 to Higher Alcohols." Science **335**(6076): 1596-1596.

Li, L. (1966). "Properties of nicotinamide adenine dinucleotide phosphate-dependent formate dehydrogenase from Clostridium thermoaceticum." J Bacteriol **92**: 405-412.

Liew, F., A. M. Henstra, K. Winzer, M. Köpke, S. D. Simpson and N. P. Minton (2016). "Insights into CO2 Fixation Pathway of Clostridium autoethanogenum by Targeted Mutagenesis." mBio **7**(3).

Lim, H. N., Y. Lee and R. Hussein (2011). "Fundamental relationship between operon organization and gene expression." Proceedings of the National Academy of Sciences **108**(26): 10626-10631.

Ljungdahl, L. G. (1986). "The Autotrophic Pathway of Acetate Synthesis in Acetogenic Bacteria." Annual Review of Microbiology **40**: 415-450.

Ljungdahl, L. G. and J. R. Andreesen (1975). "Tungsten, a Component of Active Formate Dehydrogenase from Clostridium-Thermoaceticum." Febs Letters **54**(2): 279-282.

Loubière, P., E. Gros, V. Paquet and N. D. Lindley (1992). "Kinetics and physiological implications of the growth behaviour of Eubacterium limosum on glucose/methanol mixtures." Journal of General Microbiology **138**(5): 979-985.

Lu, W. P., S. R. Harder and S. W. Ragsdale (1990). "Controlled potential enzymology of methyl transfer reactions involved in acetyl-CoA synthesis by CO dehydrogenase and the corrinoid/iron-sulfur protein from Clostridium thermoaceticum." Journal of Biological Chemistry **265**(6): 3124-3133.

Lutke-Eversloh, T. and H. Bahl (2011). "Metabolic engineering of *Clostridium acetobutylicum*: recent advances to improve butanol production." Current Opinion in Biotechnology **22**(5): 634-647.

Lutke-Eversloh, T. and G. Stephanopoulos (2008). "Combinatorial pathway analysis for improved L-tyrosine production in *Escherichia coli*: identification of enzymatic bottlenecks by systematic gene overexpression." Metab Eng **10**(2): 69-77.

Marcellin, E., J. B. Behrendorff, S. Nagaraju, S. DeTissera, S. Segovia, R. W. Palfreyman, J. Daniell, C. Licona-Cassani, L. Quek, R. Speight, M. P. Hodson, S. D. Simpson, W. P. Mitchell, M. Köpke and L. K. Nielsen (2016). "Low carbon fuels and commodity chemicals from waste gases—systematic approach to understand energy metabolism in a model acetogen." Green Chem **18**.

Martin, M. E., H. Richter, S. Saha and L. T. Angenent (2016). "Traits of selected Clostridium strains for syngas fermentation to ethanol." Biotechnology and Bioengineering **113**(3): 531-539.

Mermelstein, L. D. and E. T. Papoutsakis (1993). "In vivo methylation in Escherichia coli by the Bacillus subtilis phage phi 3T I methyltransferase to protect plasmids from restriction upon transformation of Clostridium acetobutylicum ATCC 824." Applied and Environmental Microbiology **59**(4): 1077-1081.

Meyer, C. L., J. W. Roos and E. T. Papoutsakis (1986). "Carbon monoxide gasing leads to alcohol production and butyrate uptake without acetone formation in continuous cultures ofClostridium acetobutylicum." Applied Microbiology and Biotechnology **24**(2): 159-167.

Milo, R., A. Bar-Even, E. Noor and N. E. Lewis (2010). "Design and analysis of synthetic carbon fixation pathways." Proc Natl Acad Sci U S A **107**(19): 8889-8894.

Mock, J., Y. Zheng, A. P. Mueller, S. Ly, L. Tran, S. Segovia, S. Nagaraju, M. Köpke, P. Dürre and R. K. Thauer (2015). "Energy Conservation Associated with Ethanol Formation from H2 and CO2 in Clostridium autoethanogenum Involving Electron Bifurcation." Journal of Bacteriology **197**(18): 2965-2980.

Molitor, B., K. Kirchner, A. W. Henrich, S. Schmitz and M. A. Rosenbaum (2016). "Expanding the molecular toolkit for the homoacetogen Clostridium ljungdahlii." Scientific Reports **6**: 31518.

Mörsdorf, G., K. Frunzke, D. Gadkari and O. Meyer (1992). "Microbial growth on carbon monoxide." Biodegradation **3**(1): 61-82.

Müller, V. (2003). "Energy Conservation in Acetogenic Bacteria." Applied and Environmental Microbiology **69**(11): 6345-6353.

Müller, V., S. Schmidt and E. Biegel (2009). "The ins and outs of Na(+) bioenergetics in Acetobacterium woodii." Biochimica Et Biophysica Acta-Bioenergetics **1787**(6): 691-696.

Nagarajan, H., M. Sahin, J. Nogales, H. Latif, D. R. Lovley, A. Ebrahim and K. Zengler (2013). "Characterizing acetogenic metabolism using a genome-scale metabolic reconstruction of Clostridium ljungdahlii." Microbial Cell Factories **12**(1): 1-13.

Nagaraju, S., N. K. Davies, D. J. F. Walker, M. Köpke and S. D. Simpson (2016). "Genome editing of Clostridium autoethanogenum using CRISPR/Cas9." Biotechnology for Biofuels **9**(1): 219.

Nevin, K. P., S. A. Hensley, A. E. Franks, Z. M. Summers, J. H. Ou, T. L. Woodard, O. L. Snoeyenbos-West and D. R. Lovley (2011). "Electrosynthesis of Organic Compounds from Carbon Dioxide Is Catalyzed by a Diversity of Acetogenic Microorganisms." Applied and Environmental Microbiology **77**(9): 2882-2886.

Nicolaou, S. A., S. M. Gaida and E. T. Papoutsakis (2010). "A comparative view of metabolite and substrate stress and tolerance in microbial bioprocessing: From biofuels and chemicals, to biocatalysis and bioremediation." Metabolic Engineering **12**(4): 307-331.

Nicolaou, S. A., S. M. Gaida and E. T. Papoutsakis (2011). "Coexisting/Coexpressing Genomic Libraries (CoGeL) identify interactions among distantly located genetic loci for developing complex microbial phenotypes." Nucleic Acids Res **39**(22): 152-161.

Nölling, J., G. Breton, M. V. Omelchenko, K. S. Makarova, Q. Zeng, R. Gibson, H. M. Lee, J. Dubois, D. Qiu, J. Hitti, GTC Sequencing Center Production Finishing, B. Teams, Y. I. Wolf, R. L. Tatusov, F. Sabathe, L. Doucette-Stamm, P. Soucaille, M. J. Daly, G. N. Bennett, E. V. Koonin and D. R. Smith (2001). "Genome Sequence and Comparative Analysis of the Solvent-Producing Bacterium Clostridium acetobutylicum." Journal of Bacteriology **183**(16): 4823-4838.

NRC-NAE, N. R. C. (U.S.). and C. o. A. s. E. F. P. o. A. L. T. F. pp. (2009). Liquid transportation fuels from coal and biomass: technological status, costs, and environmental impacts, National Academies Press.

Papoutsakis, E. T. (1984). "Equations and calculations for fermentations of butyric-acid bacteria." Biotechnology and Bioengineering **26**(2): 174-187.

Papoutsakis, E. T. (2008). "Engineering solventogenic clostridia." Current Opinion in Biotechnology **19**(5): 420-429.

Papoutsakis, E. T. (2015). "Reassessing the Progress in the Production of Advanced Biofuels in the Current Competitive Environment and Beyond: What Are the Successes and Where Progress Eludes Us and Why." Industrial & Engineering Chemistry Research **54**(42): 10170-10182.

Papoutsakis, E. T. and C. L. Meyer (1985). "Equations and calculations of product yields and preferred pathways for butanediol and mixed-acid fermentations." Biotechnology and Bioengineering **27**(1): 50-66.

Parkhill, J., M. Sebaihia, B. W. Wren, P. Mullany, N. F. Fairweather, N. Minton, R. Stabler, N. R. Thomson, A. P. Roberts, A. M. Cerdeno-Tarrraga, H. W. Wang, M. T. G. Holden, A. Wright, C. Churcher, M. A. Quail, S. Baker, N. Bason, K. Brooks, T. Chillingworth, A. Cronin, P. Davis, L. Dowd, A. Fraser, T. Feltwell, Z. Hance, S. Holroyd, K. Jagels, S. Moule, K. Mungall, C. Price, E. Rabbinowitsch, S. Sharp, M. Simmonds, K. Stevens, L. Unwin, S. Whithead, B. Dupuy, G. Dougan and B. Barrell (2006). "The multidrug-resistant human pathogen Clostridium difficile has a highly mobile, mosaic genome." Nature Genetics **38**(7): 779-786.

Paul, D., F. W. Austin, T. Arick, S. M. Bridges, S. C. Burgess, Y. S. Dandass and M. L. Lawrence (2010). "Genome sequence of the solvent-producing bacterium Clostridium carboxidivorans strain P7T." Journal of Bacteriology **192**(20): 5554-5555.

Payne, W. J. (1970). "Energy yields and growth of heterotrophs." Annual review of microbiology **24**: 17-52.

Peters, V., P. H. Janssen and R. Conrad (1998). "Efficiency of hydrogen utilization during unitrophic and mixotrophic growth of Acetobacterium woodii on hydrogen and lactate in the chemostat." Fems Microbiology Ecology **26**(4): 317-324.

Pfleger, B. F., D. J. Pitera, C. D. Smolke and J. D. Keasling (2006). "Combinatorial engineering of intergenic regions in operons tunes expression of multiple genes." Nat Biotechnol **24**(8): 1027-1032.

Phillips, J. R., E. C. Clausen and J. L. Gaddy (1994). "Synthesis Gas as Substrate for the Biological Production of Fuels and Chemicals." Applied Biochemistry and Biotechnology **45-6**: 145-157.

Phillips, J. R., K. T. Klasson, E. C. Clausen and J. L. Gaddy (1993). "Biological production of ethanol from coal synthesis gas." Applied Biochemistry and Biotechnology **39**(1): 559-571.

Poehlein, A., M. Cebulla, M. M. Ilg, F. R. Bengelsdorf, B. Schiel-Bengelsdorf, G. Whited, J. R. Andreesen, G. Gottschalk, R. Daniel and P. Dürre (2015). "The Complete Genome Sequence of Clostridium aceticum: a Missing Link between Rnf- and Cytochrome-Containing Autotrophic Acetogens." mBio **6**(5).

Pohlmann, A., W. F. Fricke, F. Reinecke, B. Kusian, H. Liesegang, R. Cramm, T. Eitinger, C. Ewering, M. Potter, E. Schwartz, A. Strittmatter, I. Voss, G. Gottschalk, A. Steinbuchel, B. Friedrich and B. Bowien (2006). "Genome sequence of the bioplastic-producing "Knallgas" bacterium *Ralstonia eutropha* H16." Nat Biotechnol **24**(10): 1257-1262.

Purdy, D., T. A. T. O'Keeffe, M. Elmore, M. Herbert, A. McLeod, M. Bokori-Brown, A. Ostrowski and N. P. Minton (2002). "Conjugative transfer of clostridial shuttle vectors from Escherichia coli to Clostridium difficile through circumvention of the restriction barrier." Molecular Microbiology **46**(2): 439-452.

Pyne, M. E., M. Bruder, M. Moo-Young, D. A. Chung and C. P. Chou (2014). "Technical guide for genetic advancement of underdeveloped and intractable Clostridium." Biotechnology Advances **32**(3): 623-641.

Pyne, M. E., M. R. Bruder, M. Moo-Young, D. A. Chung and C. P. Chou (2016). "Harnessing heterologous and endogenous CRISPR-Cas machineries for efficient markerless genome editing in Clostridium." Scientific Reports **6**.

Ragsdale, S. W. (1991). "Enzymology of the Acetyl-Coa Pathway of Co2 Fixation." Critical Reviews in Biochemistry and Molecular Biology **26**(3-4): 261-300.

Ragsdale, S. W. (1997). "The Eastern and Western branches of the Wood/Ljungdahl pathway: how the East and West were won." Biofactors **6**(1): 3-11.

Ragsdale, S. W., J. E. Clark, L. G. Ljungdahl, L. L. Lundie and H. L. Drake (1983). "Properties of Purified Carbon-Monoxide Dehydrogenase from Clostridium-Thermoaceticum, a Nickel, Iron-Sulfur Protein." Journal of Biological Chemistry **258**(4): 2364-2369.

Ragsdale, S. W., P. A. Lindahl and E. Münck (1987). "Mössbauer, EPR, and optical studies of the corrinoid/iron-sulfur protein involved in the synthesis of acetyl coenzyme A by Clostridium thermoaceticum." Journal of Biological Chemistry **262**(29): 14289-14297.

Ragsdale, S. W. and E. Pierce (2008). "Acetogenesis and the Wood–Ljungdahl pathway of CO2 fixation." Biochimica et Biophysica Acta (BBA) - Proteins and Proteomics **1784**(12): 1873-1898.

Ragsdale, S. W., E. Pierce, G. Xie, R. D. Barabote, E. Saunders, C. S. Han, J. C. Detter, P. Richardson, T. S. Brettin, A. Das and L. G. Ljungdahl (2008). "The complete genome sequence of Moorella thermoacetica (f. Clostridium thermoaceticum)." Environmental Microbiology **10**(10): 2550-2573.

Ramió-Pujol, S., R. Ganigué, L. Bañeras and J. Colprim (2015). "Incubation at 25 °C prevents acid crash and enhances alcohol production in Clostridium carboxidivorans P7." Bioresource Technology **192**: 296-303.

Raybuck, S. A., N. R. Bastian, W. H. Ormejohnson and C. T. Walsh (1988). "Kinetic Characterization of the Carbon-Monoxide Acetyl-Coa (Carbonyl Group) Exchange Activity of the Acetyl-Coa Synthesizing Co Dehydrogenase from Clostridium-Thermoaceticum." Biochemistry **27**(20): 7698-7702.

Richter, H., M. Martin and L. Angenent (2013). "A Two-Stage Continuous Fermentation System for Conversion of Syngas into Ethanol." Energies **6**(8): 3987.

Rose, A. H. (1971). Advances in Microbial Physiology, Elsevier Science.

Rude, M. A. and A. Schirmer (2009). "New microbial fuels: a biotech perspective." Current Opinion in Microbiology **12**(3): 274-281.

Salimi, F. and R. Mahadevan (2013). "Characterizing metabolic interactions in a clostridial co-culture for consolidated bioprocessing." BMC Biotechnology **13**(1): 95.

Salis, H. M., E. A. Mirsky and C. A. Voigt (2009). "Automated design of synthetic ribosome binding sites to control protein expression." Nat Biotechnol **27**(10): 946-950.

Savage, M. D., Z. G. Wu, S. L. Daniel, L. L. Lundie and H. L. Drake (1987). "Carbon monoxide-dependent chemolithotrophic growth of Clostridium thermoautotrophicum." Applied and Environmental Microbiology **53**(8): 1902-1906.

Schiel-Bengelsdorf, B. and P. Dürre (2012). "Pathway engineering and synthetic biology using acetogens." FEBS Letters **586**(15): 2191-2198.

Schuchmann, K. and V. Müller (2012). "A Bacterial Electron-bifurcating Hydrogenase." Journal of Biological Chemistry **287**(37): 31165-31171.

Schuchmann, K. and V. Müller (2013). "Direct and reversible hydrogenation of CO2 to formate by a bacterial carbon dioxide reductase." Science (New York, N.Y.) **342**: 1382-1385.

Serganov, A. and D. J. Patel (2007). "Ribozymes, riboswitches and beyond: regulation of gene expression without proteins." Nat Rev Genet **8**(10): 776-790.

Service, R. F. (2014). "Cellulosic ethanol at last?" Science **345**(6201): 1111.

Shen, G. J., J. S. Shieh, A. J. Grethlein, M. K. Jain and J. G. Zeikus (1999). "Biochemical basis for carbon monoxide tolerance and butanol production by Butyribacterium methylotrophicum." Applied Microbiology and Biotechnology **51**(6): 827-832.

Sheppard, C. A., E. E. Trimmer and R. G. Matthews (1999). "Purification and Properties of NADH-Dependent 5,10-Methylenetetrahydrofolate Reductase (MetF) fromEscherichia coli." Journal of Bacteriology **181**(3): 718-725.

Sillers, R., A. Chow, B. Tracy and E. T. Papoutsakis (2008). "Metabolic engineering of the non-sporulating, non-solventogenic Clostridium acetobutylicum strain M5 to produce butanol without acetone demonstrate the robustness of the acid-formation pathways and the importance of the electron balance." Metabolic Engineering **10**(6): 321-332.

Simon, H., H. White, H. Lebertz and I. Thanos (1987). "Reduction of 2-Enoates and Alkanoates with Carbon-Monoxide or Formate, Viologens, and Clostridium-Thermoaceticum to Saturated Acids and Unsaturated and Saturated Alcohols." Angewandte Chemie-International Edition in English **26**(8): 785-787.

Simpson, S. D., M. Köpke and F. Liew (2011). Recombinant Microorganisms and Methods of Use Thereof, USPTO.

Singh, K. D., M. H. Schmalisch, J. Stülke and B. Görke (2008). "Carbon Catabolite Repression in Bacillus subtilis: Quantitative Analysis of Repression Exerted by Different Carbon Sources." Journal of Bacteriology **190**(21): 7275-7284.

Sloan, J., T. A. Warner, P. T. Scott, T. L. Bannam, D. I. Berryman and J. I. Rood (1992). "Construction of a sequencedClostridium perfringens-Escherichia coli shuttle plasmid." Plasmid **27**(3): 207-219.

Stephanopoulos, G. (2011). Patent application: Converting a carbon source into a lipid comprises culturing a first organism in the presence of a carbon source and culturing a second organism in the presence of carbon dioxide, Massachusetts Inst Technology (MA)**:** 27 pp. US2011177564-A2011177561 US2011007325 2011177514 Jan 2011172011 WO2011088364-A2011177562 WOUS2011021360 2011177514 Jan 2011172011 WO2011088364-A2011177568 WOUS2011021360 2011177514 Jan 2011172011 WO2011088364-A2011177563 WOUS2011021360 2011177514 Jan 2011172011.

Strätz, M., U. Sauer, A. Kuhn and P. Dürre (1994). "Plasmid Transfer into the Homoacetogen Acetobacterium woodii by Electroporation and Conjugation." Applied and Environmental Microbiology **60**(3): 1033-1037.

Straub, M., M. Demler, D. Weuster-Botz and P. Dürre (2014). "Selective enhancement of autotrophic acetate production with genetically modified Acetobacterium woodii." Journal of Biotechnology **178**: 67-72.

Stülke, J. and W. Hillen (1999). "Carbon catabolite repression in bacteria." Current Opinion in Microbiology **2**(2): 195-201.

Subashchandrabose, S. R., B. Ramakrishnan, M. Megharaj, K. Venkateswarlu and R. Naidu (2013). "Mixotrophic cyanobacteria and microalgae as distinctive biological agents for organic pollutant degradation." Environment International **51**(0): 59-72.

Szulczyk, K. R. (2010). "Which is a better transportation fuel–butanol or ethanol?" International Journal of Energy and Environment **1**(3): 501-512.

Tan, Y., J. Liu, X. Chen, H. Zheng and F. Li (2013). "RNA-seq-based comparative transcriptome analysis of the syngas-utilizing bacterium Clostridium ljungdahlii DSM 13528 grown autotrophically and heterotrophically." Molecular BioSystems **9**(11): 2775-2784.

Thauer, R. K., A. K. Kaster, H. Seedorf, W. Buckel and R. Hedderich (2008). "Methanogenic archaea: ecologically relevant differences in energy conservation." Nat Rev Microbiol **6**(8): 579-591.

Tracy, B. P., S. W. Jones, A. G. Fast, D. C. Indurthi and E. T. Papoutsakis (2012). "Clostridia: the importance of their exceptional substrate and metabolite diversity for biofuel and biorefinery applications." Current Opinion in Biotechnology **23**: 364–381 310.1016/j.copbio.2011.1010.1008.

Tremblay, P.-L., T. Zhang, S. A. Dar, C. Leang and D. R. Lovley (2013). "The Rnf Complex of Clostridium ljungdahlii Is a Proton-Translocating Ferredoxin:NAD+ Oxidoreductase Essential for Autotrophic Growth." mBio **4**(1).

Tripathi, S. A., D. G. Olson, D. A. Argyros, B. B. Miller, T. F. Barrett, D. M. Murphy, J. D. McCool, A. K. Warner, V. B. Rajgarhia, L. R. Lynd, D. A. Hogsett and N. C. Caiazza (2010). "Development of pyrF-Based Genetic System for Targeted Gene Deletion in Clostridium thermocellum and Creation of a pta Mutant." Applied and Environmental Microbiology **76**(19): 6591-6599.

Tummala, S. B., S. G. Junne and E. T. Papoutsakis (2003). "Antisense RNA downregulation of coenzyme A transferase combined with alcohol-aldehyde dehydrogenase overexpression leads to predominantly alcohologenic Clostridium acetobutylicumfermentations." J Bacteriol **185**.

Ueki, T., K. P. Nevin, T. L. Woodard and D. R. Lovley (2014). "Converting Carbon Dioxide to Butyrate with an Engineered Strain of Clostridium ljungdahlii." mBio **5**(5): e01636-01614.

Wang, H. H., F. J. Isaacs, P. A. Carr, Z. Z. Sun, G. Xu, C. R. Forest and G. M. Church (2009). "Programming cells by multiplex genome engineering and accelerated evolution." Nature **460**(7257): 894-U133.

Wang, S. N., H. Y. Huang, J. Kahnt, A. P. Mueller, M. Kopke and R. K. Thauer (2013). "NADP-Specific Electron-Bifurcating [FeFe]-Hydrogenase in a Functional Complex with Formate Dehydrogenase in Clostridium autoethanogenum Grown on CO." Journal of Bacteriology **195**(19): 4373-4386.

Wang, S. N., H. Y. Huang, J. Kahnt and R. K. Thauer (2013). "A Reversible Electron-Bifurcating Ferredoxin- and NAD-Dependent [FeFe]-Hydrogenase (HydABC) in Moorella thermoacetica." Journal of Bacteriology **195**(6): 1267-1275.

Wang, Y., Z. T. Zhang, S. O. Seo, K. J. Choi, T. Lu, Y. S. Jin and H. P. Blaschek (2015). "Markerless chromosomal gene deletion in Clostridium beijerinckii using CRISPR/Cas9 system." Journal of Biotechnology **200**: 1-5.

Warner, J. R., P. J. Reeder, A. Karimpour-Fard, L. B. A. Woodruff and R. T. Gill (2010). "Rapid profiling of a microbial genome using mixtures of barcoded oligonucleotides." Nat Biotechnol **28**(8): 856-U138.

White, H. and H. Simon (1992). "The Role of Tungstate and or Molybdate in the Formation of Aldehyde Oxidoreductase in Clostridium-Thermoaceticum and Other Acetogens - Immunological Distances of Such Enzymes." Archives of Microbiology **158**(2): 81-84.

Wohlfarth, G. and G. Diekert (1991). "Thermodynamics of Methylenetetrahydrofolate Reduction to Methyltetrahydrofolate and Its Implications for the Energy-Metabolism of Homoacetogenic Bacteria." Archives of Microbiology **155**(4): 378-381.

Wood, H. G. (1991). "Life with CO or CO_2 and H_2 as a source of carbon and energy." The FASEB journal : official publication of the Federation of American Societies for Experimental Biology **5**(2): 156-163.

Yamamoto, I., S. M. Liu, T. Saiki and L. G. Ljungdahl (1982). "Properties of Nadp-Dependent Formate Dehydrogenase from Clostridium-Thermoaceticum, a Tungsten-Selenium-Iron Protein." Federation Proceedings **41**(4): 888-888.

Yu, M., Y. Du, W. Jiang, W.-L. Chang, S.-T. Yang and I.-C. Tang (2012). "Effects of different replicons in conjugative plasmids on transformation efficiency, plasmid stability, gene expression and n-butanol biosynthesis in Clostridium tyrobutyricum." Applied microbiology and biotechnology **93**(2): 881-889.

Zinoni, F., A. Birkmann, W. Leinfelder and A. Böck (1987). "Cotranslational insertion of selenocysteine into formate dehydrogenase from Escherichia coli directed by a UGA codon." Proceedings of the National Academy of Sciences **84**(10): 3156-3160.

Appendix A

REPRINT PERMISSIONS

A.1 Reprint Permissions for Chapter 2

Publication: B. P. Tracy, S. W. Jones, A. G. Fast, D. C. Indurthi, E. T. Papoutsakis. Clostridia: the importance of their exceptional substrate and metabolite diversity for biofuel and biorefinery applications. *Current Opinion in Biotechnology*. 2012; 23:364-381

Permission: This is a license agreement between Alan Fast and Elsevier provided by Elsevier and Copyright Clearance Center.

Table A.1: License agreement for Chapter 2 from COB

License Number	4164380948540
License date	Aug 08, 2017
Licensed Content Publisher	Elsevier
Licensed Content Publication	Current Opinion in Biotechnology
Licensed Content Title	Clostridia: the importance of their exceptional substrate and metabolite diversity for biofuel and biorefinery applications
Licensed Content Author	Bryan P Tracy, Shawn W Jones, Alan G Fast,Dinesh C Indurthi, Eleftherios T Papoutsakis
Licensed Content Date	Jun 1, 2012
Licensed Content Volume	23
Licensed Content Issue	3
Licensed Content Pages	18
Start Page	364
End Page	381
Type of Use	reuse in a thesis/dissertation
Portion	full article
Format	both print and electronic
Are you the author of this Elsevier article?	Yes
Will you be translating?	No

Publication: A. G. Fast and E. T. Papoutsakis. Stoichiometric and energetic analyses of non-photosynthetic CO2-fixation pathways to support synthetic biology strategies for production of fuels and chemicals. *Current Opinion in Chemical Engineering*. 2012; 1:380-395

Permission: This is a license agreement between Alan Fast and Elsevier provided by Elsevier and Copyright Clearance Center.

Table A.2: License agreement for Chapter 2 from CoCHE

License Number	4164430406016
License date	Aug 08, 2017
Licensed Content Publisher	Elsevier
Licensed Content Publication	Current Opinion in Chemical Engineering
Licensed Content Title	Stoichiometric and energetic analyses of non-photosynthetic CO2-fixation pathways to support synthetic biology strategies for production of fuels and chemicals
Licensed Content Author	Alan G Fast, Eleftherios T Papoutsakis
Licensed Content Date	Nov 1, 2012
Licensed Content Volume	1
Licensed Content Issue	4
Licensed Content Pages	16
Type of Use	reuse in a thesis/dissertation
Portion	full article
Format	both print and electronic
Are you the author of this Elsevier article?	Yes
Will you be translating?	No

A.2 Reprint Permissions for Chapter 3

Publication: A. G. Fast, E. D. Schmidt, S. W. Jones, B. P. Tracy. Acetogenic mixotrophy: novel options for yield improvement in biofuels and biochemicals production. *Current Opinion in Biotechnology*. 2015; 33:60-72

Permission: This is a license agreement between Alan Fast and Elsevier provided by Elsevier and Copyright Clearance Center.

Table A.3 License agreement for Chapter 3 from CoB

License Number	4164431114028
License date	Aug 08, 2017
Licensed Content Publisher	Elsevier
Licensed Content Publication	Current Opinion in Biotechnology
Licensed Content Title	Acetogenic mixotrophy: novel options for yield improvement in biofuels and biochemicals production
Licensed Content Author	Alan G Fast, Ellinor D Schmidt, Shawn W Jones, Bryan P Tracy
Licensed Content Date	Jun 1, 2015
Licensed Content Volume	33
Licensed Content Issue	n/a
Licensed Content Pages	13
Type of Use	reuse in a thesis/dissertation
Portion	full article
Format	both print and electronic

Are you the author of this Elsevier article?	Yes
Will you be translating?	No

A.3 Reprint Permissions for Chapter 4

Publication: S. W. Jones, A. G. Fast, E. D. Carlson, C. A. Wiedel, J. Au, M. R. Antoniewicz, E. T. Papoutsakis, B. P. Tracy. CO_2 Fixation by anaerobic non-photosynthetic mixotrophy for improved carbon conversion. *Nature Communications*. 2016; 7:12800

Permission: This article has been distributed under a Creative Commons CC-BY license. The material may be reused without obtaining permission from Nature Publishing Group, providing that the author and the original source of the publication are fully acknowledged.